



Sound Radiation from a Loudspeaker Cabinet using the Boundary Element Method

Fernandez Grande, Efren

Publication date:
2008

[Link back to DTU Orbit](#)

Citation (APA):

Fernandez Grande, E. (2008). *Sound Radiation from a Loudspeaker Cabinet using the Boundary Element Method*. Department of Acoustic Technology, Technical University of Denmark.

General rights

Copyright and moral rights for the publications made accessible in the public portal are retained by the authors and/or other copyright owners and it is a condition of accessing publications that users recognise and abide by the legal requirements associated with these rights.

- Users may download and print one copy of any publication from the public portal for the purpose of private study or research.
- You may not further distribute the material or use it for any profit-making activity or commercial gain
- You may freely distribute the URL identifying the publication in the public portal

If you believe that this document breaches copyright please contact us providing details, and we will remove access to the work immediately and investigate your claim.



Technical University of Denmark (DTU)

Acoustic Technology

Sound Radiation from a Loudspeaker Cabinet using the Boundary Element Method

Master Thesis by
Efren Fernandez Grande

Supervisor: Finn Jacobsen

September 30, 2008

Abstract

Ideally, the walls of a loudspeaker cabinet are rigid. However, in reality, the cabinet is excited by the vibration of the loudspeaker units and by the acoustic pressure inside the cabinet. The radiation of sound caused by such vibration can influence the overall performance of the loudspeaker, in some cases becoming clearly audible. The aim of this study is to provide a tool that can evaluate the contribution from the cabinet to the overall sound radiated by a loudspeaker. The specific case of a B&O Beolab 9 early prototype has been investigated. An influence by the cabinet of this prototype had been reported, based on subjective testing. This study aims to detect the reported problem. The radiation from the cabinet is calculated using the Boundary Element Method. The analysis examines both the frequency domain and the time domain characteristics (in other words, the steady state response and the impulse response) of the loudspeaker and the cabinet. A significant influence of the cabinet has been detected, which becomes especially apparent in the time domain, during the sound decay process.

Preface

This report presents the work carried out between February and September of 2008 as a Master Thesis project at the Technical University of Denmark (DTU).

This Master Thesis was carried out at the Acoustic Technology department, under the supervision of Finn Jacobsen. The project was done in collaboration with Bang & Olufsen, with Sylvain Choisel as the contact person from the company.

Acknowledgments

Throughout this project, there have been several people that helped and kindly contributed in different ways. Initially, I would like to thank Finn Jacobsen for his valuable guidance and help during the whole project.

I would also like to thank Peter Juhl for his support and advice concerning the Boudary Element Method, and along with Vicente Cutanda, for the development and sharing of the OpenBEM software, that has been used in this project. Salvador Barrera for his help with the Boundary Element Method calculations and explanations.

Thank the cooperation with Bang & Olufsen, especially with Sylvain Choisel, for his interest and collaboration. Yu Luan (Spark) for sharing his work and helping with the ANSYS modeling and Mogens Ohlrich for his advice and collaboration on the vibration measurements. Finally, I would like to thank Ioanna Karagali, David Fernandez and Kostas Komninos for the revision of the document and their priceless support.

This work was granted with one of the Bang & Olufsen scholarships for 2008.

Contents

1	Introduction	6
2	Theoretical Background	9
2.1	The BEM in Acoustics	9
2.1.1	Green's function	10
2.1.2	Sommerfeld's radiation condition	10
2.1.3	The integral equation (BIE)	11
3	Methodology	15
3.1	Vibroacoustic Measurements	16
3.1.1	Measurement mesh	16
3.1.2	Procedure of the measurement	18
3.2	Verification measurements	20
3.2.1	Sound pressure measurements	20
3.2.2	Laser measurements	20
3.3	Numerical calculations	20
4	Preliminary testing	23
4.1	Initial considerations	23
4.2	Description	24
4.3	Results	27
4.4	Conclusion	28
5	Preprocessing and Measurements	29
5.1	Geometry	29
5.2	Meshing	31
5.2.1	Testing of the mesh	32
5.3	Boundary Conditions (Measurement)	33
5.3.1	Laser measurements	35
5.3.2	SPL measurements	35
5.3.3	Measurement tests, validation tests	35
5.4	Solution	37

6	Results	39
6.1	Results from the vibration measurement	39
6.2	Sound pressure radiated by the loudspeakers cabinet	42
6.3	Radiation by the cabinet compared to the total radiation	44
6.4	Contribution from the cabinet to the radiated sound	47
6.4.1	Considerations regarding the cabinets radiation	53
6.5	Behavior of the cabinet in the time domain	54
6.5.1	Impulse response	54
6.5.2	Decay of the sound pressure	58
6.6	Radiation at the back of the cabinet (time domain)	63
6.7	Radiation from the bottom of the cabinet	67
6.7.1	Frequency domain (Bottom radiation)	67
6.7.2	Impulse response (bottom radiation)	69
6.7.3	Decay of the sound pressure (Bottom radiation)	69
7	Conclusions	73
	Bibliography	77
	List of Figures	79
A	Non-linear vibration of the cabinet	83
B	Deflection shapes of the cabinet	89
C	Matlab codes	92
C.1	Calculation of the sound radiated by the cabinet	92
C.2	Calculation of the sound radiated by the loudspeaker	98
C.3	Time domain characteristics (Impulse response & decay)	102
C.4	Testing of the method (Test Box)	109
D	SHELL63 Elastic Shell	112

Chapter 1

Introduction

Since the first loudspeakers were developed, there has always been a great interest for improvement, in pursuit of a higher sound quality. Generally, loudspeaker units have been the main target of such development, because they are essentially the source of sound radiation. To the contrary, less emphasis has been put on the cabinet's design, since its impact on the sound quality is not so immediate. However, a poor cabinet design can clearly influence to a significant extent the overall quality of sound radiated by the loudspeaker.

Ideally, the walls of a loudspeaker cabinet are rigid and unmoving. However, in reality, such is not the case. The cabinet is excited mechanically by the reaction forces caused by the motion of the loudspeaker units mounted on them, and by the acoustic pressure developed within the cabinet [9]. These two sources of excitation, make the cabinet vibrate, and thus radiate sound. It is of interest to know if this sound radiation is of sufficient magnitude and time duration to contribute audibly to the loudspeaker's total acoustic output.

This problem has been studied by different authors, such as Tappan, Toole and Olive, Capone, Lipshitz, Vanderkooy et al. and Karjalainen et al. However, surprisingly little literature exists on the topic [2]. The early work on the subject was generally based on steady-state measurements, where the contribution from poorly designed cabinets would become apparent in the frequency response, as in [16]. Also subjective testing was used as a tool for evaluation of the sound quality [17]. However, in this early studies, the contribution from the loudspeaker enclosure would not be estimated separately.

Later research has mainly been based on the the use of numerical methods, which have proved to be very convenient for this problem. Such is the case in refs. [9], [2] or [7] and other authors that have studied the problem, compared different methods and procedures, and examined different cabinet designs. However, most of the work in this area has primarily focused on the steady state response of the systems.

All formerly cited authors concluded that the acoustic radiation from a cabinet can significantly affect the overall performance of a loudspeaker, mainly at the lowest structural resonance frequencies of the cabinet. However, such influence depends mainly on the design of the loudspeaker.

The particular case of this study focuses on the radiation of a prototype of the Beolab 9 loudspeaker by Bang & Olufsen. During the development process of the loudspeaker, a “coloring” effect from the loudspeaker cabinet was reported based on subjective testing. The main purpose of this study is to provide a tool that can evaluate the radiation by a loudspeaker cabinet and verify if the reported problem can be detected by such a tool.

It should be remarked that in the present case of study, the shape of the cabinet is not a standard rectangular cabinet, but a curved, conical like shaped one. This is a fundamental difference between the present case of study and the previously referred work on the field.

In this report, first a brief fundamental explanation of the Boundary Element Method is presented, followed by the description of the methodology used in this project (Chapter 3). The results of some preliminary testing, done in order to verify the procedure of calculations used, are presented in Chapter 4. In Chapter 5, the model and preprocessing of the BEM is described. The results obtained are presented and discussed in Chapter 6. Finally, Chapter 7 summarizes the main conclusions that can be drawn from the study.

Chapter 2

Theoretical Background

The theoretical background of this project is mainly related to the Boundary Element Method (BEM). The BEM has been the principal tool used in this project for the calculations carried out. In this section the method is briefly presented, without going deep into it. The aim of this section is to introduce some essential concepts and the idea on which the method is based.

The BEM is a numerical method used to solve linear partial differential equations (PDEs) formulated as integral equations. In general terms, a boundary value problem governed by a certain PDE is to be solved over a certain domain. The governing PDE is formulated in an integral form by using a weighted integral equation and the Green-Gauss theorem, until the so called boundary integral equation (BIE) is formulated. The BIE consists only of boundary integrals. The problem is therefore reduced from a three-dimensional problem to a two-dimensional one. By solving this boundary integral equation, the solution to the problem over the entire domain is found.

2.1 The BEM in Acoustics

In the particular case of acoustics, which is the actual application here, the BEM makes it possible to calculate the sound field over a certain domain (sound pressure, particle velocity...), provided a certain set of boundary conditions.

The starting point is the wave equation for an homogeneous, inviscid compressible fluid,

$$\nabla^2 p_{ins} = \frac{1}{c^2} \frac{\partial^2 p_{ins}}{\partial t^2} \quad (2.1)$$

where p_{ins} is the instant pressure variation, c is the speed of sound. Assuming time harmonic waves, the wave equation can be expressed as the Helmholtz equation, which describes the propagation of the sound pressure in the medium.

$$\nabla^2 p + k^2 p = 0 \quad (2.2)$$

Due to the time-harmonic wave assumption, the time dependence has been removed from the Helmholtz equation (2.2). Under this assumption, the term $\frac{\partial^2 p_{ins}}{\partial t^2}$ from 2.1 can be expressed as $-\omega^2 e^{j\omega t} p_{ins}$. In the Helmholtz equation, the factor $e^{j\omega t}$ (which would be the only time dependent term), is omitted. The wavenumber k is defined as $k = \omega/c$

2.1.1 Green's function

If a point source (described by a delta function) is placed in the unbounded medium, it can be expressed by the inhomogeneous equation,

$$(\nabla^2 + k^2)G_k(\vec{r}, \vec{r}_0) = -4\pi\delta(\vec{r} - \vec{r}_0) \quad (2.3)$$

The solution to the above equation is the free space Green's Function, which is expressed as:

$$G(\vec{r}, \vec{r}_0) = \frac{e^{-jk(\vec{r}-\vec{r}_0)}}{|\vec{r} - \vec{r}_0|} \quad (2.4)$$

This function represents the pressure in the medium at the observation point \vec{r} , generated by a point source placed at \vec{r}_0 . This point source is a monopole, which is a mathematical abstraction, but nevertheless an essential concept in acoustics, useful to describe many important phenomena.

2.1.2 Sommerfeld's radiation condition

The Sommerfeld's radiation condition makes it possible to solve the Helmholtz equation uniquely. Therefore it is essential in acoustic radiation problems in unbounded mediums. It is a boundary condition for infinite exterior domains. Basically, it expresses the fact that the energy decreases towards infinity, decaying progressively to zero. In other words, it expresses the fact that there are no reflections coming from infinity. Quoting Sommerfeld's own words [15] : *"...the sources must be sources, not sinks of energy. The energy which is radiated from the sources must scatter to infinity; no energy may be radiated from infinity into the field"*.

The Sommerfeld's radiation condition for an acoustic problem may be stated as:

$$\lim_{r \rightarrow \infty} [r(p - \rho_0 c v_r)] = 0 \quad (2.5)$$

where r is the radial coordinate of the spherical system, $\rho_0 c$ is the characteristic impedance of air, p is the sound pressure and v_r is the radial component of the particle velocity.

2.1.3 The integral equation (BIE)

As mentioned previously, given a boundary problem, the BEM makes it possible to calculate the solution on the domain of the problem (for instance a general boundary problem as below).

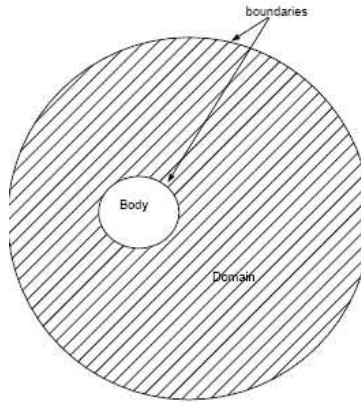


Figure 2.1: *Simple Boundary Problem Sketch. In a sound radiation problem the domain is governed by the wave equation. In this particular project the outer boundary condition is the Sommerfield radiation condition -Infinity-, and the inner boundary condition is the velocity of the body*

To arrive to the integral equation, starting from the Helmholtz equation, the starting point is the vector identity [5]:

$$G(\nabla^2 + k^2)p - p(\nabla^2 + k^2)G = \nabla \cdot (G\nabla p - p\nabla G) \quad (2.6)$$

Integrating equation (2.6) over the volume V (which is the volume of the sphere of radius a that encloses all points outside S) yields,

$$-\int_V p(\nabla^2 + k^2)GdV = \int_V \nabla \cdot (G\nabla p - p\nabla G)dV \quad (2.7)$$

Such a sphere of volume V is very large, its radius goes towards infinity, in order to enclose all points of the domain.

The Gauss theorem ¹ is applied to the right side of (2.7). Thus, it is possible to transform the previous volume integral into a surface integral.

$$-\int_V p(\nabla^2 + k^2)GdV = \int_S (G\nabla p - p\nabla G)ndS + I_A \quad (2.8)$$

The term I_A in (2.8) depends on the radius a of the sphere used to integrate the volume in (2.7). The term I_A can be shown to vanish towards infinity, because both Green's function and the pressure satisfy the Sommerfeld's radiation condition (see above: (2.1.2)) as in [5]. Thus, I_A is zero. Equation (2.8) can be as well expressed as:

$$4\pi \int_V p(r)\delta(r - r_0)dV = \int_S (p(r)\frac{\partial G}{\partial n} + jkz_0v(r)G)dS \quad (2.9)$$

The left side of (2.9) is the solid angle seen from the observation point, or field point, which is:

$$\begin{aligned} & 0, & \text{if } r_0 \text{ is inside } S \\ & 4\pi p, & \text{if } r_0 \text{ is outside } S \\ & C(r_0) = 4\pi + \int_S \frac{\partial}{\partial n}(\frac{1}{R})dS, & \text{if } r_0 \text{ is in the boundary of } S \end{aligned}$$

Bearing all the previous in mind, the integral equation can be formulated as:

$$C(P)p(P) = \int_S (p(Q)\frac{\partial G(P,Q)}{\partial n} + jkz_0v(Q)G(P,Q))dS \quad (2.10)$$

The previous equation (2.10) relates the pressure on any point Q on the surface S of the body with any point P in the domain, as well as the velocity of the body in its surface (in the case that it is vibrating).

There is as well a more complete integral equation, in which the scattering case is also taken into account. An additional term representing an incident wave is included. In this case the previous equation (2.10) is then [6],

¹The Gauss theorem or divergence theorem is a conservation theorem that relates the flow through a surface to the flow inside the surface. Intuitively, it states that the sum of all sources minus the sum of all sinks inside a surface, equals the net flow through the surface (whether outwards or inwards). The volume integral is equal to the surface integral over the boundary.

$$C(P)p(P) = \int_S (p(Q) \frac{\partial G(P, Q)}{\partial n} + jkz_0 v(Q) G(P, Q)) dS + 4\pi p^I(P) \quad (2.11)$$

Therefore, this equation relates as well the pressure and velocity at any point Q belonging to the surface S of the body (Q is on S), with any point P in the domain. $p(Q)$ and $v(Q)$ are respectively the sound pressure and vibration velocity at Q , $G(P, Q)$ is the free space Green's function relating Q with a field point P . z_0 is the characteristic impedance of the medium (ρc). p^I is the incident pressure in the case of a scattering problem (if the problem is purely a radiation problem the term p^I disappears).

This Boundary Integral Equation -BIE- (2.11), makes it possible to know the pressure at any point P in the domain. However, this equation should be implemented numerically in order to be solved. In general terms, equation (2.11) is discretized into elements along the body surface, and the equation is expressed as a matrix equation. By solving such matrix equation, the pressure on the nodes is calculated, that is the pressure throughout the surface of the body. Once that the pressure at the surface is known, the pressure at any field point can be as well obtained.

In this section, the numerical implementation of the BIE is not looked at, since the aim of it is just to illustrate and briefly explain some of the mathematical foundations in which the BEM is based (namely such an integral equation). For a more detailed explanation refer to ref. [5] [1] [8].

Chapter 3

Methodology

The aim of this project is to study the radiation by a loudspeaker cabinet, which is vibrating and radiating sound simultaneously with the loudspeaker units. There is the fundamental problem that it is difficult to measure the radiation from the loudspeaker cabinet, due to the fact that the loudspeaker units are radiating simultaneously. Hence, the BEM is a very appropriate solution to calculate the radiation from the cabinet (without the contribution of the loudspeaker loudspeaker units).

The method presented here can be used for other radiation problems involving a vibrating body, not only a loudspeaker cabinet. It is applicable to many other cases, and it is especially useful for problems in which the source of interest cannot be separated from other sources radiating simultaneously (i.e: automotive problems, machinery, etc).

In this section, the general procedure followed in order to calculate the sound pressure radiated by a loudspeaker cabinet is presented. Initially, a general description is provided, followed by a more detailed explanation of the measurements, testing and calculations carried out.

In order to determine the sound radiated by the loudspeakers cabinet with the BEM, it is necessary to know what is the velocity on its surface (it is the boundary condition of the problem). The velocity of the cabinet is measured directly. When the velocity is known, it is possible to calculate the sound pressure radiated by the cabinet (without the direct contribution of the loudspeaker units).

Some verification measurements are performed as well, in order to check that the calculations are correct and get a better understanding of the results. These verifi-

cation measurements consist, firstly of sound pressure measurements, and secondly of laser measurements on the loudspeaker membrane (to also calculate the total SPL with the BEM).

Therefore, the procedure used for the study can be divided into a measurement stage (which comprises both vibroacoustic measurements and verification measurements) and a numerical calculation stage, using the BEM.

3.1 Vibroacoustic Measurements

The vibroacoustic measurements are performed with accelerometers, placed directly on the surface of the body. A measurement mesh along the surface of the body is defined, consisting of a set of specific positions where the acceleration is measured. These positions (the measurement mesh) are the same as the mesh used for the BEM model. (See Sect. 5).

Generally, the effects of loudspeaker cabinets radiation manifest themselves primarily at the cabinet's resonance frequencies between 100 Hz and 300 Hz [2]. Concerning the resolution, the measurement mesh was designed so that all the modes up to more than 300 Hz can be measured and comprised in the study with sufficient resolution. For this purpose a preliminary modal analysis of the body is very useful. It is helpful to have an idea of how the vibration and the deflection shapes look like.

In the specific case of loudspeakers, the cabinet vibrates due to both structural excitation from the drivers and acoustic excitation from the pressure within the cabinet [9]. The effect from both sources of vibration, is inherently accounted for by the measurements of the normal velocity performed on the surface of the cabinet (BEM boundary condition).

3.1.1 Measurement mesh

The loudspeaker cabinet was measured at more than 100 different measurement positions. The lower section of the loudspeaker, where the woofer of the loudspeaker lies, was measured at four different heights. Each of the heights had between 16 and 18 positions around the circumference of the loudspeaker. The upper part (where the midrange unit lies), was measured at three different heights with 8 positions at each of the heights. Finally, the circumference just above the woofer, where the vibration levels are the highest, was measured in a finer mesh, consisting of 32 positions along the circumference of the cabinet. The measurement mesh is shown in the following figure 3.1 (note that the measurement mesh is the same as the BEM mesh shown in figure 5.3)

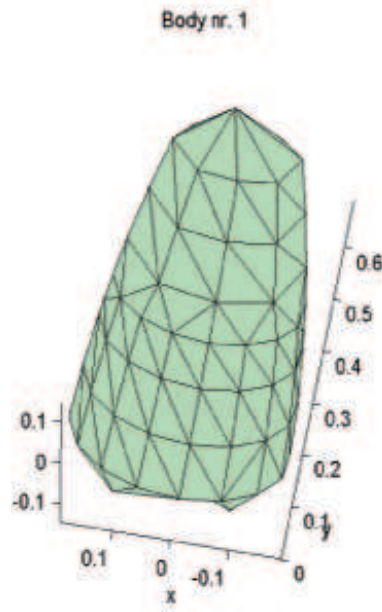


Figure 3.1: *Measurement mesh of the Beolab 9. The velocity was measured at every node of the mesh*

Generally, it can be said that the circumference of the speaker was “sampled” with at least 16 measurement positions (going up to 18 or 30 in some of the cases), and at four different heights. The upper part of the speaker, despite it is not vibrating with very high amplitudes was meshed with a similar resolution.

Based on the modal study carried out on the Beolab9 by Yu Luan [10], where the deflection shapes of the cabinet were looked at, it can be assured that the mesh is fine enough to go up to 300 Hz, with a resolution of approximately 6 measurement positions/nodes per wavelength. This measurement mesh assures that all the modes up to 300Hz are measured. However, the mesh can go up to higher frequencies (around 400 Hz and more), with less accuracy, but still providing acceptable results. In principle, using this measurement mesh, deflection shapes with up to three wavelengths in the radial direction of the structure ($n=3$) can be measured, with a resolution of 6 positions per wavelength (from [10] it can be seen that all the modes below 300 Hz have a maximum of 3 wavelengths per circumference).

An example of a deflection shape (309 Hz) of a conical cabinet, from Yu Luan’s work, is shown below [10].

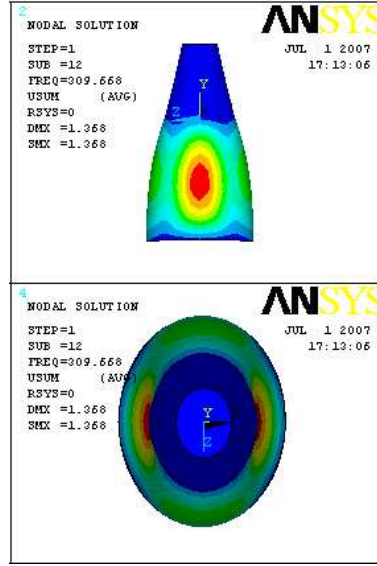


Figure 3.2: Example of the deflection shape of a conical cabinet at 309 Hz. Image from [10]

It should as well be remarked that the most efficient modes in terms of sound radiation from the cabinet are those in the lower frequency range, where big areas of the cabinet are vibrating in phase. The acoustic radiation from a cabinet affects the overall performance of a loudspeaker only at the lowest structural resonance frequencies of the cabinet, if at all [16] [2]. Therefore, the mesh designed is sufficient for the present study, considering the frequency range of concern.

3.1.2 Procedure of the measurement

When studying the sound radiated by a specific body, the phase information is essential (the phase information tells us how the different parts of the body are vibrating, and how the total sound radiation is built up with the contribution from each part of the body). Therefore, in order to have a reliable phase information, it is necessary to set a reference point in the body. Relative to this reference point, the phase of the rest of the measurement positions can be determined (the phase is calculated relative to the reference point). In other words, it could be said that the reference point has zero phase, and the phase of all the remaining positions represent the “delay” between the reference point and each position. It is essential that this reference is not placed in a nodal line in any of the modes of interest.

The general procedure for the measurement is the following: The magnitude of the acceleration of the reference point $|R|$, the magnitude of the acceleration of each position $|S|$, and the complex transfer function between both positions $\hat{H} = \hat{S}/\hat{R}$ are measured. Based on those three measurements, the complex acceleration at each position \hat{S} , which includes magnitude and phase information, can be obtained simply as:

$$\hat{S} = \hat{H} \cdot |R|$$

In the previous expression, \hat{S} is the complex acceleration of a measurement position (where the phase information is included, referenced to the reference point). A more thorough explanation of how to obtain it, is presented below:

Three quantities are measured:

- the magnitude of the velocity of the reference point: $|R|$
- the magnitude of the velocity of the measurement position: $|S|$
- the complex transfer function between the reference and the measurement position: $\hat{H} = |H|e^{j\phi_H}$

Considering that the magnitude of \hat{H} is $|H| = |S/R|$ and the phase is $\phi_H = \phi_S - \phi_R$, the complex transfer function can be expressed as:

$$\hat{H} = |H|e^{j\phi} = \frac{\hat{S}}{\hat{R}} = \frac{|S|}{|R|}e^{j(\phi_S - \phi_R)} \quad (3.1)$$

Since R is the reference, it has phase zero, therefore

$$\hat{R} = |R|e^{j\phi_R} = |R|e^0 = |R| \quad (3.2)$$

The previous equation also shows that the phase of the transfer function and the measurement position is the same, $\phi_H = \phi_S$.

From 3.1 and 3.2, it is straightforward to express the complex quantity \hat{S} as:

$$\hat{S} = \hat{H} \cdot \hat{R} = \hat{H} \cdot (|R|e^{j\phi_R}) = \hat{H} \cdot |R| \quad (3.3)$$

where \hat{S} is expressed only in terms of the measured quantities \hat{H} and $|R|$.

From the derivation above, it is clear that \hat{S} is the vibration at a certain position, with a certain magnitude and a certain phase relative to the reference. The phase has been referenced to a position of the cabinet (the reference point) instead of to the electrical input. The reason for this is the stability of the measurement. By not choosing the electrical reference, the influence of the phase distortion from the loudspeaker is prevented, and the possible error is smaller.

These measurements provide the vibration velocity information necessary for the numerical calculations to be carried out. They provide both the magnitude and the phase at every position. These measured velocities at every position will be input into the BEM, in order to calculate what is the radiated sound pressure from the body.

3.2 Verification measurements

There are some simple measurements that can be performed to verify the results obtained. These measurements are not essential for the calculations, but they are very useful for validation and for achieving a better understanding of the results.

3.2.1 Sound pressure measurements

According to what has been explained before, the SPL radiated by the body is also measured. This is done in order to compare the calculated sound pressure radiated by the body with the measured one. In the present study, the measurement corresponds to the total sound pressure radiated by the speaker, with both the contribution from the cabinet and the loudspeaker units.

Due to the fact that the BEM numerical study is done in an infinite medium, that is in the free-field, the measurements should be performed preferably under anechoic conditions (to avoid reflections from surfaces which are not accounted for in the numerical model). If the measurements were not performed under such anechoic conditions, the reflections from the surrounding bodies would influence the measurement.

3.2.2 Laser measurements

Another set measurements that could be performed for verification, involves measuring the velocity of the loudspeaker's membrane. Thus, the radiated pressure from the loudspeaker can be calculated with the BEM and be compared with the pressure measurements. These vibration measurements should be performed with a laser, since the accelerometers are too heavy compared to the membrane, and their load would affect the vibration severely.

3.3 Numerical calculations

The second part of the method is based in calculations by means of the Boundary Element Method. The numerical study was carried out using the OpenBEM¹ software [6]. ANSYS and Solid Works were as well used for the preprocessing of the model. In this section, the procedure to perform such calculations is explained.

Initially, a mesh is designed according to the geometry of the body. In this mesh, the vibration velocity at each node should be known, thus, it is measured as explained in 3.1. Each node of the mesh corresponds to a measurement position. Finally, the

¹OpenBEM is an open software based on Matlab, developed by Peter Juhl and Vicente Cutanda from the University of Southern Denmark, Odense

velocities are input into the BEM as the Boundary Conditions and the sound field is obtained.

In this specific project, the meshes were defined manually in ANSYS and afterwards exported to OpenBEM software. This manual procedure makes it possible to get a better control over the mesh geometry, and guarantees a fairly good correspondence between the actual body geometry and the mesh used for the numerical calculations (hence, it guarantees a good correspondence between the nodes and the measurement positions, which should be the same).

It is important to bear in mind the frequency range of interest, since a certain minimum resolution of the mesh is needed, in order for the results to be accurate enough. A minimum of 6 nodes per wavelength should be used. Such resolution generally provides enough accurate results and a sufficient small error [5]. Below this limit, the results are biased and can be severely affected. Above this resolution the results are more precise (generally, the higher the mesh resolution, the more accurate the results will be).

In this project, focused on the Beolab9 prototype, the frequency range of concern goes up to around 250 or 300 Hz, where the cabinet is radiating most significantly. The maximum element length was of approximately 0.1 m. A minimum density of 6 nodes per wavelength (wavelength in the structure, mainly in the circumferential dimension) was guaranteed for the frequency range of concern, which in principle is more than enough. However, the resolution of the mesh at low frequencies, where the radiation from the cabinet is higher, is much more fine (the deflection shapes are rather simple -no more than one or two wavelengths around the circumference of the loudspeaker- [10] so that the mesh resolution is very fine at the lower frequencies -much more than 6 elements/wavelength-). Thus, based on the wavelength of the vibration in the structure, the resolution of the mesh has been designed to provide enough accurate results.

Chapter 4

Preliminary testing

It is important to test the calculation method and the procedure, to make sure that the calculated sound pressure radiated by the loudspeaker's cabinet is correct. It is also important to examine the method in order to have a better understanding of the results. Therefore, testing is an essential stage of the project, prior to the final investigation. It provides the wanted verification and evaluation of the method.

4.1 Initial considerations

In this project, the sound pressure radiated by a loudspeaker cabinet is calculated. Since it is difficult to measure the cabinet's radiation separately, the calculations can not be verified by simple comparison with measurements¹. Therefore, a test case is very convenient, prior to the study of the loudspeaker's cabinet radiation itself.

The test case used for verification is a wooden box in which one of the walls is vibrating. This structure is in principle similar to a vibrating loudspeaker cabinet. In this case, all the sound pressure radiated is due to the vibration of the body itself, without any other source (such as the loudspeaker units). Thus, it is possible to compare the calculations with simple pressure measurements.

Another possible verification test is to measure the velocity of the loudspeaker units, via laser measurements. This would make it possible to calculate the total radiated pressure by the loudspeaker (cabinet + units) with the BEM, and compare it with sound pressure measurements. However, it is preferable to do the testing based on the

¹The sound pressure radiated by the cabinet cannot be measured directly by simple measurements because the loudspeaker units are radiating simultaneously.

vibration of the box structure rather than on laser measurements of the loudspeaker units. The reason is that we are interested in the radiation from the loudspeaker's cabinet, which is much lower than the radiation directly from the units. Thus, if the radiation from the units is included in the calculations, the weight of the cabinet radiation is minimized (and the weight of the units radiation is magnified). Furthermore, considering that the unit's radiation is calculated by a different procedure² than the cabinet's radiation, the test box case is a much more reliable verification. Nevertheless, the calculation including both the radiation of the cabinet and the units (laser measurements) will also be performed, since it is a useful verification of the results, but it is not the best test to verify the calculation method.

4.2 Description

The purpose of the test is to examine the method explained in Chapter 3 - Methodology. For that purpose, the method is used to calculate the pressure radiated by a vibrating box and compare the calculations with measurements.

The box used for the testing is a cubic box of $46 \times 46 \times 46 \text{ cm}$, made of five rigid wooden plates, and a sixth plate on top. This latter plate is a 1 mm thick aluminum plate with an inertial exciter attached in the center which excites the plate causing the vibration. The test-box structure is shown in Figure 4.1.



Figure 4.1: *Test Box used for the verification of the procedure*

²The sound pressure radiated by the unit is measured via laser measurements, instead of accelerometers.

The box is a convenient test structure for the method used in the project. If the modeling body was a simple plate (instead of a box), near singular integration would be involved in the calculations. If the box is present, such near singular integration is not necessary, and the problem is simpler and more similar to the loudspeaker cabinet case.

Modeling the box is rather straightforward due to its simple geometry. The meshing has been done using triangular elements (SHELL63 in ANSYS) with a maximum distance between nodes of 14cm . As it will be explained in section 4.3 the top frequency limit of the calculation, due to resolution considerations, is approximately 150Hz . The maximum “usable” frequency range of the box in the testing reaches to approximately that same frequency $150\text{-}200\text{ Hz}$ (because due to the input levels used in the inertial transducer in order to produce the wanted SPL, the transducer is overloaded, giving rise to much distortion, especially above 200 Hz).

The BEM mesh of the test-box is shown in Figure 4.2

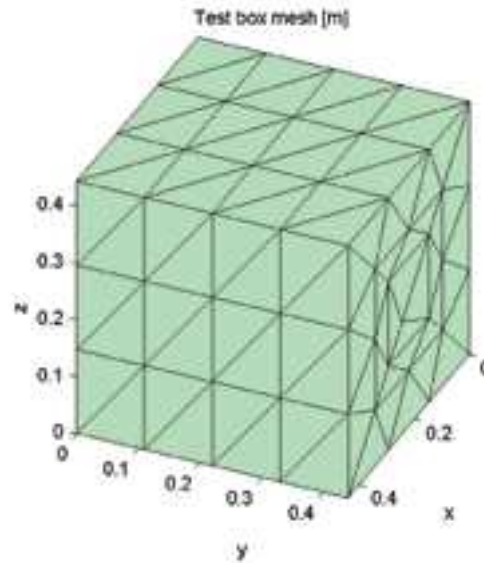


Figure 4.2: *Mesh of the test box used for the BEM calculations. The maximum element length is of 16cm*

The measurement has been performed as explained in Chapter 3-Methodology. A block diagram of the measurement setup is shown in figure 4.3

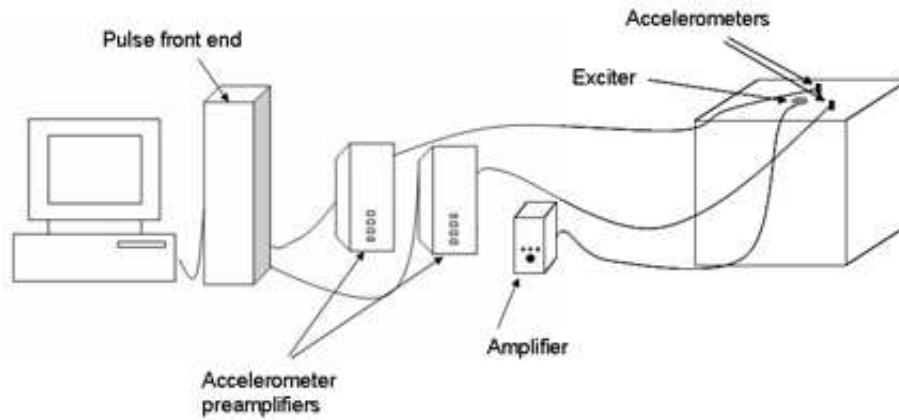


Figure 4.3: *Block diagram of the measurement*

The normal velocity of the box has been measured at every node, via vibroacoustic measurements. Both amplitude and phase have been measured. The reference point was set near the exciter, because at that position all the modes are present.

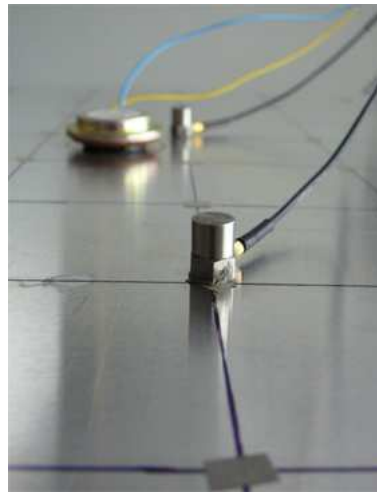


Figure 4.4: *Image of the measurement*

The velocity of every single node is measured (one measurement per node of the mesh). The measured data is input in the calculations as the normal velocity boundary condition. Using the BEM, based on such measurements, the sound field in the domain is calculated and the sound pressure at any point around the box is known.

In the BEM calculations, anechoic conditions are assumed (free-space); in other words, no reflections are taken into account. The sound pressure measurements, in order to be consistent with such anechoic conditions, have been performed inside an anechoic chamber. Thus, for the sake of comparison, calculations and measurements

are carried out under similar conditions.

4.3 Results

In Figure 4.5 the measured sound pressure and the sound pressure calculated with the BEM are shown.

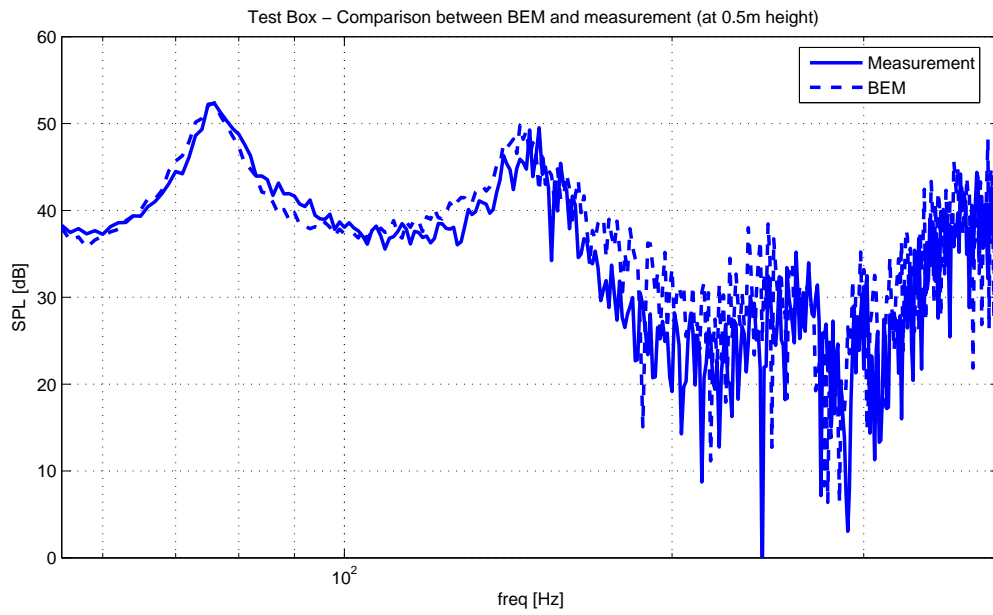


Figure 4.5: Comparison between the BEM calculation and the measured SPL

The agreement between calculations and measurement is generally very good, especially at low frequencies.

At higher frequencies the deviations are larger. This is related to the resolution of the mesh. Based on some preliminary study of the wavelengths and natural frequencies in the structure, and according to the rule of thumb of 6 nodes/wavelength, it can be assumed that the top frequency limit of the calculation is below 150 Hz. This frequency (actually 140 Hz) corresponds to the (1,3) mode of the plate, which has a resolution of approximately 6 nodes/wavelength. Above this frequency, the resolution of the mesh is not sufficient compared to the wavelengths in the structure, and greater deviations occur as the frequency increases, especially above 180 Hz (where the resolution of the mesh is becoming very coarse compared to the wavelength dimensions).

Apart from the coarser resolution of the BEM mesh, another explanation for this

greater deviation at higher frequencies (above 150 Hz) is the distortion of the box-transducer. This is apparent from the rapid fluctuations in the frequency response from 180 Hz on (the sound is very distorted in this frequency range). In the low frequency range, where these fluctuations are less rapid, the calculations are very precise. However, the overall agreement is good. If the box was behaving more linearly, the agreement between measurement and calculations would be expected to be even better.

The load of the accelerometers was also considered and examined. The normal velocity of the plate was measured with and without the load of an accelerometer, that was attached at different positions. In principle it did not affect the vibration of the plate of the box importantly.

4.4 Conclusion

A preliminary test was performed to verify that the calculation method used in the project is valid. The results of this test are satisfactory. The agreement between measurements and calculation is fairly good, especially at low frequencies, in the frequency range where the mesh satisfies the 6 nodes/wavelength resolution. The method has been proved to be appropriate for the purpose of this project, to the sound radiation of a vibrating loudspeaker cabinet.

Chapter 5

Preprocessing and Measurements

In this section, the Boundary Element Method preprocessing required for calculating the radiation from a loudspeaker's cabinet is presented. The specific case of the B&O Beolab 9 cabinet is investigated.

In first place, the geometry and the meshing of the cabinet's model is presented. Some testing of the mesh is also shown in this section. The Boundary Conditions of the problem are as well examined. The required set of Boundary Conditions consists basically of the velocity of the cabinet surface, which is obtained from empirical vibroacoustic measurements. Such measurements are briefly explained in this section. After this preprocessing stage, the problem can be solved with the BEM.

In short, this section focuses on the specific case of study of the Beolab9. It basically presents the BEM preprocessing prior to the solution of the problem.

5.1 Geometry

The loudspeaker modeled in this study is an early prototype of the Beolab9 loudspeaker manufactured by Bang & Olufsen. The loudspeaker is shown in Figure 5.1.

The cabinet has a characteristic curved shape, with an elliptical cross-section all along its height, which is narrowing from the bottom to the top resembling somehow a conical shape. There are three drivers in the speaker, a woofer and a midrange unit placed directly on the surface of the cabinet, and the third driver is a tweeter placed "on top" of the speaker, in the Acoustic Lens[©] device.



Figure 5.1: *Beolab9. Side view (left). Top view (centre). View without the screen cover (right)*

The actual cabinet of the loudspeaker is shown on the right side of Figure 5.1 (in the other two figures, the cabinet is covered with a screen, which is the exposed visible part). The cabinet is the structure to which the vibration of the driver is transmitted, and presumably it is radiating sound.

The cabinet surface is basically smooth, except for the cavities to which the drivers are attached. However, for simplicity, these irregularities in the geometry are disregarded in the modeling and the cabinet shape is simplified. Since the frequency range of concern is basically low frequency (up to about 300 Hz), the shortest wavelength considered is of more than $1m$, and these irregularities can be neglected without any significant effect. Thus, the geometry can be simplified to a smooth cabinet, as shown in Figure 5.2.

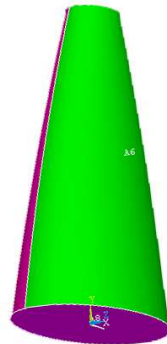


Figure 5.2: *Beolab9 simplified geometry in which the mesh was based*

5.2 Meshing

The mesh is designed using triangular elements (of three nodes per element). The type of element used is SHELL63 (in ANSYS), triangular element of six degrees of freedom at each node (see Appendix D). The element sizes vary along the surface. The resolution of the mesh is finer around the woofer. The mesh is shown in Figure 5.3 ¹.

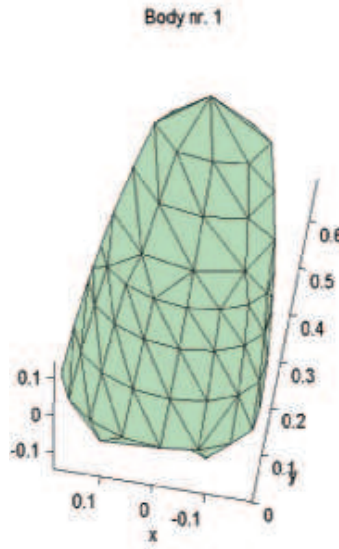


Figure 5.3: *Meshing of the Beolab 9 used for the BEM calculations*

The maximum dimension of the elements (the maximum separation between nodes) is of 13cm . According to the rule of thumb of 6 elements per wavelength, with this mesh, considering the deflection shapes of the cabinet (see [10]) the resolution of the mesh is sufficient below 300 Hz. The frequency range of concern goes up to no more than this 300 Hz limiting frequency.

Depending on the number of wavelengths in the structure around the circumferential dimension, the resolution of the mesh is different. The mesh provides a minimum resolution of about 18 nodes/wavelength if there is one wavelength in the structure ($n=1$) in the circumferential dimension. If there are two wavelengths ($n=2$) around the circumference, it provides a resolution of 8 to 10 nodes/wavelength. If there are three wavelengths ($n=3$) in the structure, it provides a resolution of 5 to 6 nodes/wavelength. Above this limit, the resolution is coarser (but the frequency range of concern is nevertheless below it).

¹Note that the BEM mesh is the same as the measurement mesh

Therefore, the meshing used is more than sufficient for the frequency range of interest up to 300 Hz. Below this frequency limit, the resolution of the mesh is more than sufficient.

The mesh was created manually in order to have a better control of the node coordinates and achieve a better correspondence between the BEM mesh and the measurement positions (since the velocity at each node is measured in order to determine the Boundary Conditions). Therefore, it is important to make sure that the coordinates of each measurement position match with the coordinates of each of the nodes.

The mesh was created in ANSYS, and afterwards exported to OpenBEM (in Matlab), where the calculations were carried out.

5.2.1 Testing of the mesh

Once the mesh has been created, it is important to verify that it is working properly. For this purpose a simple test was carried out. The test consists on placing a point source in the origin of coordinates, and evaluate what the velocity is in the normal direction at each node (in other words, calculate what is the normal velocity produced by the point source at each node). Using those velocities as the set of Boundary conditions, the sound pressure calculated by the BEM should equal that of the point source calculated analytically.

Expressed in a more intuitive way, it could be said that the test consists on calculating what is the pressure produced by a point source with the BEM, using the mesh as a "midpoint" to verify that it is indeed "working" properly. The BEM results are then compared with the analytical solution.

Figure 5.4 presents the results of the test. It is apparent from it that the mesh is working properly, and that its resolution is clearly sufficient. The BEM results agree with the analytical solution, and the error is very small. In the frequency range of main interest, the error is sufficiently low. At 200 Hz the error is below 2.5% and at 300 Hz it is below 5%. At 400 Hz (frequency which is already out of the main range of interest) the error is still below 10%. On the other hand, above 500 Hz, the mesh resolution is not sufficient, and the results from the calculations break down (the error at 700 Hz is of about 25%).

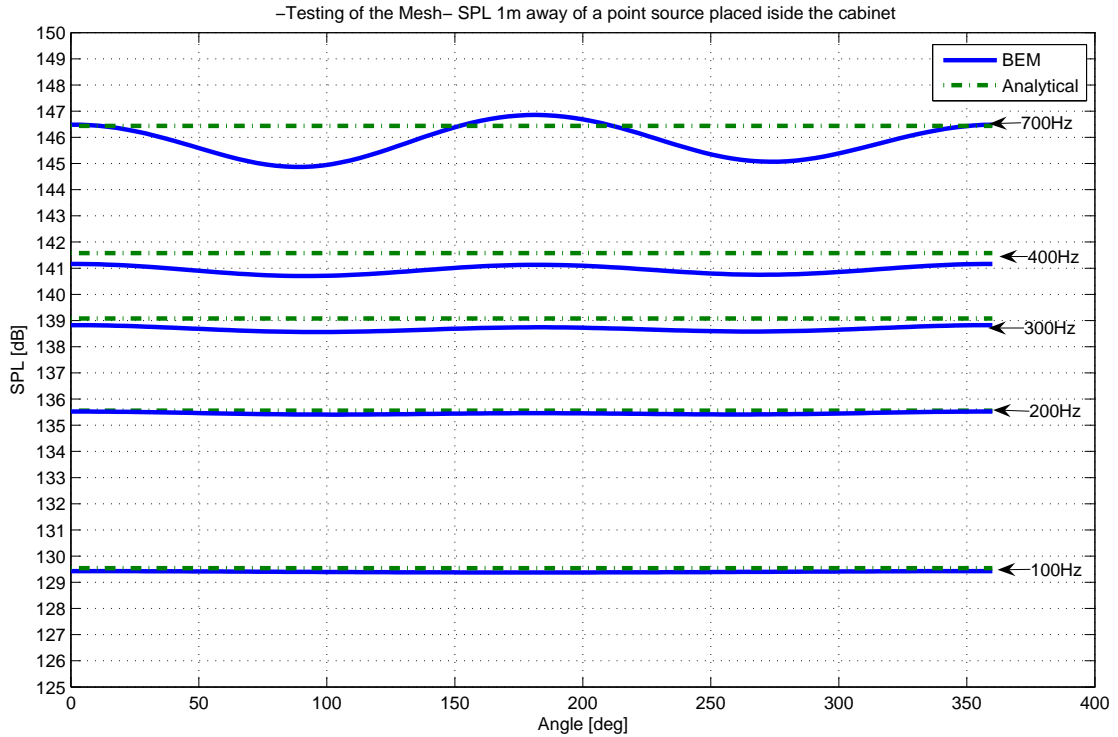


Figure 5.4: *Testing of the mesh. Sound pressure produced by a monopole placed at the origin. The figure compares the sound pressure calculated analytically and with the BEM using the loudspeaker mesh, for different frequencies.*

The mesh has been shown to be working properly, and according to the previous discussion, its resolution is appropriate for the case of study in this project.

5.3 Boundary Conditions (Measurement)

As it has been explained in Chapter 3 (Methodology), the Boundary Conditions of the problem have to be determined via vibroacoustic measurements. In a radiation problem such as the present, the boundary conditions consist of the velocity on the surface of the radiating body. In the present case we are interested in the velocity of the loudspeaker cabinet. This vibration velocity should be measured.

The detailed procedure of the measurement, and the measurement method have been explained in section 3 (method). Here, only the setup used for measuring the loudspeaker cabinet's velocity is briefly explained.

As mentioned previously, the measurement grid (the measurement positions) along the loudspeaker cabinet's surface, should be the same as the nodes of the BEM mesh.

In principle the velocity at each node is measured. Thus, there are 100 measurement positions and a reference position (used to determine the phase of the vibration. See Chapter 3 (Methodology)). It is important that the coordinates of the measurement positions and the coordinates of the nodes are the identical.



Figure 5.5: *Some pictures of the vibration measurement*

The reference position is selected to be just above the woofer, because the vibration levels are dominant there and in principle every mode is present in that position.

A block diagram of the measurement is shown in Figure 5.6

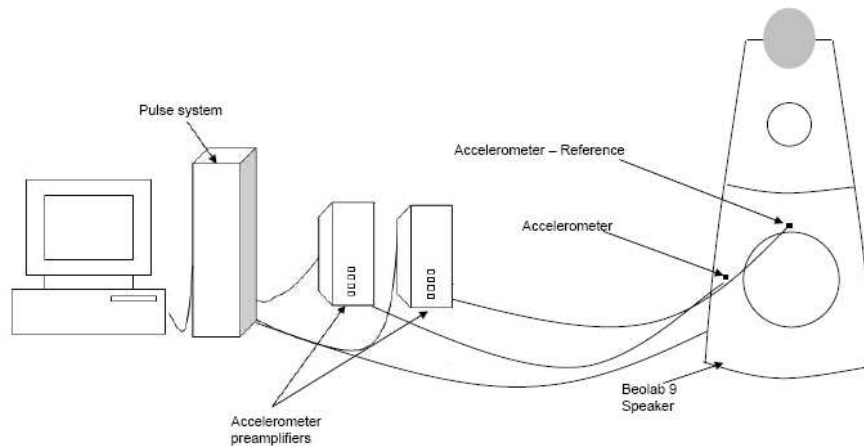


Figure 5.6: *Block diagram of the vibration measurement*

The type of excitation used for the measurement was pseudorandom noise, with a frequency span of 800 Hz and 800 lines. In this case, it is very convenient to use such an excitation signal, due to the great amount of measurement positions involved (more

than 100 positions). Pseudorandom noise measurements optimize very much the time required for performing the measurements.

5.3.1 Laser measurements

In order to measure the velocity of the loudspeaker membrane, laser measurements are required. Accelerometers cannot be used because the membrane is very light, and their load would affect severely the vibration.

Based on the laser measurements, the total sound pressure radiated by the speaker (cabinet + drivers) can be calculated with the BEM. These calculations can be compared to the sound pressure measurements, for verification. It is interesting to inspect the accuracy of the calculation of the total sound radiated by the speaker.

5.3.2 SPL measurements

Besides the vibroacoustic measurements, sound pressure measurements were also carried out, in order to compare the calculations with the measurements, and have an idea of what is the contribution of the cabinet, relative to the total radiated pressure.

The idea is to measure the total sound pressure radiated by the loudspeaker (both drivers and cabinet), and compare it with the calculations. In order to do so, it is necessary to measure under anechoic conditions, since for the BEM calculations free-space is assumed (no reflections from other bodies). The pressure measurements were therefore done in an anechoic chamber, to provide such free-space condition.

5.3.3 Measurement tests, validation tests

The results from the measurements were carefully processed and examined, position by position. Apart from the calibration of the transducers, all the measured positions were compared with the reference to make sure that the order of magnitude was correct and that there were no errors in the measurement that could bias the results. There were no apparent errors present in the data.

Estimation of the maximum expected pressure

Based on the vibration measurements, the maximum expected pressure radiated by the cabinet can be estimated. Since the velocity on the surface of the body is known, by evaluating the volume velocity of the body, the radiated sound pressure can be estimated.

The estimation was done to have an idea of the order of magnitude of the radiated sound pressure. By doing so, the BEM calculations can be compared with the estimation, to make sure that they are in the same range.

The volume velocity is expressed as the particle velocity u times the surface S :

$$Q = Su \quad (5.1)$$

The volume velocity of the body can be approximated by multiplying each node velocity by the surface around it. It is a discrete space approximation in which the area surrounding each node is assumed to be vibrating with similar velocity. The loudspeaker surface is therefore approximated by 101 surface “cells”. Since the frequency range of concern is very low, this approximation is sufficiently accurate.

Once the volume velocity Q has been determined, the sound pressure radiated can be also determined by

$$p = \frac{j2\pi f \rho Q_{cab}}{4\pi R_{fp}} e^{-jkR_{fp}} \quad (5.2)$$

where Q is the volume velocity, R_{fp} is the distance to the field point (the point where the sound pressure is calculated), f and k are the frequency and the wavenumber respectively. Therefore, it is straightforward to estimate the sound pressure radiated from the body (the loudspeaker cabinet in this case).

The maximum expected radiation of the Beolab 9 cabinet (for an input of 100mV amplitude broadband noise), is of approximately **46.5dB** at 85 Hz and at 150 Hz. In principle, considering the vibration velocity levels, it is a reasonable result.

This volume velocity approach is accurate if the velocity of all the positions is in phase and the structure is smaller than a quarter of a wavelength in air. In the present test, the low frequency condition is fulfilled. However, the velocities of all points are not vibrating in phase. At the low frequency modes, which are the ones radiating the most, the whole cabinet is vibrating almost in phase, so the estimation of the SPL is reasonably good, but it is still overestimated by 3 or 4 dB (as will be apparent in the following Chapter 6).

5.4 Solution

Once the geometry and the meshing have been made and verified, and the necessary set of boundary conditions for the problem have been measured, the problem can be solved using the BEM. With the information collected, the sound pressure radiated by the cabinet can be predicted at any point of the domain. The BEM software used is OpenBEM, a software based on Matlab codes, developed by P.Juhl and V.Cutanda, freely distributed by them [6].

The details on the implementation of the BEM and the computation process are out of the scope of this report. Only the results of the BEM study are presented. The codes produced in order to solve the problem using the BEM are included in Appendix C (codes of Matlab). Some explanation is found in the comments of the codes. The steps followed, the general procedure and the ideas behind the Matlab codes are reflected in the comments.

Chapter 6

Results

The aim of this project is to evaluate the contribution of the cabinet to the overall sound radiated by the loudspeaker. In the present chapter, the results of the study are presented and discussed.

In first place, the results from the measurements performed on the cabinet's surface are presented. Subsequently, the results obtained from the BEM calculations are examined. These results calculated with the BEM show what is the actual radiation from the loudspeaker's cabinet. Therefore, they are essential in understanding the contribution from the cabinet to the total radiated sound. Based on these results, the problem is analyzed in both frequency and time domain. The sound radiated by the cabinet is compared to the sound by the loudspeaker unit and to the total sound radiated by the loudspeaker. Moreover, some additional measurements concerning the non-linear behavior of the cabinet were done. However, these linearity measurements are presented in Appendix A, since they are not the main focus of the study, but they are nevertheless useful to understand better the problem studied in the present project.

For the sake of simplicity, from this point on we will refer to:

- the loudspeaker's cabinet as “cabinet”
- the loudspeaker's unit as “unit”
- the whole loudspeaker, consisting of both unit and cabinet as “loudspeaker”

6.1 Results from the vibration measurement

In this section, the results from the vibration measurements are presented. As explained in Chapter 5, the vibration on the loudspeaker's cabinet was measured at

more than 100 positions (according to the measurement mesh designed). By analyzing the vibration data obtained from the measurements, it is possible to get an idea of which frequencies might be contributing more to the sound radiated by the cabinet, which positions are vibrating with greater amplitudes, etc. In general terms, these vibration data provide a first idea about how the vibration and the actual radiation from the cabinet is.

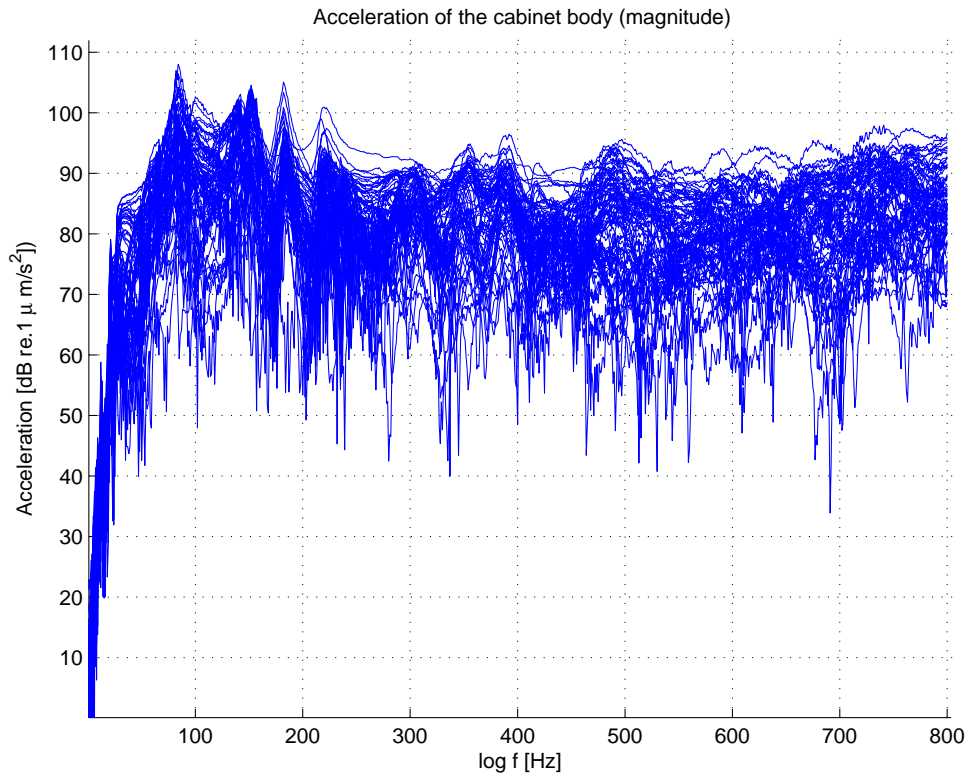


Figure 6.1: *Acceleration on the cabinets surface at all the measurement positions*

From Figure 6.1, it is possible to localize the natural frequencies of the cabinet and to know at which ones it is vibrating with greater level. Such an investigation provides an idea of the frequencies that could be more relevant to the sound radiation. In principle, the main concern is in the low frequency modes (since their radiation efficiency is expected to be greater).

It is straightforward to localize the main frequencies of vibration. Based on the data of figure 6.1, the main frequencies concern are 85 Hz, 145-150 Hz, 185 Hz and 220 Hz.

An investigation on the deflection shapes of some natural frequencies was done. By looking at the normal velocities at different positions, it was apparent that at low frequency the cabinet is vibrating almost in phase, as a whole. Contrarily, at higher frequencies the phase starts to change along the structure, and the deflection shapes become more complicated.

In Appendix B, the deflection shapes of some modes of the cabinet are presented. At 85 Hz and below, the cabinet is vibrating in a “pulsating mode” like shape. At 150Hz, the deflection shape resembles the one of $n=2$ circumferential modes (the front and the back of the cabinet are vibrating in phase, while the sides are vibrating in anti-phase with the front and back). Even though the deflection shapes are not clearly defined (they do not correspond to the analytical standard shapes of simple cylindrical bodies), it is interesting to see how the cabinet is vibrating at different natural frequencies.

These results just provide an initial idea of the vibration levels, the deflection shapes, what are the main frequencies that could be problematic, etc. This is useful information, but it is no more than just a first insight in to the vibration, the investigation of the cabinet’s sound radiation -based on BEM calculations-, is presented in the following sections.

6.2 Sound pressure radiated by the loudspeakers cabinet

Based on the vibration measurements on the surface of the loudspeaker's cabinet, the sound pressure level radiated by the cabinet has been calculated with the BEM, as explained in Chapter 3. The details about the preprocessing of the BEM model are included in Chapter 5. In the present section, the results of the calculation are presented and discussed.

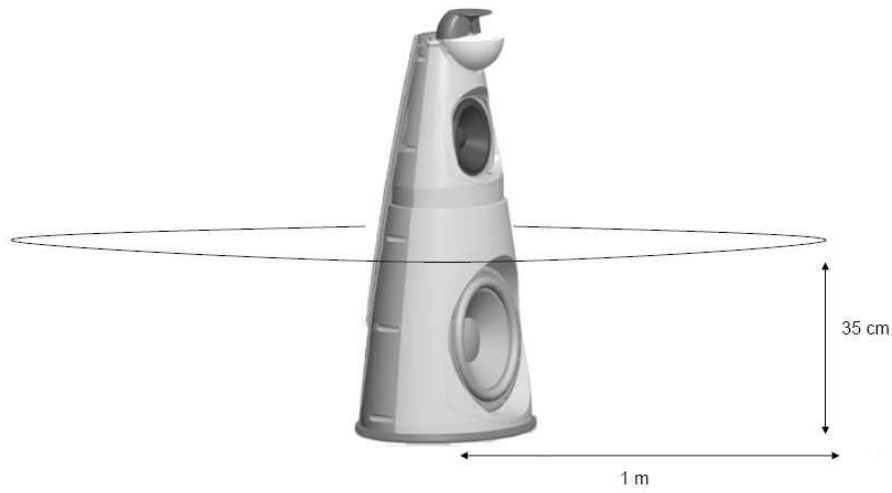


Figure 6.2: *Field points at which the sound pressure was calculated*

Figure 6.2 shows the field points defined in the domain at which the sound pressure has been calculated. These field points are set around the azimuth angle (with a resolution of 1 degree) at 1 meter distance from the radial direction and 35 cm height. The calculation has been done for frequencies from 50 to 400 Hz (with 1 Hz resolution).

The sound pressure radiated by the cabinet is presented in a surface plot, showing the SPL against the frequency and the polar angle (azimuth angle). The color corresponds to the SPL. The phase can be plotted in a contour plot, where each line is an isobar -all points of each line have the same phase-. Each transition between isobars corresponds to a $\pi/4$ change in the phase.

Figures 6.3 and 6.4 show both the magnitude (in dB) and the phase of the sound pressure.

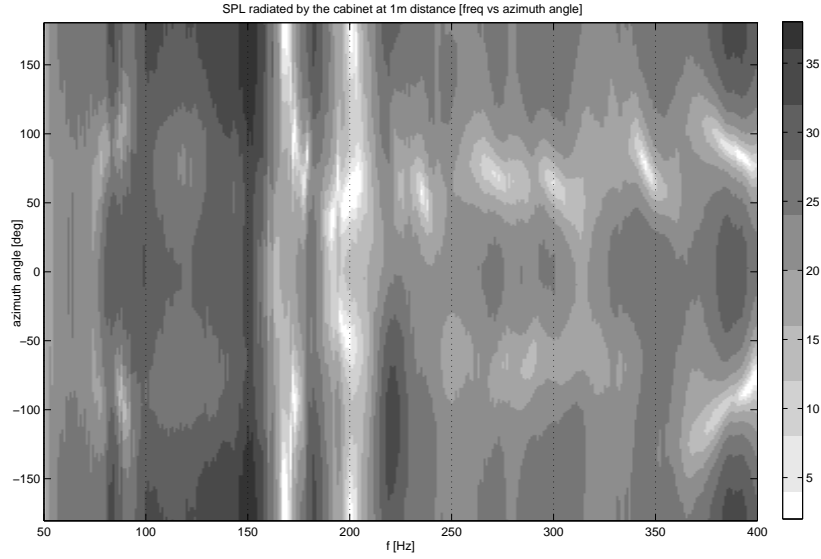


Figure 6.3: *SPL radiated by the loudspeakers cabinet, at 1m distance and 0.35 m height, around the azimuth angle (polar angle around the loudspeaker)*

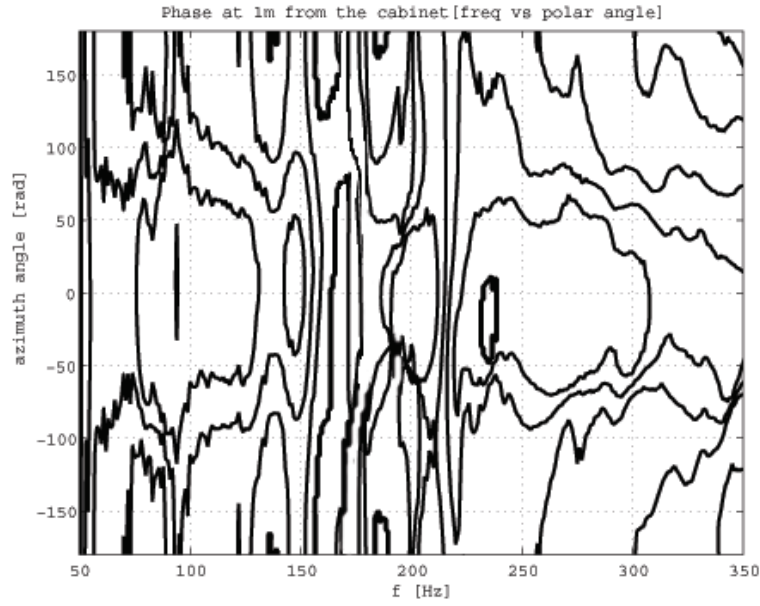


Figure 6.4: *Phase of the pressure radiated by the loudspeakers cabinet, at 1m distance and 0.35 m height around the azimuth angle. The isobars represent a $\pi/4$ phase change*

From Figure 6.3 it is evident that the highest sound pressure levels are in the frequency range between 80 Hz and 180 Hz. The sound pressure is particularly high at 150 Hz, 85 Hz and 180 Hz. However, the most important sound radiation is at 150

Hz. The highest sound pressure levels are found towards the back of the cabinet. The results presented here agree with conclusions drawn from the data shown in figure 6.1.

Based on the previous results, the frequencies at which the cabinet is radiating the most have been identified. They can be plotted in a more conventional polar plot, which shows the SPL along the polar angle (“around” the cabinet).

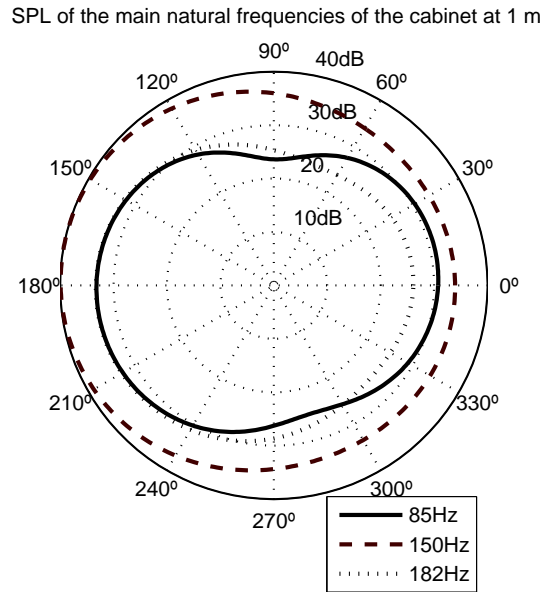


Figure 6.5: *SPL radiated by the loudspeakers cabinet, along the polar angle at 1m distance. 85 Hz (solid), 150Hz (dashed) and 182 Hz (dotted)*

6.3 Radiation by the cabinet compared to the total radiation

In order to estimate the contribution of the cabinet to the radiated sound, it is important to know the total radiation from the loudspeaker. In this section, the total sound pressure radiated by the loudspeaker is compared to the one radiated by the cabinet.

While the cabinet radiation has been calculated with the BEM (it is the same as in the previous section 6.2), the total sound pressure from the speaker has been measured in an anechoic chamber - achieving the “free-space” condition also assumed in the calculations -.

For the following comparison, three positions (three field points) are used as observation points. Those positions are placed in the front, the side and the back of the loudspeaker, at 1 m distance in the radial direction and 0.35 m height from the ground.

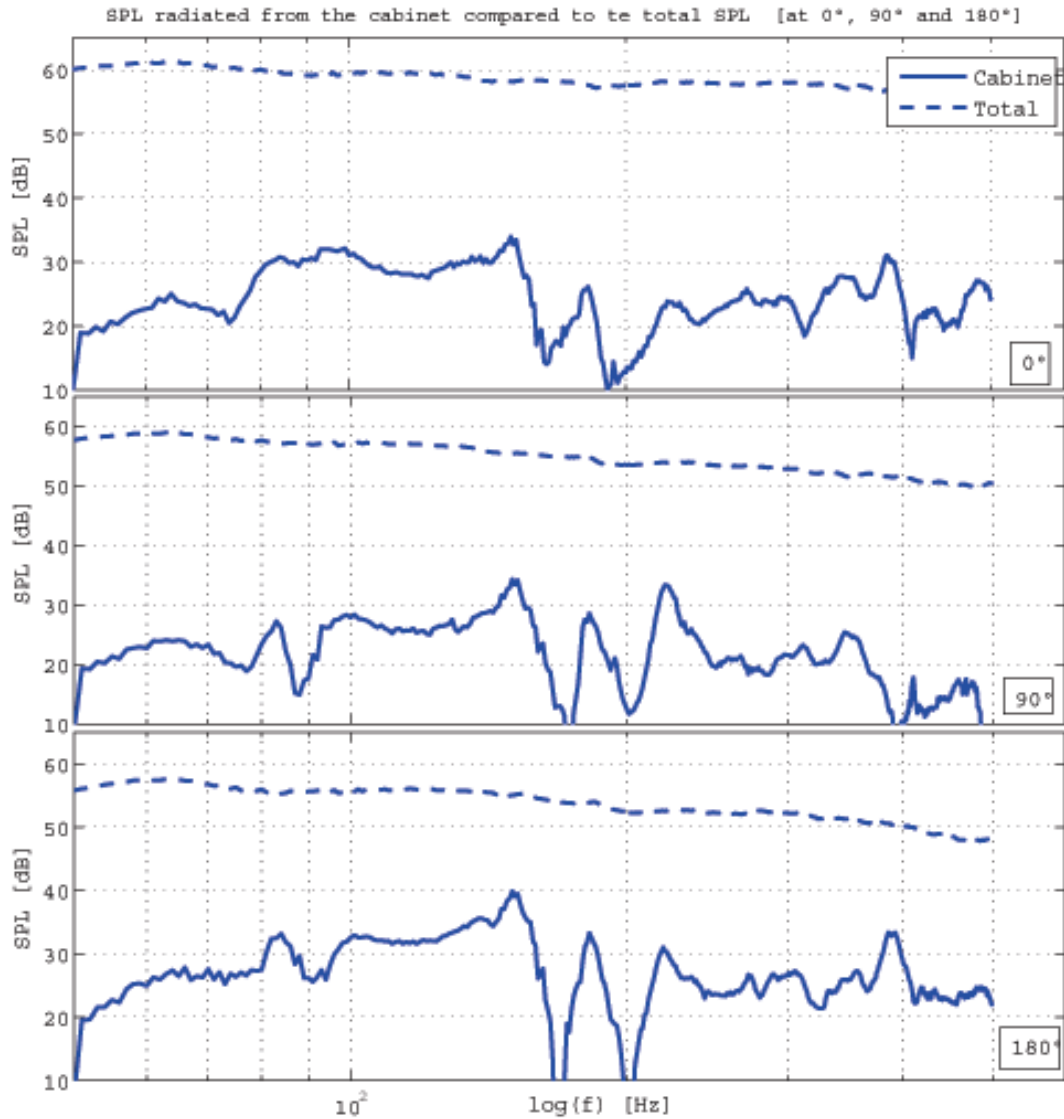


Figure 6.6: *SPL radiated by the loudspeakers cabinet, at 1m distance, compared to the total radiated pressure by the loudspeaker. The top figure shows the radiation in the front direction -0°-, the medium figure shows the lateral radiation -90°-, and the bottom figure the back radiation -180°-*

Figure 6.6 shows the radiation from the cabinet compared to the total radiated pressure. It is obvious that the radiation by the cabinet is in all cases much lower than the total sound pressure. Thus, the influence of the cabinet does not seem too significant in terms of magnitude. The most important contribution from the cabinet can be found in the back of the loudspeaker, in the frequency range between 80 and 150 Hz.

For a more clear comparison of the radiation from the speaker and the cabinet,

the results can be summarized in one same plot. In such plot it is apparent how the radiation from the cabinet and the loudspeaker is changing differently depending on the position of the observation point.

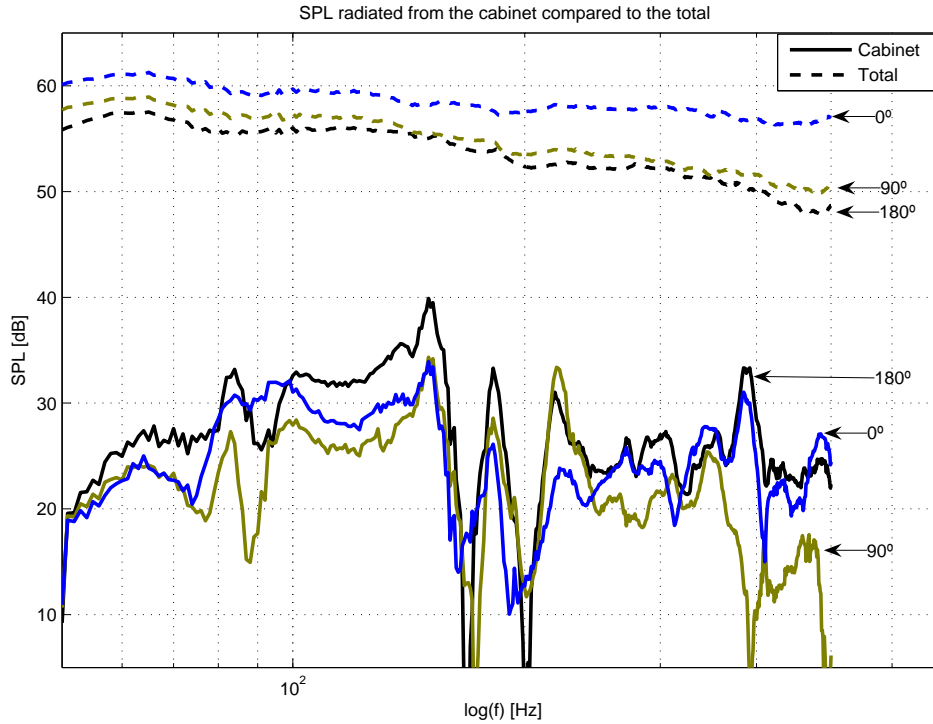


Figure 6.7: *SPL radiated by the loudspeakers cabinet, at 1m distance, compared to the total radiated pressure by the loudspeaker. The front (blue), lateral (green) and back (black) radiation are plotted together*

It is obvious from figure 6.7 that the main radiation from the cabinet is taking place in the front and in the back of the cabinet.

Results presented in section 6.2 and in figures 6.6 and 6.7 indicated that the radiation from the cabinet is greater in the back. Contrarily, the sound radiation of the loudspeaker is weaker in the back¹. The combination of this two facts, result in an increased influence from the cabinet towards the back of the loudspeaker.

Summarizing the results of this section, it should be highlighted that the SPL radiated by the cabinet is much lower than the total radiated sound. However, the greater radiation from the cabinet and the weaker radiation from the speaker towards the

¹These two facts are reasonable if we consider that most of the front area of the loudspeaker is “occupied” by the loudspeaker units, while most of the cabinets net surface is in the back of the speaker.

back, result in a higher contribution from the cabinet at the back than at the front. This contribution at the back of the cabinet seems to be the most important one, and it could affect to some extent the total radiation from the speaker.

These results agree with those in refs. [9], [2] and [16]. However, there is a fundamental difference with ref.[9], since in their study, the contribution of the cabinet was greater on axis (in front of the loudspeaker). This difference may be related with the geometry of the cabinet, since their work focused only on rectangular shapes, where the vibration transmitted to the back would be different than in the case of a curved “elliptical” cabinet. Also the different radiation efficiency may be of importance. However, this hypothesis should be further investigated.

6.4 Contribution from the cabinet to the radiated sound

In the previous section, the radiation from the cabinet was compared to the total radiated sound by the loudspeaker. It is clear that such a comparison is important in order to get an idea of how the cabinet could influence the “final” sound radiated by the loudspeaker. The results presented so far are useful, but it is difficult to withdraw certain conclusions from them. In this section, a more thorough approach to the problem is formulated.

The total radiated sound by the loudspeaker can be determined by simple sound pressure measurements (as was done in the previous section). However, another interesting approach is to calculate the total sound radiation with the BEM. In this case the calculations are based on the velocity of the loudspeaker unit, which is measured via laser measurements (to avoid the influence of loading the membrane with accelerometers).

Using the BEM, both the total pressure by the loudspeaker (including the radiation from the cabinet and the loudspeaker unit) and the pressure radiated only by the unit (as if the cabinet was completely rigid) can be calculated separately.

In the present study, both pressure measurements and BEM calculations have been carried out and compared. Using the BEM, the pressure radiated by the cabinet, by the loudspeaker units, and by the whole loudspeaker (cabinet and units) has been calculated. These calculations are compared to the measurements of the total pressure as well. The observation points used for the study were in the front, the side and the back of the loudspeaker, at 1 m distance and 0.35 m height. In this section mainly the results obtained for the front and the back positions are shown.

It should be noted that the BEM calculations require some more time than the pressure measurements -since they involve laser measurements and the calculations

themselves-, but they render it possible to obtain results which would not be easily acquired otherwise. It is also very interesting to compare the BEM calculations with the measurements, and it is a very useful verification tool.

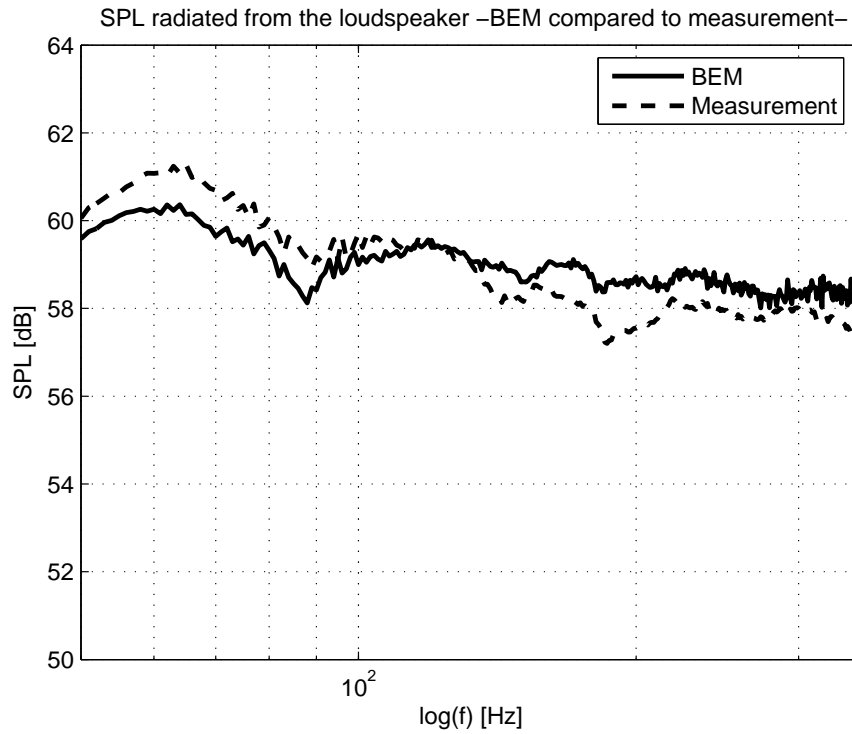


Figure 6.8: Comparison of measurements and BEM calculations of the total radiation from the loudspeaker. The observation point is in **front** of the loudspeaker at 1 m distance and 0.35 m height

In Figure 6.8, the total pressure radiated by the loudspeaker in the front direction is presented, where both calculated and measured pressure are plotted. It seems that there is a very good agreement between measurements and calculations, with a maximum difference of 1 dB SPL.

In the case where the observation point is placed in the back of the loudspeaker (Figure 6.9), measured and calculated results are rather similar, but the agreement is not as good as it was at the front of the loudspeaker (Figure 6.8).

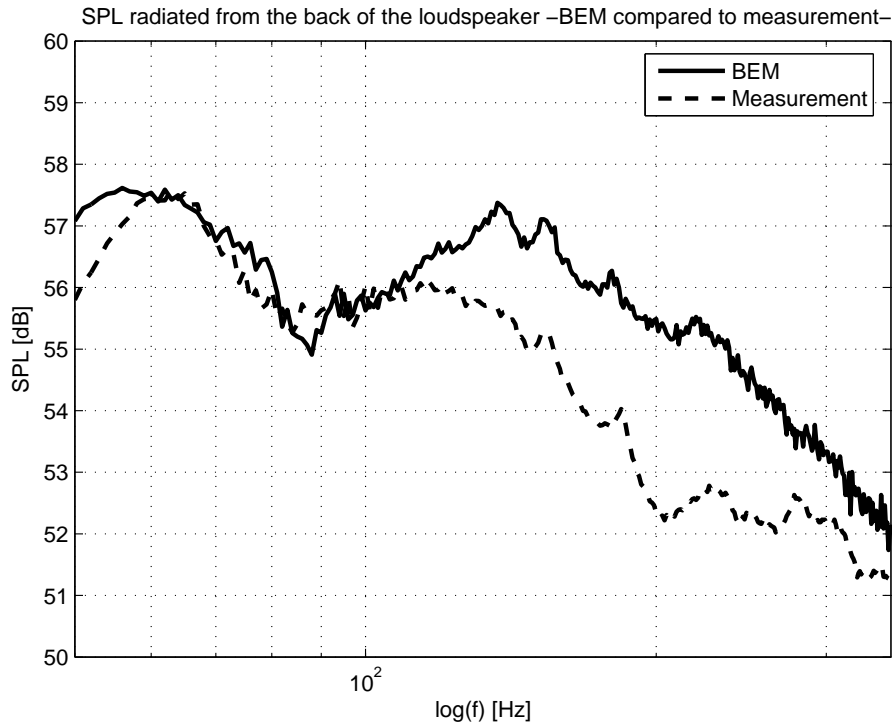


Figure 6.9: Comparison of measurements and BEM calculations of the total radiation from the loudspeaker. The observation point is in the **back** of the loudspeaker at 1 m distance

At the back of the cabinet (Figure 6.8), the agreement is generally good, particularly at low frequencies. However, there is a significant deviation around the 200 Hz frequency range, where the measured pressure is 3 dB lower than the calculations. This can be explained by the fact that the measurements were not performed in a strictly free-space condition (free of any sort of reflections). The loudspeaker was standing on a platform surface (instead of being suspended in the air), thus being sensitive to reflection paths from the platform. The lower sound pressure around 200 Hz seems to be caused by a “ground reflection” from the platform². However the agreement is fairly good, and despite the amplitude difference, both curves follow quite similar fluctuations.

²It is apparent from figure 6.8 that the reflection from the platform is not so present in the measurements in the front of the speaker, because in this case it was placed in the edge of the platform, not giving rise to the possibility of important reflections from it.

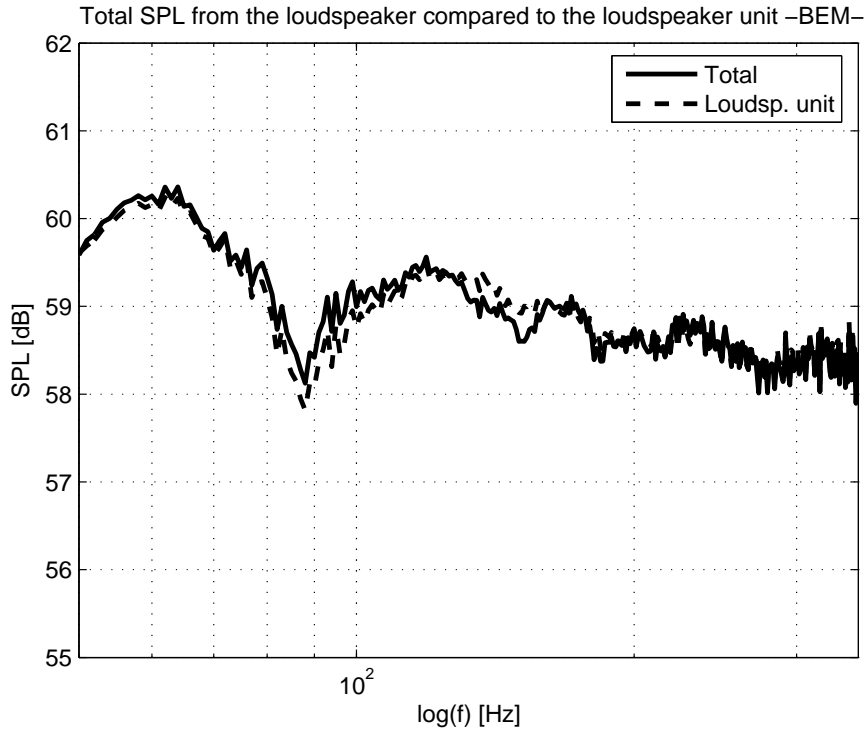


Figure 6.10: *SPL of the loudspeaker unit compared to the total SPL (cabinet + unit) in front of the loudspeaker calculated with the BEM. The observation point is at 1 m distance (at the front)*

The comparison between the pressure radiated by the unit and the total is shown in figure 6.10. The observation point is placed in front of the loudspeaker, 1 m away.

There is a very slight difference between the radiation from the loudspeaker unit and the total pressure in the front. However, such a difference is insignificant, showing no apparent influence from the cabinet. If we consider that the SPL difference between cabinet and loudspeaker is of more than 25 dB (see Figure 6.7), no significant influence from the cabinet can be expected. For cabinet resonances to be visible in the frequency response, a steady-state output of at least -20 dB relative to the output from the units themselves is required [16]. Thus, it is clear that in this case, the total sound pressure is mainly produced by the loudspeaker unit itself.

Similar calculations and measurements were performed as well in the back of the loudspeaker, for an observation point placed at 1 meter distance (at 180° azimuth). The results are presented in different figures, initially showing the calculations of the loudspeaker unit and the total (figure 6.11), then compared with the measurements (figure 6.12), and finally plotted along with the cabinet's SPL (figure 6.13).

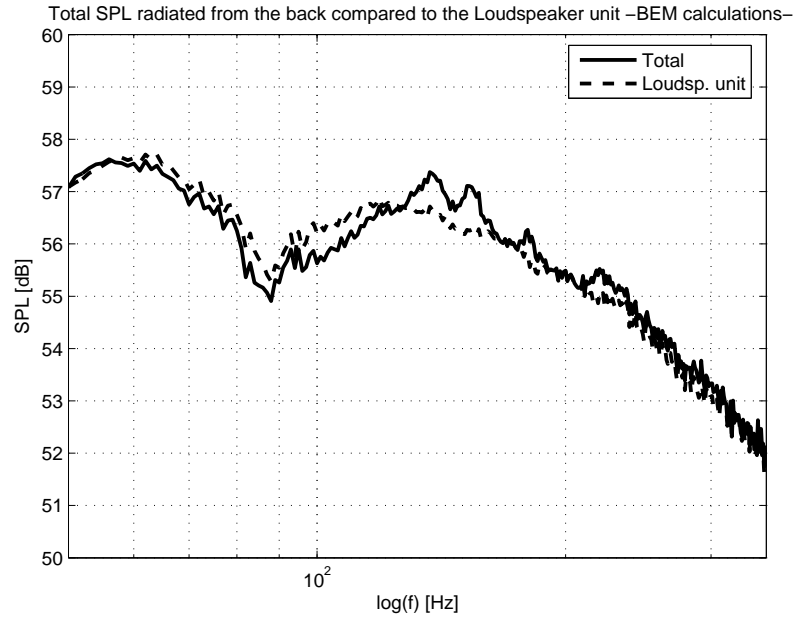


Figure 6.11: *SPL of the loudspeaker unit compared to the total SPL (cabinet + unit) calculated with the BEM. The observation point is at 1 m distance (in the back).*

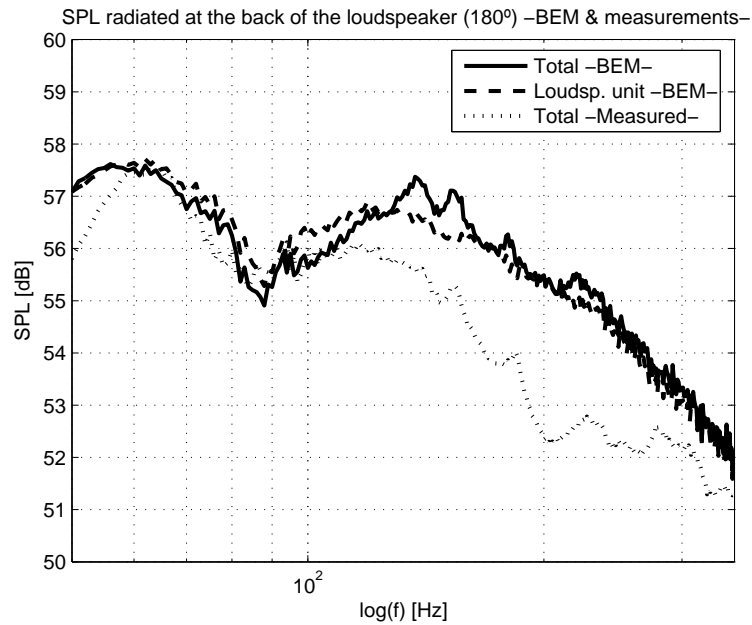


Figure 6.12: *SPL of the loudspeaker unit compared to the total SPL (from the BEM calculations and from the measurements). The observation point is at 1 m distance (in the back).*

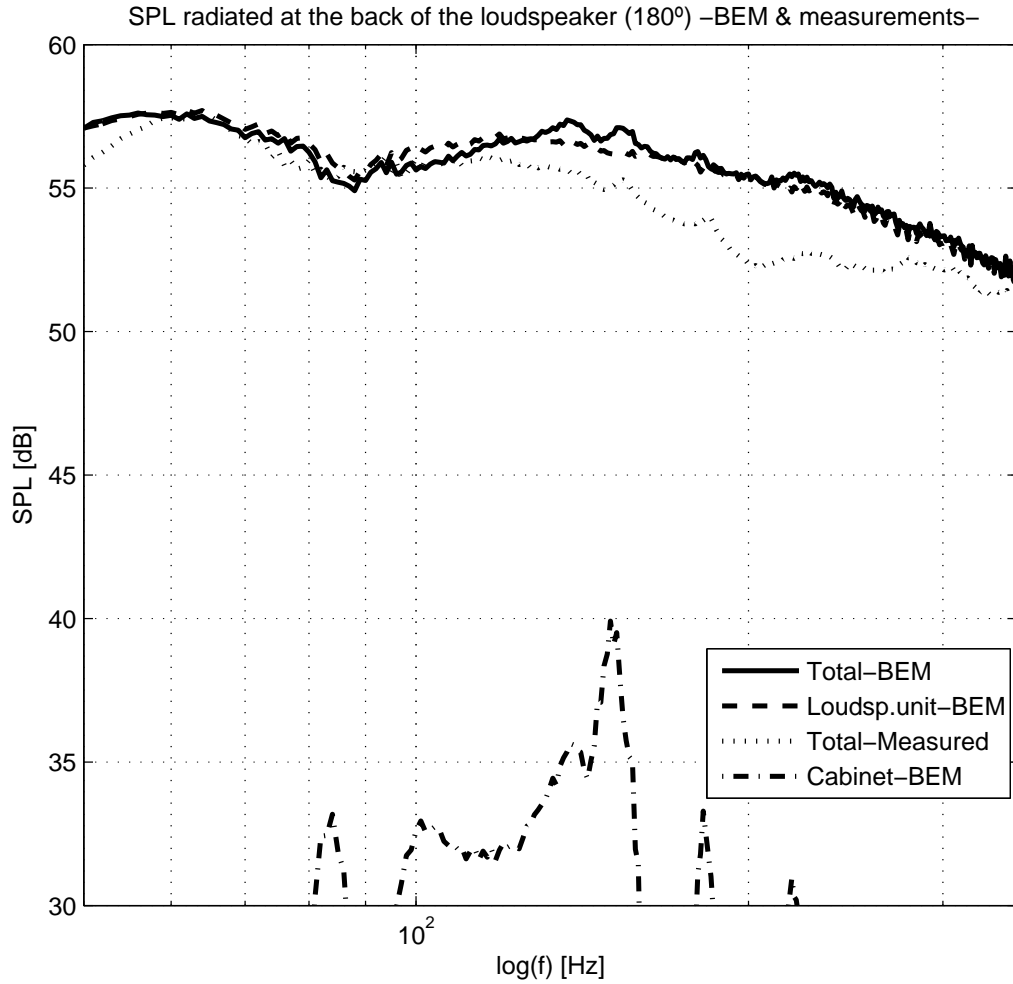


Figure 6.13: *SPL radiated by the loudspeaker unit compared to the total and to the cabinet. The observation point is at 1 m distance (in the back).*

On the contrary to figure 6.10, it is apparent from figures 6.11, 6.12 and 6.13 - which show the pressure at the back of the cabinet-, that there is a visible influence by the cabinet on the total radiated pressure. This influence is noticeable from the peaks which appear around 150 Hz and 184 Hz in the total radiated pressure by the loudspeaker. From figure 6.11, it is apparent that such peaks are not present in the driver's radiation, while they are present in the total sound pressure curve.

In figure 6.12, it can be seen how these peaks also appear in the measurements of the total pressure, confirming that they are actually present in the total radiation (the measurements are plotted along with the BEM calculations).

Finally, in Figure 6.13, the calculated and measured data of the total sound radiation is compared to the radiation of the cabinet. It is evident that the peaks appearing in the curve of the total sound pressure correspond to the peaks of the cabinet's frequency response. Thus, there is little doubt that such peaks are due to the contribution of the cabinet. This is a very interesting result, since it shows how the cabinet has an influence on the final sound radiated by the loudspeaker, and confirms the greater influence of the cabinet in the back side of it. However, the magnitude of the cabinet's contribution is rather small. The magnitude of the peaks in the total pressure is hardly 1 dB SPL. Therefore, it seems that the cabinet is indeed affecting the frequency response of the loudspeaker, but not too drastically though.

6.4.1 Considerations regarding the cabinets radiation

It can be concluded from the results presented in section 6.3 and section 6.4 that the cabinet radiation has not a drastical impact in the frequency response of the loudspeaker, at least in terms of sound pressure level. However, there is still an influence from the cabinet that should be examined more thoroughly.

All in all, it is important to bear in mind the fact that the influence of the cabinet has only been inspected from the frequency domain so far. The contribution from the cabinet to the total radiation of sound could be greater in the time domain. Particularly, the narrow frequency peaks and dips present in the cabinet's frequency response (figures 6.6 and 6.7), point towards a low damping characteristic that might have an influence in the behavior of the loudspeaker, which might be especially apparent in the time domain.

It should be remarked that even for cases in which the disturbance from the cabinet to the steady-state response may be too small to be readily discerned, it is still potentially audible [9].

6.5 Behavior of the cabinet in the time domain

While in the previous section the results were based on the frequency domain, in the present section they are based on the time domain.

So far, the frequency response of the loudspeaker and the cabinet have been examined. The cabinet has not a severe influence in the loudspeaker's frequency response (in terms of SPL). Nonetheless, the frequency response of the cabinet has some resonances with a rather low damping which are of concern. These frequency peaks appear at 80 Hz, 150 Hz, 184 Hz and 220 Hz.

The low damping, displayed as narrow peaks in the frequency domain, results in a long decay of the sound in the time domain. In the present case of study, this low damping can lead to the case where the impulse response of the cabinet is longer than the impulse response of the unit. In other words, it may happen that while the contribution of the cabinet is small relative to the total when reproducing a stationary signal (such as the broadband noise used for the measurements), it becomes greater in the decay of sound, after the loudspeaker unit stops vibrating. This can result in a blurred, smeared sound, which would produce an unclear perception, and which is especially disturbing when listening to sounds with some kind of transient or impulsive components (which is generally the case in most signals).

Based on the frequency response of the loudspeaker unit and the cabinet calculated with the BEM, the time domain behavior can be analyzed. If the frequency response is transformed back to the time domain, by means of Inverse Fast Fourier Transforms (IFFT), it is possible to obtain the impulse response, and hence know how the decay of the sound from the loudspeaker is. The time domain characteristics are thus obtained for free-space conditions as well.

6.5.1 Impulse response

The impulse response (IR) of a system is the output when a short transient signal, mathematically described as a Dirac delta function (or Kronecker, in the case of discrete systems), is presented to the system. A Dirac delta function consists of all frequencies with equal amplitude. Since all frequencies are presented simultaneously to the system, it is possible to calculate its frequency response by Fourier transforming it. Similarly, the impulse response can be calculated from the frequency response by inverse transforming it.

The impulse response provides useful information about the loudspeaker characteristics. It is a good measure for evaluating the “transparency” of the loudspeaker to sound. This property is related to how clear the sound of the loudspeaker is perceived, or in other words, to which extent the loudspeaker is modifying the reproduced

signal. Long impulse responses indicate unclear sound reproduction, while on the contrary, short impulse responses indicate clear reproduction, with little influence from the speaker to the sound (flat frequency response, low phase inaccuracy, etc.).

In the frequency response of the Beolab9 cabinet, there are some peaks which indicate a long impulse response. On the other hand, the frequency response of the loudspeaker unit is rather flat, indicating a relatively short impulse response. If this is the case, the impulse response of the cabinet could be longer than the loudspeaker unit, and the sound from the cabinet may become audible. This situation would clearly compromise the quality of the sound reproduction, and therefore it is of great concern.

Figures 6.14 and 6.15 show the impulse responses of the cabinet and the loudspeaker unit at 1 m distance in front of the loudspeaker, based on the sound pressure calculated with the BEM (presented in section 6.3 and 6.4). Figure 6.16 shows the impulse response of the loudspeaker unit measured in the near field of the loudspeaker³. The fact that it was measured in the near field helps to minimize the influence of the cabinet.

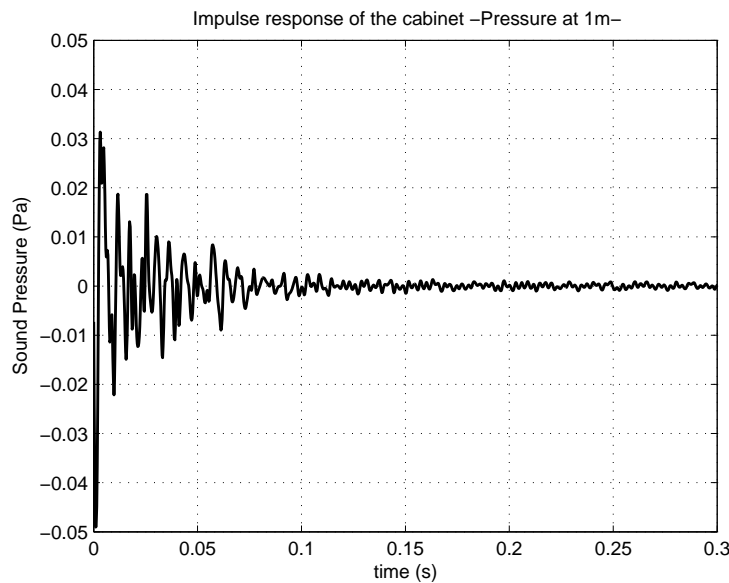


Figure 6.14: *Impulse response of the Beolab 9 cabinet. The impulse response is based on the BEM calculations of the sound pressure at 1 m distance. The observation point is placed in front of the loudspeaker (0° azimuth)*

³The impulse response of the loudspeaker included here was measured at Bang & Olufsen and kindly provided by them to be used in the present project.

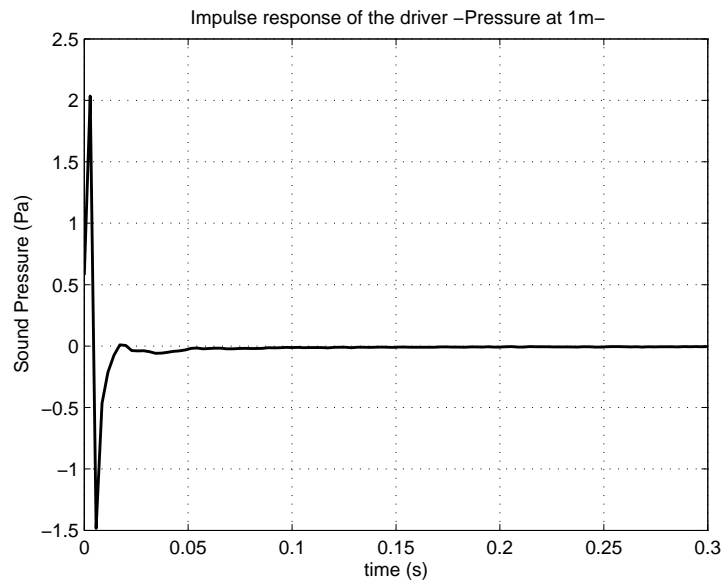


Figure 6.15: *Impulse response of the Beolab 9 woofer (loudspeaker unit) ⁴. The impulse response is based on the BEM calculations of the sound pressure at 1 m distance. The observation point is placed in front of the loudspeaker (0° azimuth)*

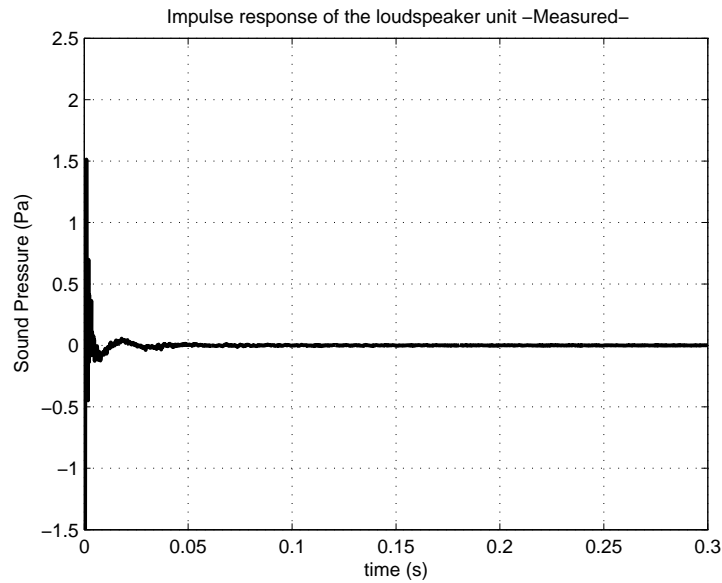


Figure 6.16: *Near field measurement of the impulse response of the Beolab 9 woofer.*

⁴The impulse response has been filtered at 300 Hz due to some noise from the laser measurements present at 350Hz. The filtering does not influence the results, and it is necessary for a clear visualization of the data.

Figures 6.14 and 6.15 indicate that the sound from the cabinet is decaying at a much slower rate than the sound by the unit. However, the amplitude scale of the figures is not the same. For a better comparison, the impulse responses are plotted in Figure 6.17 using the same amplitude scale and identical time span (until 300ms).

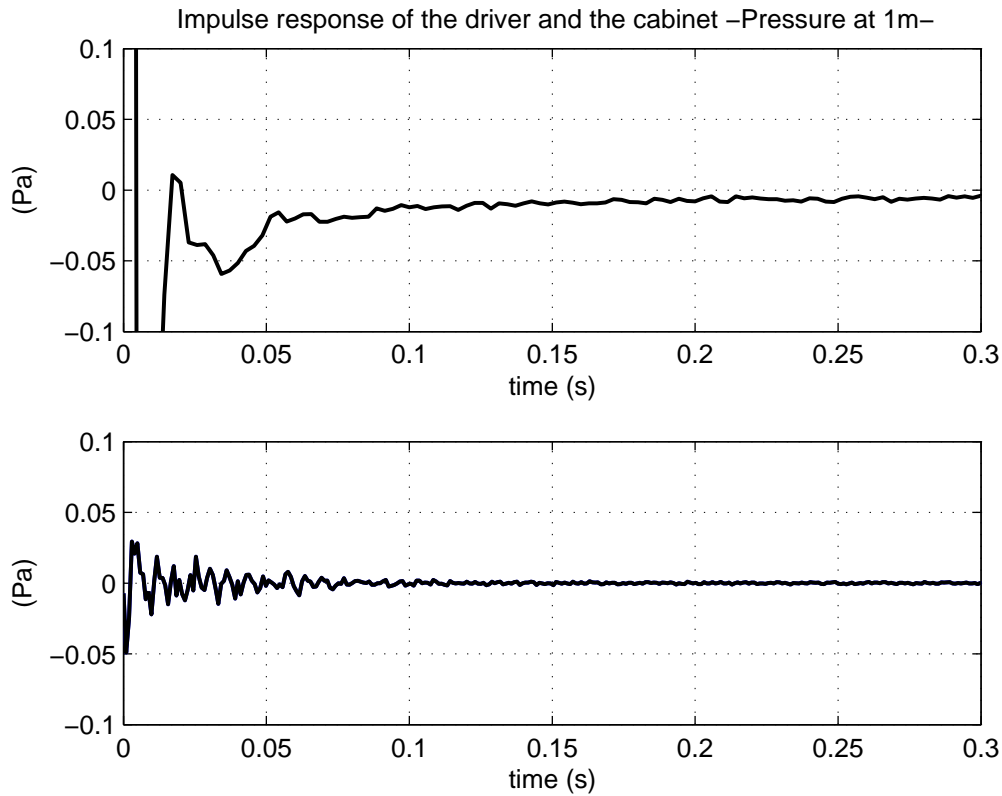


Figure 6.17: Comparison of the cabinet (up) and woofer (below) impulse responses. Note that the amplitude axis is different than from figures 6.13, 6.14 and 6.15

It is apparent from figure 6.17 that the order of magnitude of the loudspeaker unit and the cabinet is similar. This fact indicates that there is indeed an influence by the cabinet. Moreover, the main frequency components of the decays are different -it is apparent that the fluctuations in the case of the cabinet are much more rapid than in the woofer-. If this would be the case, the problem could be magnified. This is studied in the following section 6.5.2, where the spectrum of the signals throughout the decay is analyzed.

6.5.2 Decay of the sound pressure

From the impulse responses studied in section 6.5.1, it seems rather obvious that the frequency components of the cabinet's decay are rather different than the unit's decay. In other words, the distribution of energy during the decay is different in the case of the loudspeaker unit and the cabinet.

In order to study the spectral characteristics of the sound throughout the decay, the impulse responses can be segmented using short time windows, analyzing at different instants the spectrum of the decay by means of Fast Fourier Transforms (FFTs). Intuitively, this can be seen as “splitting” the impulse response in different consecutive sections, to analyze them separately. It is thus a time-frequency representation of the signal that shows which frequencies are dominating the decay of the sound pressure.

The time window used for the FFT analysis is shown in Figure 6.18. It is a *cosine tapered window* also known as *Tukey window*. This window provides a smooth transition to zero at the beginning and the end of the window, without modifying too much the amplitude of the original signal. The length of the time window is of $58ms$, which corresponds to $60samples$. The consecutive windows were overlapped half the size of the window. The signal has been analyzed in intervals of approximately $20ms$, starting from $0ms$ and $30ms$ and reaching up to $150ms$. For the FFT analysis, each of the windowed signals is zero-padded to $N=256$ points (in order to achieve a better spectral resolution).

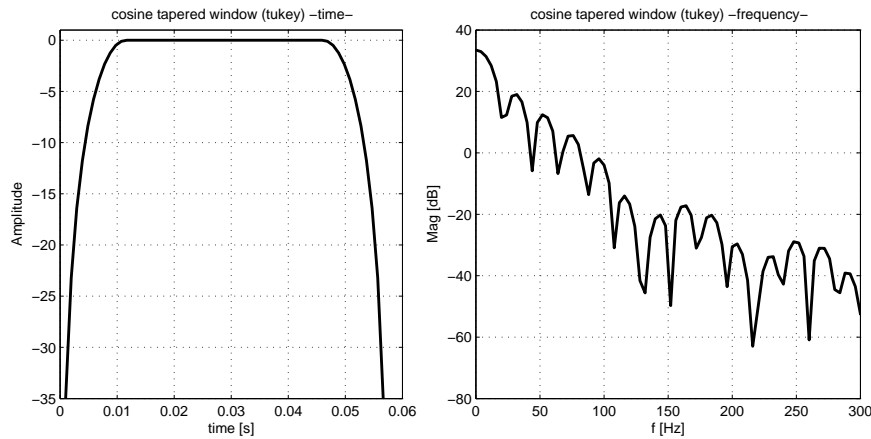


Figure 6.18: Time and frequency response of the cosine tapered window (or Tukey window) used for the frequency analysis of the decay

In Figure 6.19 and 6.20 a Waterfall plot of the decay of the cabinet and the loudspeaker unit is presented. The spectrum of the signals at 0, 30, 50, 70, 100 and 150 ms is shown.

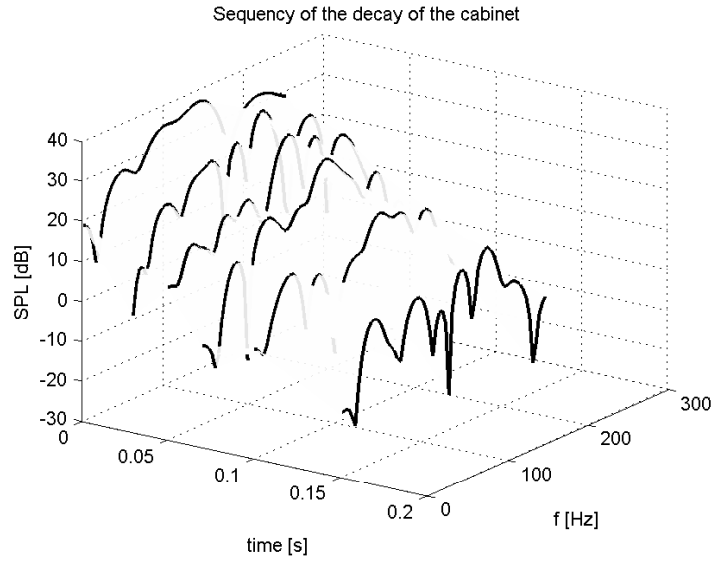


Figure 6.19: Waterfall plot of the cabinet's decay. The spectrum sections are at 0, 30, 50, 70, 100 and 150 ms

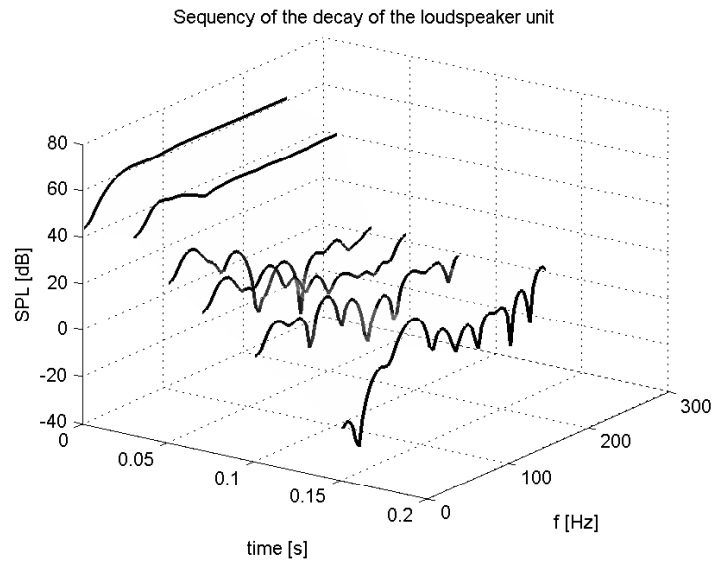


Figure 6.20: Waterfall plot of the loudspeaker unit's decay. The spectrum sections are at 0, 30, 50, 70, 100 and 150 ms

In Figure 6.21 the spectrum of the cabinet and the unit through the decay are plotted at different instants. In this way, it is easier to compare the SPL at different frequencies at different moments in time, and therefore get a better understanding of how the cabinet could be influencing the decay.

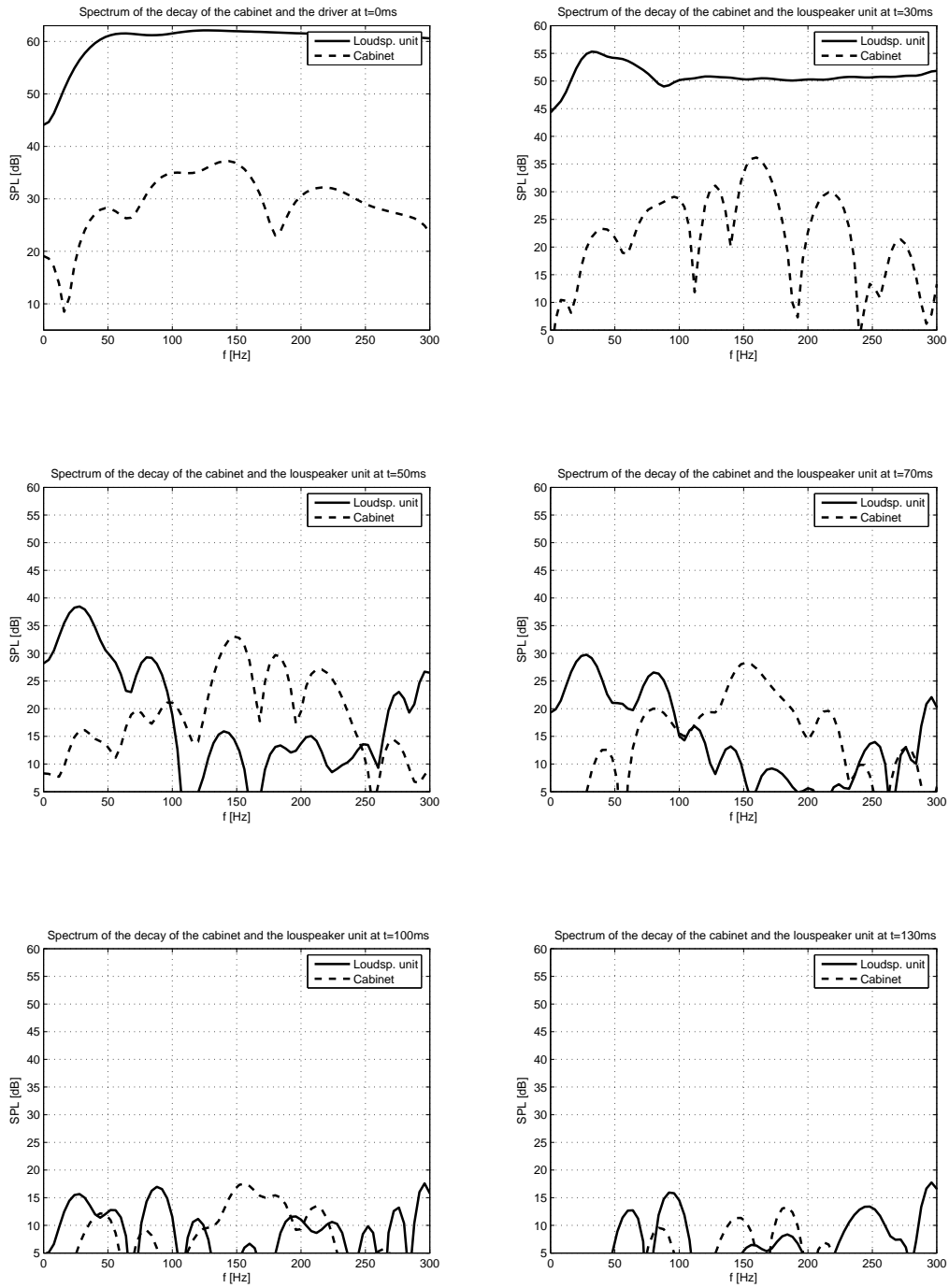


Figure 6.21: Comparison of the cabinet's -dashed line-, and the loudspeaker unit's decay-solid line- at different moments in time. 0 and 30 ms (top), 50 and 70 ms (middle), 100 and 130 ms (bottom)

It is obvious that at $0ms$ (in the moment of the impulse), the cabinet is radiating much less than the unit (it is equivalent to the stationary state situation). Nonetheless, the decay rate of the cabinet is much slower than the one of the unit, and soon it is taking over the decay process.

If the sequence of the decay is analyzed, it is clear that already at $50ms$ and until the end of the decay, the cabinet is dominating in the frequency range from 100 to 250 Hz. At $50ms$ the SPL of the cabinet is 18 dB higher than the loudspeaker unit. The energy of the unit's decay is localized mainly in the low frequency end, at around 50 Hz (at the lower resonance frequency of the woofer). It is clear that the cabinet is affecting to a great extent the total impulse response of the loudspeaker.

From the results presented here, there is no doubt that the cabinet is playing a significant role in the radiated sound by the loudspeaker. Not only its contribution is of the same order of magnitude as the loudspeaker's unit (contributing to the total), but in some cases the sound radiated by it is taking over the loudspeaker unit, being much greater.

Moreover, the different frequency components of both decays may produce a different outcome regarding the subjective perception. In terms of loudness sensation, given the same SPL, the human hearing is more sensitive to the 100-250Hz frequency range than to the 50 Hz range. This can be illustrated in figure 6.22 by the equal loudness level contours for pure tones⁵ (the lines show at which SPL, pure tones of different frequencies are perceived equally loud. For example: a 50 Hz pure tone of 50 dB is as perceived as loud as a 30 dB 150 Hz tone) -ISO 226 (2003) [14] [11]-.

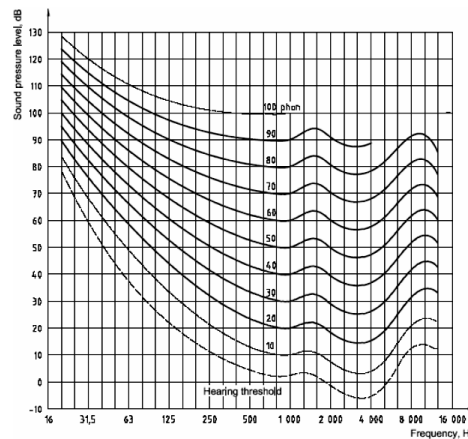


Figure 6.22: *Equal loudness level contours. Sounds presented binaurally from the frontal direction. The absolute threshold curve is also shown - from ISO 226 (2003) [14]*

⁵The curves in figure 6.22 cannot be used directly to predict the subjective loudness of complex signals, because they do not reflect the effect of masking, temporal perception, etc.

The results presented in this section so far, indicate that the cabinet of the loudspeaker is clearly influencing the total sound radiated by the loudspeaker. Figure 6.23 shows the decay of the unit and the cabinet in a time-frequency representation, where the SPL radiated by each is plotted as a surface. The figure illustrates how the cabinet is dominant during most of the decay process for the frequency range above 100 Hz (in such a plot it is easy to visualize which contribution of the two is greater).

The results obtained, suggest that even if the disturbance from the cabinet is not clearly apparent in the frequency steady-state response, such disturbance can become apparent in the time domain, provided that the damping of the cabinet's natural frequencies is low enough (long impulse response).

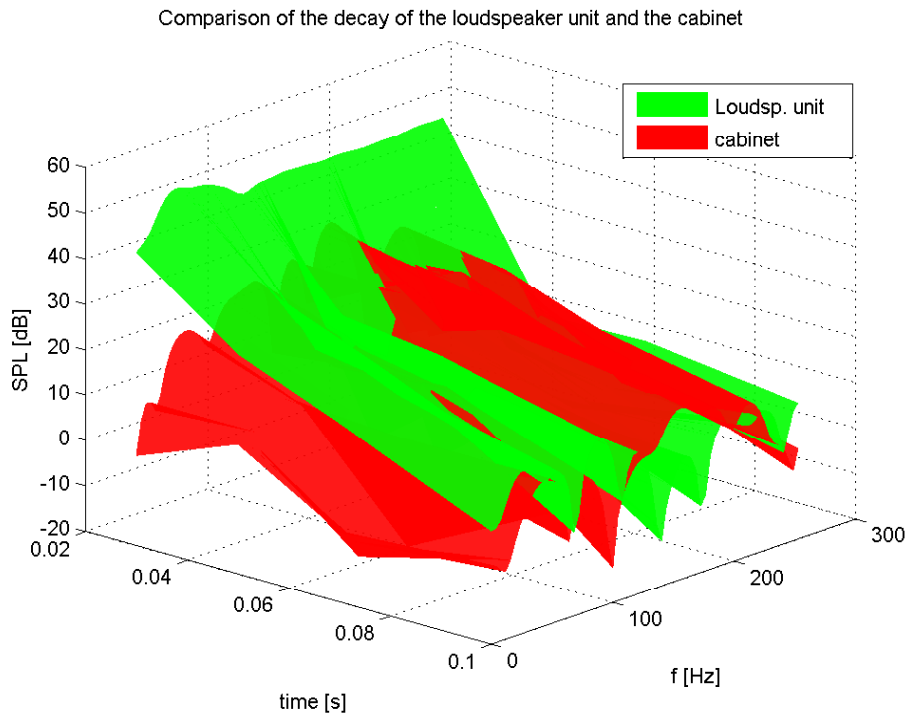


Figure 6.23: Surface plot illustrating the cabinet's (red) and the loudspeaker unit's decay (green)

Throughout the section, the time domain characteristics of the loudspeaker have been examined, and the contribution of the cabinet has been evaluated. Nevertheless, the results studied so far in section 6.5, only deal with the case in which the observation point is placed in the front of the loudspeaker (0° azimuth). This is not a very “critical” case, because in this position the influence of the loudspeaker unit is maximized, while the cabinet's influence is minimized. It could be said it is the “best” of the possible cases. In the following sections, some more critical cases are studied.

6.6 Radiation at the back of the cabinet (time domain)

It has been seen throughout the results of the project that the sound radiation from the cabinet is greater in the back than in the front of the loudspeaker. When looking at the time domain characteristics in section 6.5, only the position in front of the loudspeaker has been investigated. In this section, the time domain characteristics of the radiation of the cabinet and the unit are considered, when the observation point is placed in the back of the cabinet.

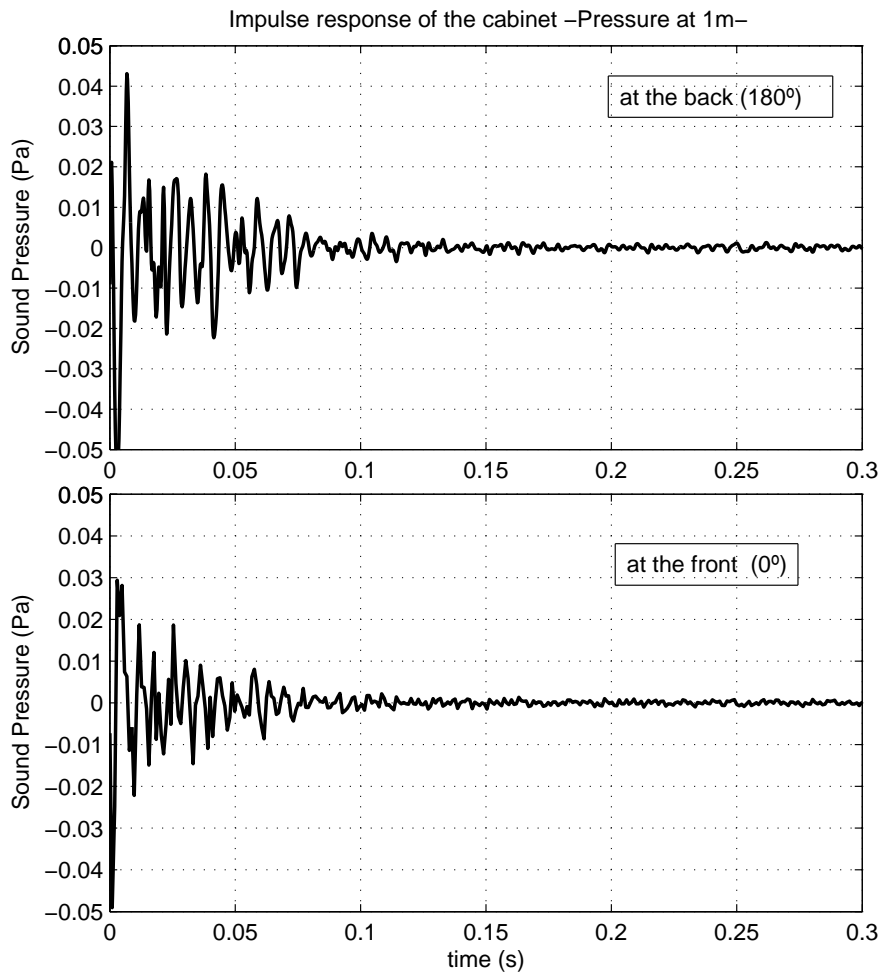


Figure 6.24: Comparison of the impulse responses of the cabinet in the back (top) and in the front (bottom) of the loudspeaker

The impulse response in the back of the cabinet is shown in Figure 6.24. It is com-

pared to the impulse response in the front of the cabinet (the same as in figure 6.14). It is obvious that the amplitude of the impulse response is greater at the back, and the decay is somewhat longer, as would be expected from the spectral data previously analyzed.

In a similar way as in section 6.5.2, the decay of the cabinet can be looked at in a frequency-time representation, to see how the spectrum is changing over time. In this way, the decay of the sound radiated by cabinet at the back and at the front of the loudspeaker can be compared. Figure 6.25 shows such a comparison.

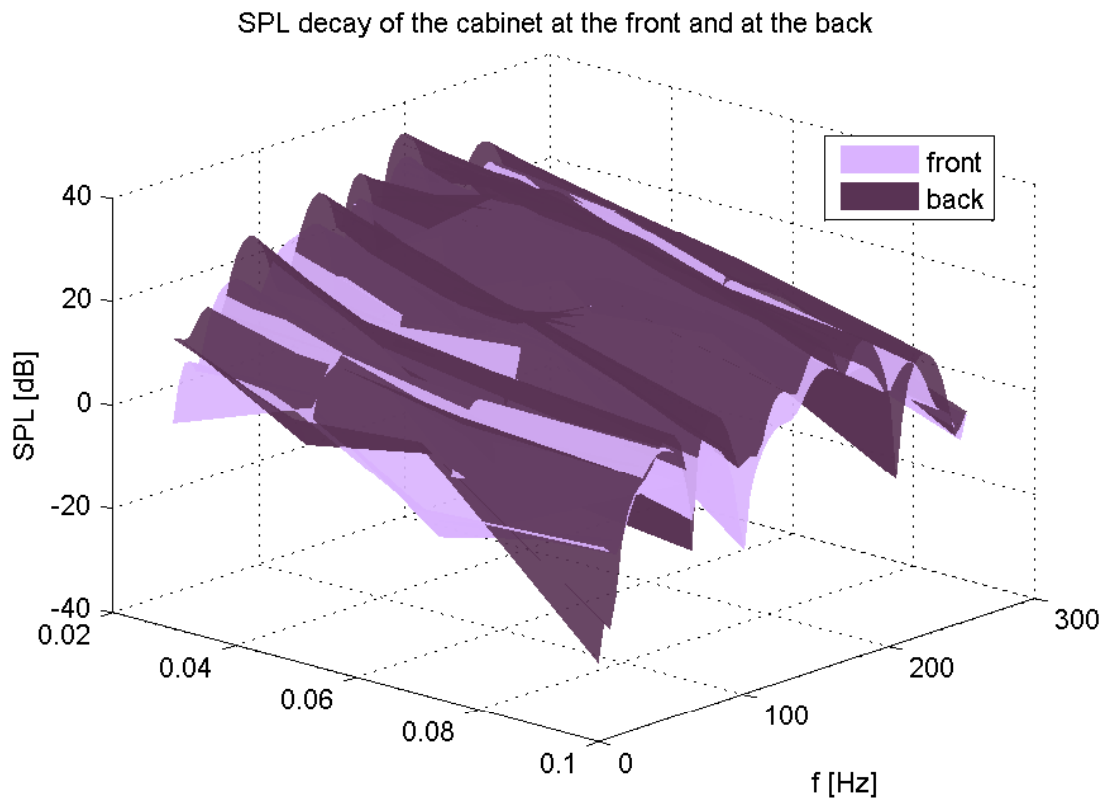


Figure 6.25: Comparison of the cabinet's SPL decay in the back and at the front of the loudspeaker

Figure 6.25 confirms the result that the magnitude of the sound radiated by the cabinet is greater in the back of the loudspeaker than in the front during the decay of the sound. Hence, considering that the unit is radiating less at the back, the cabinet is expected to play an even more important role in the decay of the overall sound.

Figure 6.26 shows a comparison between the SPL from the cabinet and from the unit at the back of the loudspeaker, at different instants of the sound pressure decay.

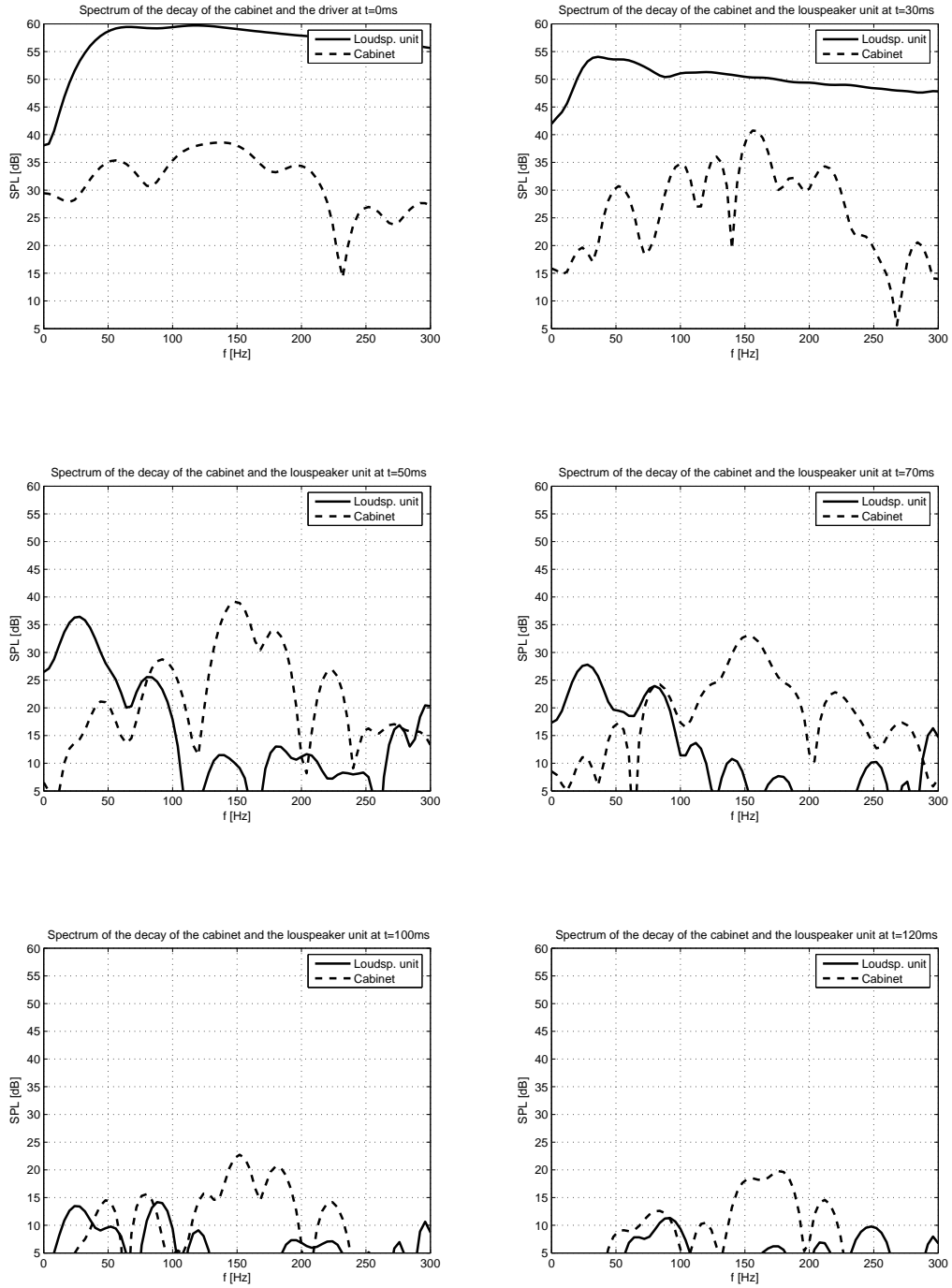


Figure 6.26: Comparison of the cabinet's -dashed line-, and the unit's decay -solid line- at different instants in time. 0 and 30 ms (top), 50 and 70 ms (middle), 100 and 120 ms (bottom). The observation point is in the **back** of the loudspeaker (180° azimuth)

It can be seen that from a very early stage of the decay ($35ms$) the amplitude of the cabinet is greater than the amplitude of the unit, and very soon the cabinet is radiating much more than the unit. Already after $50ms$, the SPL of the cabinet at 150 Hz is 20 dB greater than the unit's SPL. It is clear that the cabinet is very dominant in the decay of the sound (it is a very short period of time, but there is a very significant amplitude difference). This dominance is apparent in figure 6.27, which shows in a surface plot the SPL by the cabinet (in red) and the unit (in green) during the decay. The results shown in the figure make it easy to visualize the great contribution from the cabinet to the total sound radiated by the loudspeaker.

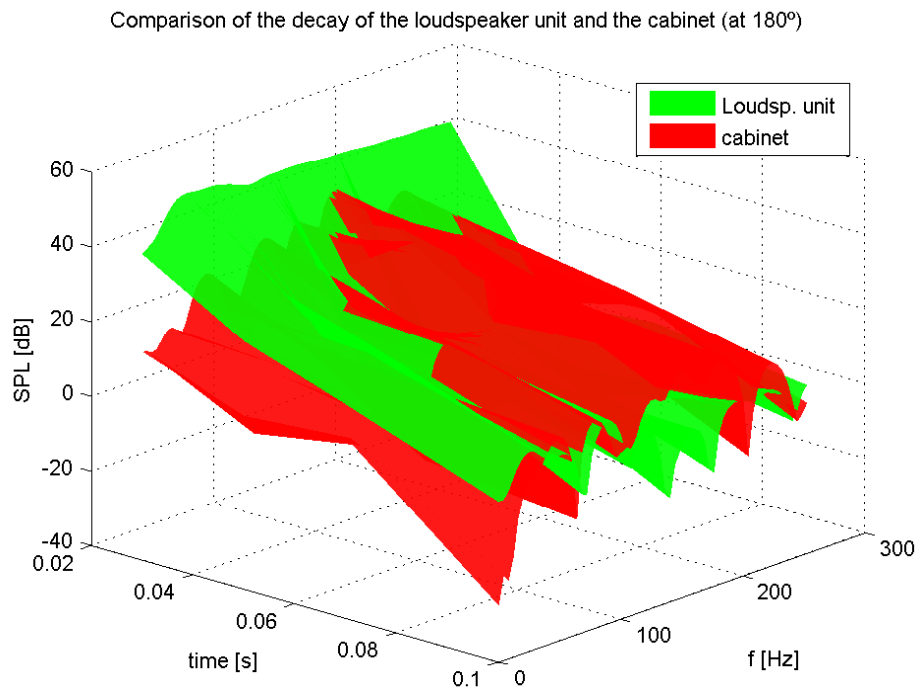


Figure 6.27: Surface plot illustrating the decay of the of the cabinet (red) and the loudspeaker unit (green) at the back of the cabinet

From the results shown in this section, it can be concluded that the greater contribution of the cabinet towards the back of the loudspeaker is also apparent in the time domain. This confirms that the problem of the cabinet being audible is found to a greater extent at the back part of the loudspeaker, where the efficiency of the cabinet's radiation is higher. It is thus clear that the problem is even more critical in the back region of the loudspeaker.

Generally, the rest of the conclusions that can be drawn from this section are similar to those drawn in sections 6.5.2 and 6.5.3, when the observation point was placed in the front of the speaker. The main difference is that in this case, the weight of the radiation from the cabinet compared to the loudspeaker unit is even greater.

6.7 Radiation from the bottom of the cabinet

The bottom of the loudspeaker's cabinet is also vibrating, with a particularly high amplitude at the lower frequency range (below 100 Hz). Such vibration levels could in principle play a significant role in the radiation of sound by the cabinet. However, the bottom vibration is not affecting too significantly the general characteristics of the sound radiated by the rest of the cabinet.

The Beolab 9 loudspeaker is designed to be placed on the floor. In such a situation, the bottom of the cabinet is not directly exposed to the medium, and not radiating directly into it. Thus, it is interesting to consider separately the case where the bottom is radiating directly into the medium, to understand better how it affects the sound radiated by the cabinet.

Besides, it should be noted that in all the pressure measurements carried out throughout the project, the loudspeaker was standing on a platform (and not suspended in air, which would be a free-space condition). Thus, it is not clear that including the vibration from the bottom in the calculations would model the measurement conditions more accurately. Moreover, it was verified in section 6.4, that the model considering the bottom of the cabinet not radiating to the medium, is a good approximation to the measurement conditions. Therefore, after such verification, and to avoid misleading results, the radiation from the bottom of the cabinet is considered separately, to evaluate the possible contribution from it to the total cabinet's radiation.

In this section, the loudspeaker is modeled as if it was suspended in air, and as if the bottom of the cabinet was radiating normally into the medium. Based on an initial investigation, the bottom is expected to play an influencing role only in the low frequency end. Therefore, the resolution of the measurement mesh was designed to be usable until 200 Hz (in order to economize the measurement and calculation time).

6.7.1 Frequency domain (Bottom radiation)

The BEM calculations were carried out both including the vibration from the bottom and without including it. The sound pressure radiated in both cases is very similar. The order of magnitude does not change generally, nor the spatial profile of how the sound is radiated into the medium. The most important changes can be seen at low frequencies, where the cabinet is vibrating as a whole, following a pulsating mode pattern. However, the general sound radiation by the cabinet with and without the contribution from the bottom is very similar.

In the following figure, the spectrum of the SPL radiated by the cabinet is shown. The two cases of the cabinet with the bottom vibrating and considered as rigid are shown for comparison.

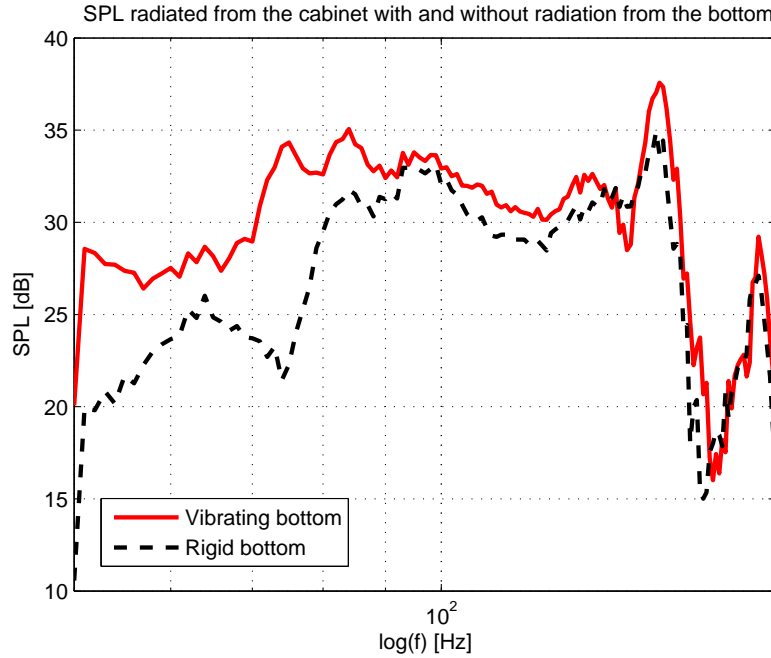


Figure 6.28: Comparison of the sound pressure radiated by the cabinet when the bottom is rigid (blue) and when it is vibrating (black)

It can be seen from Figure 6.28 that the radiation from the bottom is mainly affecting the results below 90 Hz. Above 90 Hz, both curves follow a very similar pattern. The vibration of the bottom is not changing the fundamental sound radiation characteristics from the cabinet. However, there are some relevant differences which worth to be mentioned.

Initially, the SPL at low frequencies is considerably greater (the bottom vibration contributes to a greater radiation by the zeroth order mode -at 85 Hz-, and below 85 Hz). Also the level is greater at some other natural frequencies of the cabinet -such as the 150 Hz one-. Furthermore, in most of the frequencies the overall SPL is slightly higher (about 1 dB more) than before.

It is as well very relevant the fact that some of the main peaks of the frequency response of the cabinet (such as 84 Hz and 150 Hz) are narrower. Narrower frequency peaks would reveal a longer decay time of the modes, which could emphasize the sound from the cabinet in the total sound radiated by the speaker. The best way to find out to investigate it is by looking at the time domain response of the cabinet, as has been done in previous sections.

6.7.2 Impulse response (bottom radiation)

It has been seen that the influence of the bottom radiation in the frequency domain is not too severe. However, the narrowing of some peaks in the frequency response and the increased sound pressure of the low frequency end, are expected to play a role in the radiation of the cabinet. In an analogous way as done in previous sections, the impulse response was calculated from the spectrum of the SPL 1 meter away. The Impulse response (with the bottom of the cabinet radiating in free-space) is shown in Figure 6.29

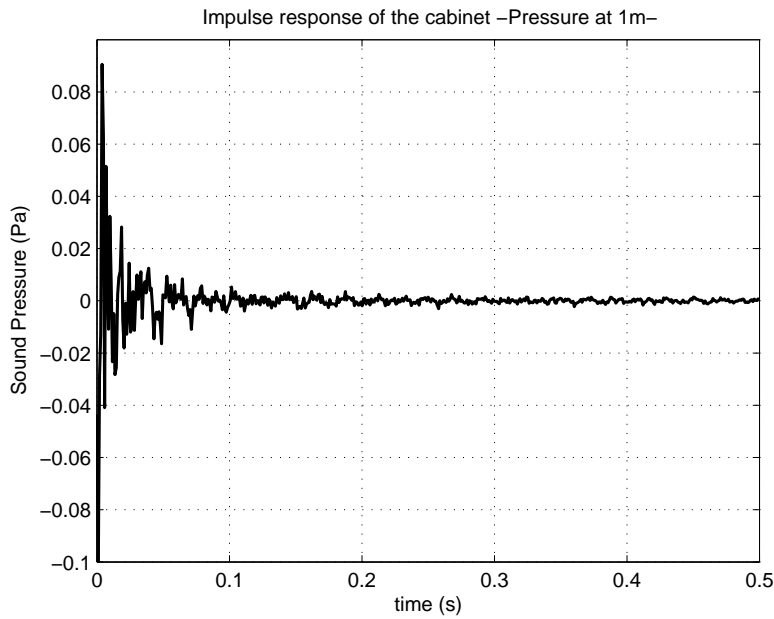


Figure 6.29: *Impulse response of the loudspeakers cabinet (where the bottom has been assumed to be radiating into the free-space domain)*

If the impulse responses of the cabinet with and without the contribution from the bottom (the bottom radiating or not radiating to the medium) are compared to each other (see Figure 6.14), it is apparent that the impulse responses are similar, but the response is slightly longer and of noticeably higher amplitude if the bottom is contributing. This result could be expected, based on the spectrum shown in figure 6.28 -especially due to the low frequency boost-.

6.7.3 Decay of the sound pressure (Bottom radiation)

The decay of the sound pressure of the cabinet with the bottom radiating to the medium, can be calculated, and plotted at different instants of time, compared to the decay of the loudspeaker unit. The results are shown in Figure 6.30 (next page)

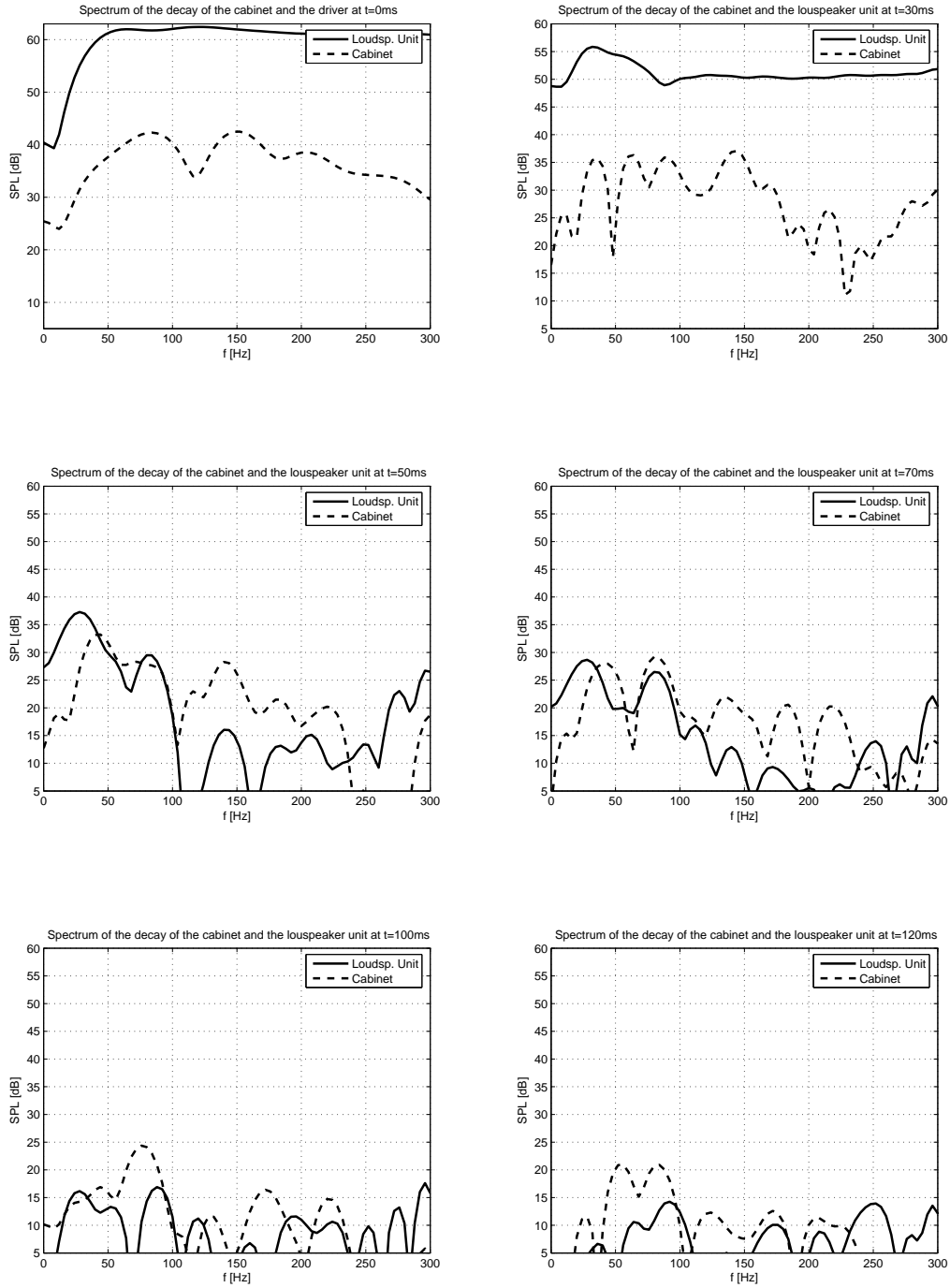


Figure 6.30: Comparison of the cabinet's -dashed line-, and the loudspeaker unit's decay -solid line- at different instants in time. 0 and 30 ms (top), 50 and 70 ms (middle), 100 and 120 ms (bottom). The cabinet is considered to be radiating in full free-space, and the radiation from the bottom of the cabinet is included.

It is clear from Figure 6.30 the fact that the cabinet is taking over an important part of the decay of the sound. The results in this case are very similar to the case where the radiation from the bottom is not considered (see figure 6.21), with the fundamental difference than in this case, the cabinet is much more present in the decay at the lower frequency range (around 50-80 Hz). Nevertheless, the results are pretty much the same in both cases.

The decay of the cabinet and the loudspeaker unit are plotted in the following figure, showing the SPL of both, and illustrating which one of the two is greater.

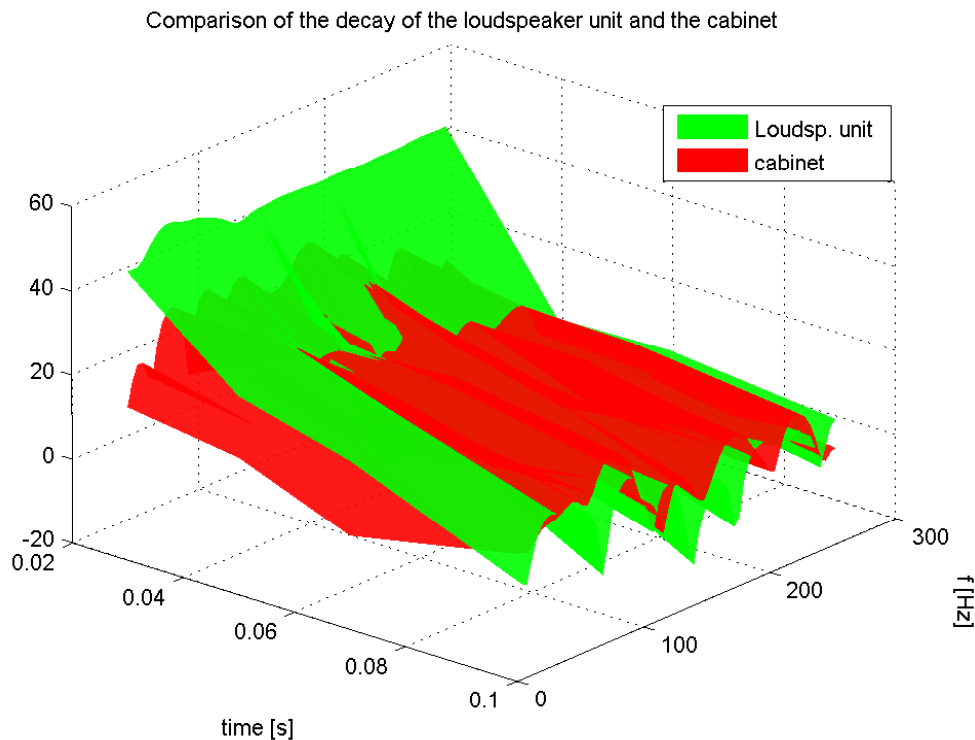


Figure 6.31: Surface plot illustrating the decay of the of the cabinet (red) and the loudspeaker unit (green) when the radiation from the cabinet into the domain is considered.

The conclusions that can be drawn from the results presented in this section, are that the bottom of the cabinet is not influencing too significantly the radiation from the cabinet. It has only an important contribution in the very low frequency range (50-100 Hz), but otherwise its influence is not too severe. However, it is preferable to study it separately, since the measurement setup is not emulating a complete free-space condition (the bottom of the cabinet is not radiating to the medium directly).

In any case, it seems clear that the contribution from the bottom of the cabinet boosts the low frequency end of the sound pressure radiated by it.

Chapter 7

Conclusions

The Boundary Element Method (BEM) has been proved to be an adequate tool for studying the sound radiation by a loudspeaker cabinet. The BEM is particularly useful in this case study due to the fact that it is difficult to measure the sound pressure by the cabinet separately, because of the simultaneous radiation by the unit.

The normal velocity of the cabinet's vibration has been examined, and some deflection shapes investigated. The maximum velocity levels were measured at 85, 150 and 182 Hz, in the front side of the speaker, close to the woofer. At low frequencies the cabinet is vibrating as a whole, while at higher frequencies the deflection shapes become more complicated.

The most significant radiation from the cabinet is in the frequency range between 80 Hz and 200 Hz. The SPL is particularly high at 150 Hz, 85 Hz and 185 Hz. The low frequencies seem to be radiating more due to the higher vibration levels and the higher radiation efficiency.

While the sound radiation from the cabinet is greater in the back of the loudspeaker, the unit's radiation is weaker there. The result of this, is in an increased influence from the cabinet towards the back of the loudspeaker.

Studying the frequency steady-state response of the loudspeaker, no important influence from the cabinet was found in the front direction. To the contrary, in the back side of the loudspeaker, there is a clear influence from the cabinet. The frequency response at the back reveals some noticeable peaks at 140, 150, 185 and 220 Hz, which correspond to the cabinet's natural frequencies¹. However, such influence does not

¹Such peaks are not present in the units radiation, but they are indeed present in the total frequency

seem too significant in terms of the SPL.

The results obtained, suggest that even if the disturbance from the cabinet is not clearly apparent in the steady-state frequency response, such disturbance can become apparent in the time domain, provided that the damping of the cabinet's natural frequencies is low enough (long impulse response).

In the present study, although the contribution from the cabinet to the total radiated pressure is not too apparent in the frequency response, when investigating the time domain, a very significant influence from the cabinet to the total radiation by the speaker has been found. The cabinet's impulse response is noticeably longer than the unit's.

The study revealed that just after a short period of time, the sound radiated by the cabinet is dominating in the decay of the loudspeaker's sound. Despite that the SPL generated by the unit is much higher than that of the cabinet in a steady-state situation (i.e. when reproducing a stationary signal, such as broadband noise), as soon as the signal ceases, the sound pressure of the unit drops, while the cabinet keeps "ringing" for a longer time. At the natural frequencies of the cabinet, its SPL was found to be much greater than the unit's during most of the decay process. Also in the time domain, the influence of the cabinet is more severe in the back than in the front.

An influence by the cabinet has been detected, especially apparent in the time domain, in the frequency range between 80 and 180 Hz. Such an influence would in principle compromise the quality of the sound reproduction. These results agree with the subjective testing that initially indicated the problem in the developing process of the loudspeaker.

The radiation from the bottom of the cabinet plays an important role at low frequencies, especially below 100 Hz. However, it does not change the fundamental sound radiation characteristics of the rest of the cabinet at higher frequencies.

The cabinet's vibration is changing non-linearly depending on the input level to the system. This non-linear behavior indicates that for increased reproduction levels, the cabinet's relative contribution might be greater, thus becoming even more audible.

The results obtained from this study, agrees fundamentally with those in refs. [9], [2] and [16]. In this project, the decay of the sound has also been investigated using a time-frequency representation, that reveals a different spectral distribution of the energy in the case of the cabinet and the unit throughout the decay process.

response of the loudspeaker, indicating an apparent influence of the cabinet.

Recommendations for future work

In the present study, the Boundary Element Method calculations have been based on vibration measurements performed on the cabinet. It would be interesting to study the possibility of basing the BEM calculations on a FEM (Finite Element Method) study instead of measurements. By doing so, the cabinet's radiation could not only be calculated, but also predicted before any prototype would have to be manufactured. This approach would have the drawback of requiring a very thoroughly detailed and "expensive" modeling.

This project focused on the sound radiation by the loudspeaker system, and the influence of the cabinet. The vibration of the system was just briefly examined. A greater insight into it could be very revealing. Basically, it would be useful to study in greater detail how the structural properties and shape of the cabinet and the loudspeaker system influence the sound radiation.

It should be noted that throughout the study, free-field conditions were assumed. However, it could be of interest to study how would a different environment affect the results. For instance, study the effect of placing the loudspeaker inside a listening room (in a usual listening environment, with reflections from walls and ceiling, for instance). Based on the measurements on the cabinet and the unit, it would be possible to model such a situation by introducing some reflecting surfaces. Such a study would reveal if the effect of reflections would increase or not the influence of the cabinet.

The study carried out evaluated the contribution of the cabinet only based on measurements and calculations. Such evaluation does not take into account subjective matters of human perception. It should be noted that this type of study is more of a quantitative approach, rather than a qualitative one. Therefore, it would be very interesting to relate it with a subjective analysis of the influence of sound radiated by loudspeaker cabinets.

Bibliography

- [1] *FEM-BEM Notes*. Bioengineering Institute of the University of Auckland, New Zealand, 2005.
- [2] Kevin J. Bastyr and Dean E. Capone. On the acoustics radiation from a loudspeaker's cabinet. *J. Audio Eng.Soc.*, 51:234–243, April 2003.
- [3] Finn Jacobsen and D. Bao. Acoustic decay measurements with a dual channel analyzer. *Journal of Sound and Vibration*, 115(3):521–537, 1987.
- [4] Finn Jacobsen and Peter M Juhl. Radiation of sound. Acoustic Technology (Technical University of Denmark), Physics Department (University of Southern Denmark), August 2006.
- [5] Peter M. Juhl. *The Boundary Element Method for Sound Field Calculations*. PhD thesis, Technical University of Denmark (DTU), August 1993.
- [6] Peter M. Juhl and Vicente Cutanda Henriquez. *OpenBEM -Open source Matlab codes for the Boundary Element Method-*. <http://www.openbem.dk/>, -.
- [7] Matti Karjalainen, Veijo Ikonen, Poju Antsalu, Panu Maijala, Lauri Savioja, Antti Suutala, and Seppo Pohjolainen. Comparison of numerical simulation models and measured low-frequency behaviour of loudspeaker enclosures. *Journal of the Audio Engineering Society (JAES)*, 49:1148–1165, 2001.
- [8] Stephen Kirkup. *The Boundary Element Method in Acoustics*. www.boundary-element-method.com, 1998/2007.
- [9] Stanley Lipshitz, Michael Heal, and John Vanderkooy. An investigation of sound radiation by loudspeaker cabinets. *J. Audio engineering Society (JAES)*, 19-22:F–4, February 1991. Audio rsearch Group, Univ. of Waterloo, Ontario, Canada.
- [10] Yu Luan. Modeling structural acoustic properties of the beolab 9 loudspeaker. Master's thesis, Acoustic Technology (AT), Technical University of Denmark (DTU), January 2008.
- [11] Brian C. J. Moore. *An Introduction to the Psychology of Hearing*. Academic Press, 2003.

-
- [12] Philip M. Morse and K. Uno Ingard. *Theoretical Acoustics*. MIT, 1968.
 - [13] Mogens Ohlrich. *Structure Borne Sound and Vibration*. Acoustic Technology, DTU, 2006.
 - [14] Torben Poulsen. Acoustic communication. hearing and speech (v2.0). Acoustic Technology, Technical University of Denmark (DTU), Denmark, August 2005.
 - [15] Arnold Sommerfeld. *Partial Differential Equations in Physics*. Cambridge University Press, New York, 1949.
 - [16] Peter W. Tappan. Loudspeaker enclosure walls. *Journal of the Audio Engineering Society (JAES)*, 10:224–231, July 1962.
 - [17] F.E. Toole and S.E. Olive. The modification of timbre by resonances: Perception and measurement. *J. Audio Engineering Society.*, 36:122–142, March 1988.

List of Figures

2.1	Simple Boundary Problem Sketch. In a sound radiation problem the domain is governed by the wave equation. In this particular project the outer boundary condition is the Sommerfield radiation condition -Infinity-, and the inner boundary condition is the velocity of the body .	11
3.1	Measurement mesh of the Beolab 9. The velocity was measured at every node of the mesh	17
3.2	Example of the deflection shape of a conical cabinet at 309 Hz. Image from [10]	18
4.1	Test Box used for the verification of the procedure	24
4.2	Mesh of the test box used for the BEM calculations. The maximum element length is of 16cm	25
4.3	Block diagram of the measurement	26
4.4	Image of the measurement	26
4.5	Comparison between the BEM calculation and the measured SPL	27
5.1	Beolab9. Side view (left). Top view (centre). View without the screen cover (right)	30
5.2	Beolab9 simplified geometry in which the mesh was based	30
5.3	Meshing of the Beolab 9 used for the BEM calculations	31
5.4	Testing of the mesh. Sound pressure produced by a monopole placed at the origin. The figure compares the sound pressure calculated analytically and with the BEM using the loudspeaker mesh, for different frequencies.	33
5.5	Some pictures of the vibration measurement	34
5.6	Block diagram of the vibration measurement	34
6.1	Acceleration on the cabinets surface at all the measurement positions .	40
6.2	Field points at which the sound pressure was calculated	42
6.3	SPL radiated by the loudspeakers cabinet, at 1m distance and 0.35 m height, around the azimuth angle (polar angle around the loudspeaker) .	43

6.4	Phase of the pressure radiated by the loudspeakers cabinet, at 1m distance and 0.35 m height around the azimuth angle. The isobars represent a $\pi/4$ phase change	43
6.5	SPL radiated by the loudspeakers cabinet, along the polar angle at 1m distance. 85 Hz (solid), 150Hz (dashed) and 182 Hz (dotted)	44
6.6	SPL radiated by the loudspeakers cabinet, at 1m distance, compared to the total radiated pressure by the loudspeaker. The top figure shows the radiation in the front direction -0° -, the medium figure shows the lateral radiation -90° -, and the bottom figure the back radiation -180° - .	45
6.7	SPL radiated by the loudspeakers cabinet, at 1m distance, compared to the total radiated pressure by the loudspeaker. The front (blue), lateral (green) and back (black) radiation are plotted together	46
6.8	Comparison of measurements and BEM calculations of the total radiation from the loudspeaker. The observation point is in front of the loudspeaker at 1 m distance and 0.35 m height	48
6.9	Comparison of measurements and BEM calculations of the total radiation from the loudspeaker. The observation point is in the back of the loudspeaker at 1 m distance	49
6.10	SPL of the loudspeaker unit compared to the total SPL (cabinet + unit) in front of the loudspeaker calculated with the BEM. The observation point is at 1 m distance (at the front)	50
6.11	SPL of the loudspeaker unit compared to the total SPL (cabinet + unit) calculated with the BEM. The observation point is at 1 m distance (in the back).	51
6.12	SPL of the loudspeaker unit compared to the total SPL (from the BEM calculations and from the measurements). The observation point is at 1 m distance (in the back).	51
6.13	SPL radiated by the loudspeaker unit compared to the total and to the cabinet. The observation point is at 1 m distance (in the back).	52
6.14	Impulse response of the Beolab 9 cabinet. The impulse response is based on the BEM calculations of the sound pressure at 1 m distance. The observation point is placed in front of the loudspeaker (0° azimuth) . . .	55
6.15	Impulse response of the Beolab 9 woofer (loudspeaker unit) ² . The impulse response is based on the BEM calculations of the sound pressure at 1 m distance. The observation point is placed in front of the loudspeaker (0° azimuth)	56
6.16	Near field measurement of the impulse response of the Beolab 9 woofer.	56
6.17	Comparison of the cabinet (up) and woofer (below) impulse responses. Note than the amplitude axis is different than from figures 6.13, 6.14 and 6.15	57
6.18	Time and frequency response of the cosine tapered window (or Tukey window) used for the frequency analysis of the decay	58
6.19	Waterfall plot of the cabinet's decay. The spectrum sections are at 0, 30, 50, 70, 100 and 150 ms	59

6.20	Waterfall plot of the loudspeaker unit's decay. The spectrum sections are at 0, 30, 50, 70, 100 and 150 ms	59
6.21	Comparison of the cabinet's <i>-dashed line-</i> , and the loudspeaker unit's decay <i>-solid line-</i> at different moments in time. 0 and 30 ms (top), 50 and 70 ms (middle), 100 and 130 ms (bottom)	60
6.22	Equal loudness level contours. Sounds presented binaurally from the frontal direction. The absolute threshold curve is also shown - from ISO 226 (2003) [14]	61
6.23	Surface plot illustrating the cabinet's (red) and the loudspeaker unit's decay (green)	62
6.24	Comparison of the impulse responses of the cabinet in the back (top) and in the front (bottom) of the loudspeaker	63
6.25	Comparison of the cabinet's SPL decay in the back and at the front of the loudspeaker	64
6.26	Comparison of the cabinet's <i>-dashed line-</i> , and the unit's decay <i>-solid line-</i> at different instants in time. 0 and 30 ms (top), 50 and 70 ms (middle), 100 and 120 ms (bottom). The observation point is in the back of the loudspeaker (180° azimuth)	65
6.27	Surface plot illustrating the decay of the of the cabinet (red) and the loudspeaker unit (green) at the back of the cabinet	66
6.28	Comparison of the sound pressure radiated by the cabinet when the bottom is rigid (blue) and when it is vibrating (black)	68
6.29	Impulse response of the loudspeakers cabinet (where the bottom has been assumed to be radiating into the free-space domain)	69
6.30	Comparison of the cabinet's <i>-dashed line-</i> , and the loudspeaker unit's decay <i>-solid line-</i> at different instants in time. 0 and 30 ms (top), 50 and 70 ms (middle), 100 and 120 ms (bottom). The cabinet is considered to be radiating in full free-space, and the radiation from the bottom of the cabinet is included.	70
6.31	Surface plot illustrating the decay of the of the cabinet (red) and the loudspeaker unit (green) when the radiation from the cabinet into the domain is considered.	71
A.1	Velocity of the cabinet, measured in the reference point, for different input levels (broadband noise was used).	84
A.2	Amplitude transfer function of the velocity of the loudspeaker cabinet at 84 Hz.	85
A.3	Amplitude transfer function of the velocity of the loudspeaker cabinet at 150 Hz.	85
A.4	Amplitude transfer function of the velocity of the loudspeaker cabinet at 185 Hz.	86
A.5	Amplitude transfer function of the velocity of the loudspeaker cabinet at 220 Hz.	86

A.6	Normalized velocity of the cabinet and the unit when reproducing a tone of 80 Hz. The overtones are a result of the non-linear distortion processes in the unit and cabinet.	87
B.1	Magnitude of the velocity around the circumference of the cabinet at 83 Hz	89
B.2	Magnitude of the velocity around the circumference of the cabinet at 99 Hz	90
B.3	Magnitude of the velocity around the circumference of the cabinet at 140 Hz	90
B.4	Magnitude of the velocity around the circumference of the cabinet at 182 Hz	91
B.5	Magnitude of the velocity around the circumference of the cabinet at 210 Hz	91
D.1	SHELL63 Elastic Shell	112

Appendix A

Non-linear vibration of the cabinet

An electrical input level of 100 mV amplitude has been used in all the measurements of the Beolab 9. Such input level (using broadband noise) was chosen because it produces a SPL of around 80 dB at 1m distance, which a reasonable listening level. However, it is important to examine the influence of using different input levels on the loudspeaker behavior.

In principle, the higher the input level, the more the cabinet vibrates (the vibration of the loudspeaker unit increases and more vibration is transmitted to the cabinet). Thus, the sound radiated by it is also expected to be greater¹. Just to get an idea of this phenomenon, the vibration of the cabinet was measured at different input levels. The vibration was measured in the reference point (which is situated just above the woofer). This point was chosen because it is a representative point of the vibration of the cabinet, since all the natural frequencies are present and the vibration levels are rather high.

¹The SPL radiated by the cabinet at different levels was not calculated, since it would involve to repeat all the measurements and calculations at different input levels.

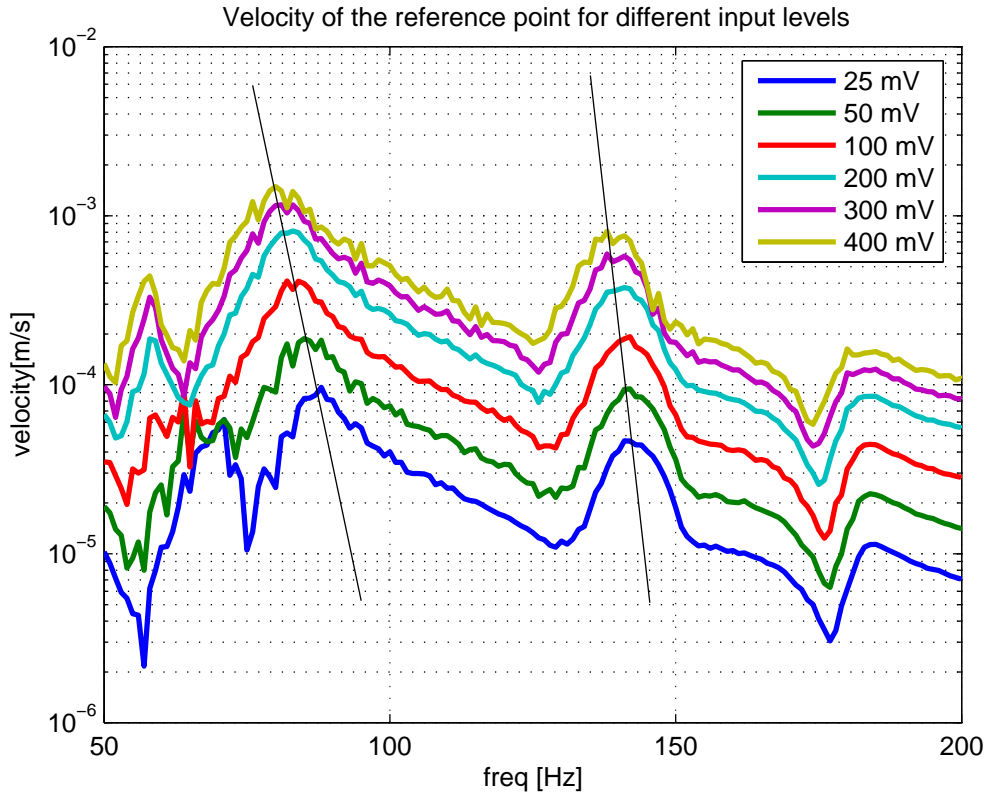


Figure A.1: *Velocity of the cabinet, measured in the reference point, for different input levels (broadband noise was used).*

Figure A.1 shows the spectrum of the vibration velocity measured at the reference point of the cabinet for different input levels ranging from 25 mV (which produces a very low SPL) to 400 mV (which produces a very high SPL).

It is obvious from the results that the vibration of the cabinet is not linear. Depending on the input level of the vibration, the peaks of the frequency response are shifting considerably. This is also apparent on the amplitude transfer function of the vibration velocity, at different frequencies, as shown in figures A.2 to A.5.

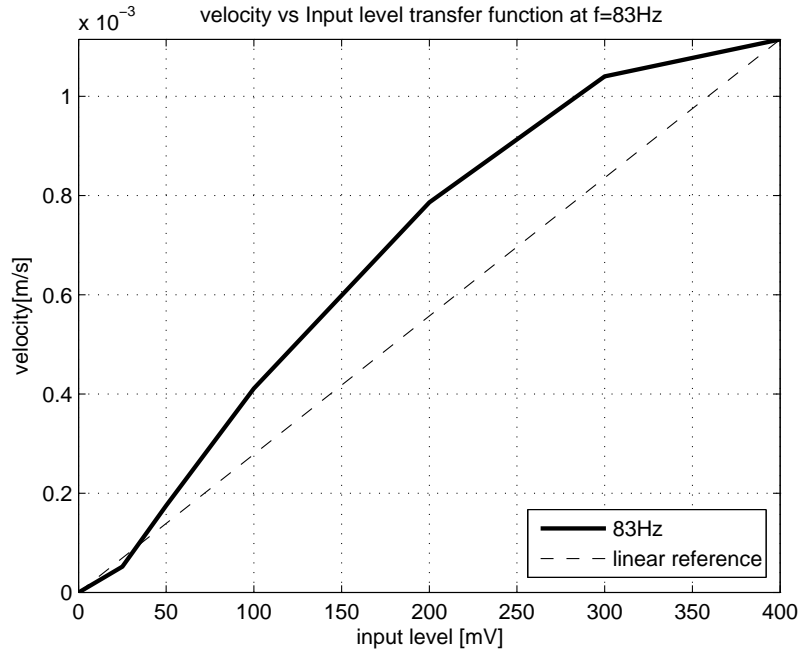


Figure A.2: Amplitude transfer function of the velocity of the loudspeaker cabinet at 84 Hz.

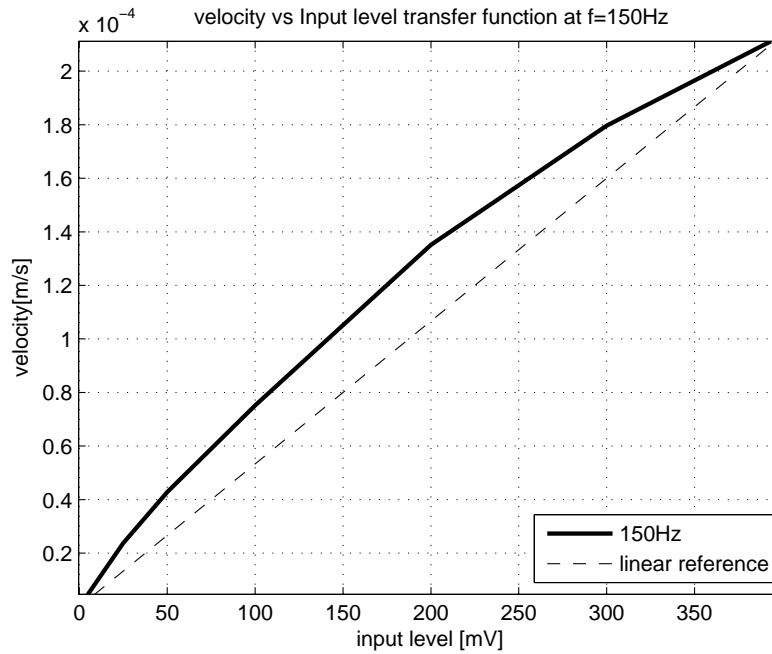


Figure A.3: Amplitude transfer function of the velocity of the loudspeaker cabinet at 150 Hz.

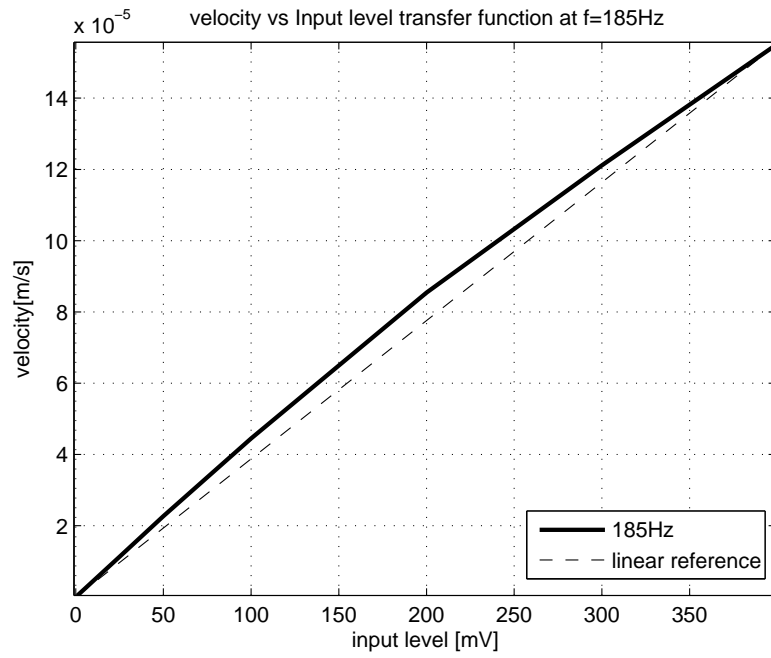


Figure A.4: Amplitude transfer function of the velocity of the loudspeaker cabinet at 185 Hz.

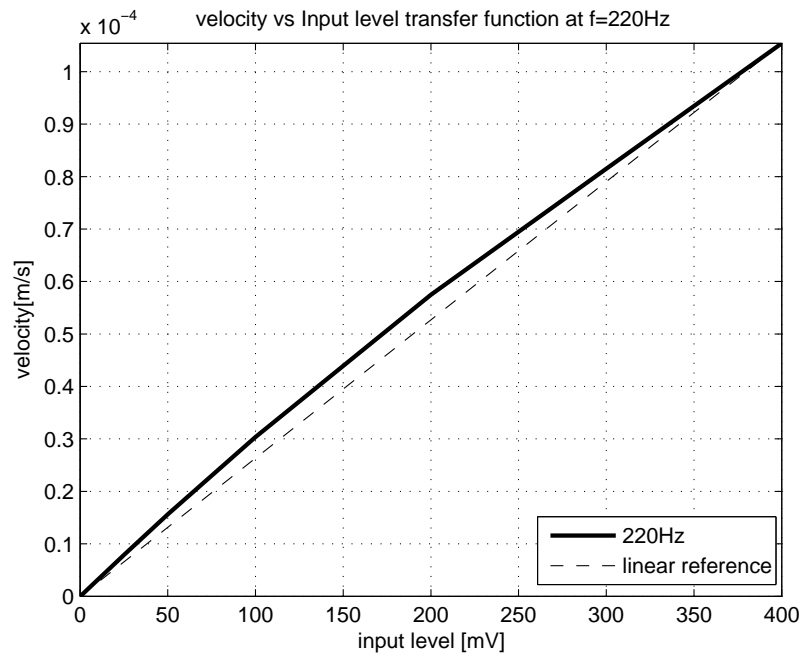


Figure A.5: Amplitude transfer function of the velocity of the loudspeaker cabinet at 220 Hz.

It is apparent from figures A.2 to A.5 that the amplitude transfer function is clearly non-linear, especially for the lower natural frequencies. At higher frequencies, there is a certain non-linear characteristic, but less severe than at lower frequencies. It can be seen from the figures that the vibration levels is increasing non-linearly with the input level. Thus, the higher the input level, the relatively higher the vibration of the cabinet will be.

However, it is reasonable to find a nonlinear vibration in the cabinet, especially considering that the loudspeaker unit is already vibrating nonlinearly (distortion, etc.). To evaluate this phenomenon, a simple measurement was carried out. A tone of 80 Hz was presented, and both the vibration of the loudspeaker unit and the cabinet was measurement (the loudspeaker unit was measured with a laser, and the cabinet using an accelerometer). The distortion from both systems can therefore be compared, and verify if the cabinet distortion is caused by the previous distortion of the unit, or if the cabinet is also distorting by itself.

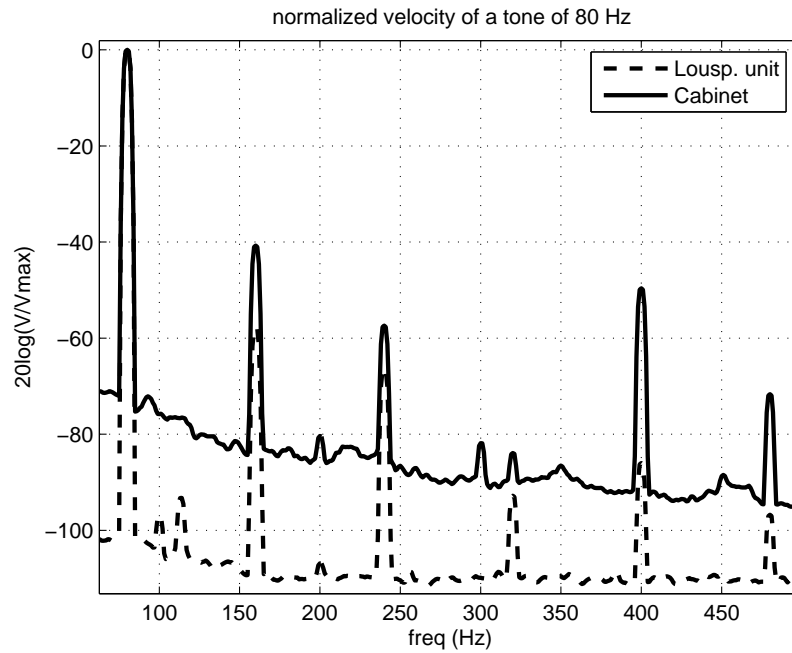


Figure A.6: Normalized velocity of the cabinet and the unit when reproducing a tone of 80 Hz. The overtones are a result of the non-linear distortion processes in the unit and cabinet.

The background noise present in the “floor” of the cabinets vibration is due to the fact that it was measured with accelerometers (while the unit was measured with the laser). The level of the figures is normalized to the amplitude of each of the main tones (at 80 Hz). In this way, the level of the overtones is relative to the main vibration of

the input tone.

Form Figure A.6 it is apparent that the cabinet is also contributing to the distortion. The level of the harmonics of the cabinet is greater than the level of the harmonics of the unit. At low frequencies (160 Hz and 240 Hz), the distortion in the harmonics of the cabinet is about 15 to 20 dB higher than the those of the unit.

It can be concluded from this section that the relative contribution from the cabinet to the radiated sound would increase with greater input levels. In other words, the louder the signal reproduced by the loudspeaker, the greater the contribution by the cabinet. Therefore, at high sound pressure levels, the problem of the cabinet being audible would be magnified.

Appendix B

Deflection shapes of the cabinet

The appendix shows the magnitude of the velocity in the surface of the cabinet at a height of 36 cm from the ground. The plots show the magnitude of the velocity around the circumference of the cabinet. In the the nodes and antinodes can be identified, to get an idea of how the deflection shapes look like.

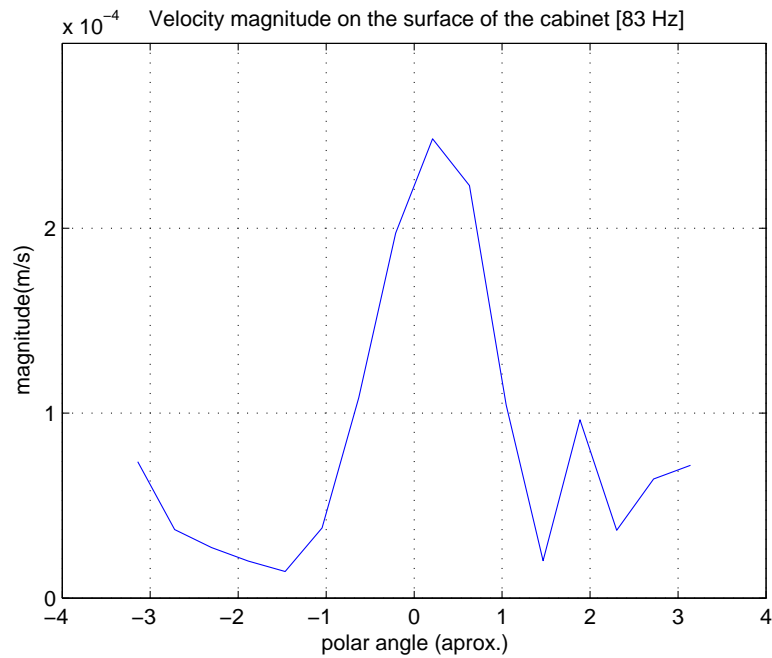


Figure B.1: *Magnitude of the velocity around the circumference of the cabinet at 83 Hz*

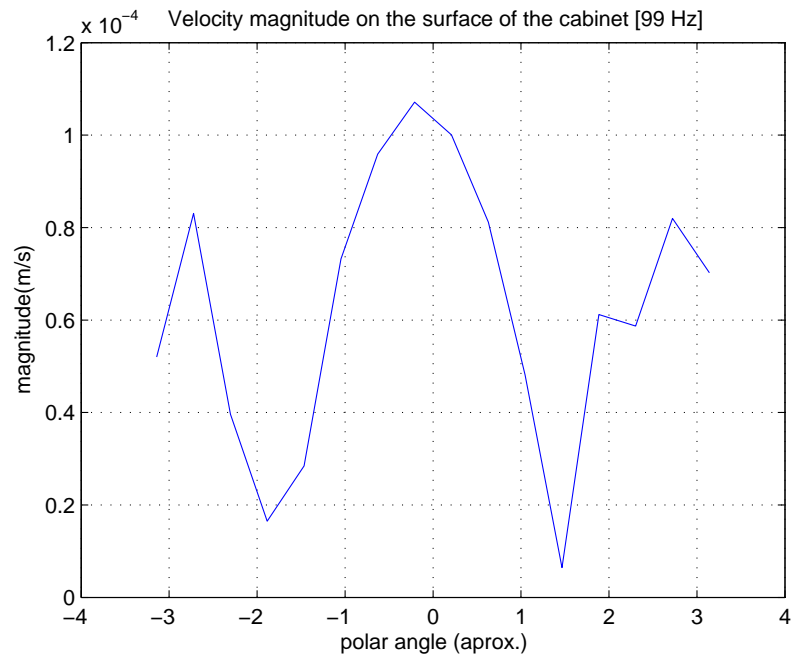


Figure B.2: *Magnitude of the velocity around the circumference of the cabinet at 99 Hz*

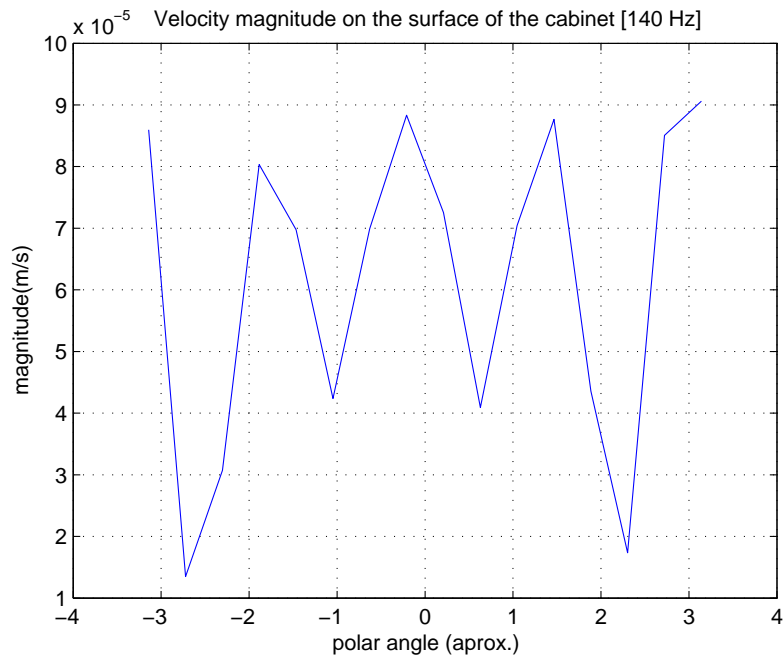


Figure B.3: *Magnitude of the velocity around the circumference of the cabinet at 140 Hz*

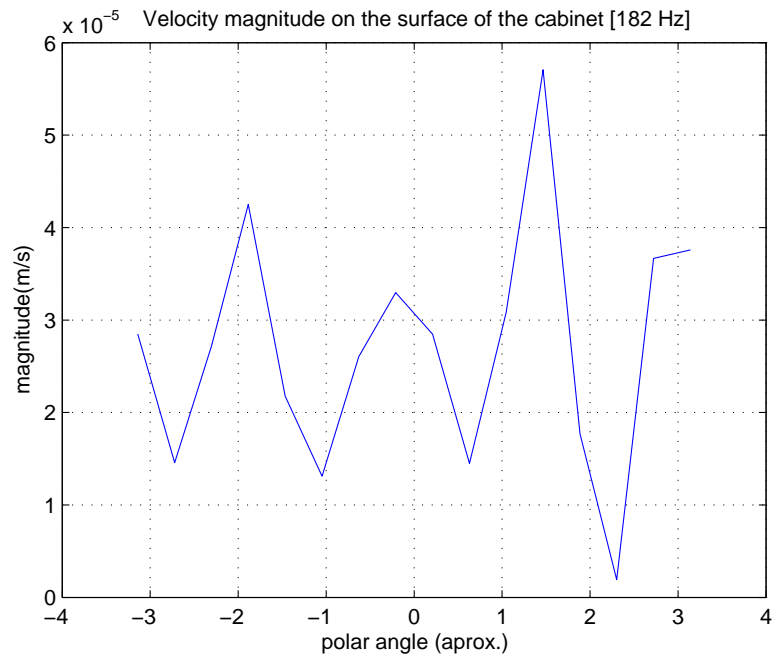


Figure B.4: *Magnitude of the velocity around the circumference of the cabinet at 182 Hz*

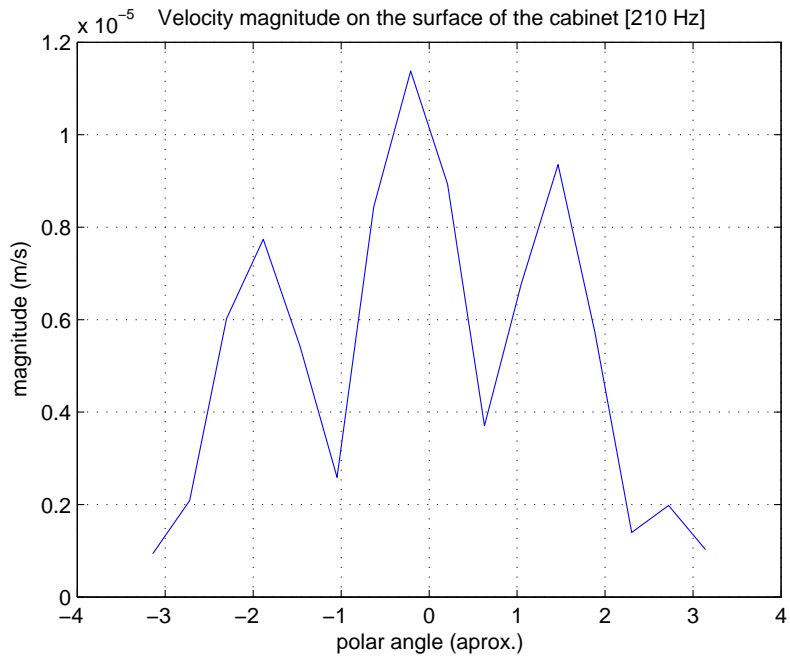


Figure B.5: *Magnitude of the velocity around the circumference of the cabinet at 210 Hz*

Appendix C

Matlab codes

C.1 Calculation of the sound radiated by the cabinet

[cabinetradiation.m]

```
%% Vibrating loudspeaker, based in measurements
%% INITIALIZATION
%clear;
clc;
open('workspace_vibrating_cabinet(24-6-08).mat'); %Opens the script
which
%contains the data obtained from the measurements
v_cabinet=ans.v_cabinet;

%pressure measured 1m in front of the speaker

p_35=ans.p_35; p_35=p_35';
p_back_35=ans.p_back_35; p_back_35=p_back_35';
p_side_35=ans.p_side_35; p_side_35=p_side_35';

pFP_allf=zeros(360,600);

%%
for f=1:600

Rfp=1; % radius of the arc of field points (half a circle in the z-
y plane)

k=2*pi*f/343; % Wavenumber, m-1
nsingON=1; % Deal with near-singular integrals
```

```

% CONDICIONES AMBIENTALES
pa = 101325;          % Presion Atmosferica (Pa)
t = 20;              % Temperatura ( C)
Hr = 50;             % Humedad relativa (%)
[rho , c , cf , CpCv , nu , alfa]=amb2prop(pa , t , Hr , 1000);

%% Read Geometry (mesh)
% Read nodes and topology.
nodes=readnodes('Node_list_ok.lis');
elements=readelements('Element_list_ok.lis');

M=size(nodes,1); N=size(elements,1);
% check geometry and add body numbers
[nodesb , topologyb , toposhrinkb , tim , segmopen]=bodyfind(nodes , elements)
;axis equal;
topologyb=toposhrinkb;

%% BC's: Velocity (vibrating cabinet)

% Calculate the BEM matrices and solve the pressures on the surface
%[A,B,CConst]=TriQuadEquat(nodesb , topologyb , topologyb , zeros(N,1) , k ,
    nsingON); % quadrilateral
[A,B,CConst]=TriQuadEquat(nodesb , topologyb , topologyb , ones(N,1) , k ,
    nsingON); % triangular
B=i*k*rho*c*B;
pf=A\(-B*v_cabinet(:,f+1));

% Field points

%This is for fieldpoints around the loudspeaker , polar diagram
%0 degrees is the front of the loudspeaker
Mfp=360; % Number of field points
height=0.35; %height of the field points. Apparently at 35cm is the
    highest sound radiation
theta=linspace(0,2*pi,Mfp)';
%xyzFP=Rfp*[cos(theta) height*ones(Mfp,1) sin(theta)];%my try
xyzFP=Rfp*[sin(theta) height*ones(Mfp,1) cos(theta)];%any try
%plot fieldpoints , to make sure that they are well defined
% figure; plot3(xyzFP(:,1),xyzFP(:,2),xyzFP(:,3)); xlabel('x'); ylabel
    ('y'); zlabel('z');

% Calculate field points
%[Afp,Bfp,Cfp]=point(nodesb , topologyb , topologyb , zeros(N,1) , k , xyzFP ,
    nsingON); % quadrilateral
[Afp,Bfp,Cfp]=point(nodesb , topologyb , topologyb , ones(N,1) , k , xyzFP ,
    nsingON); % triangular
pfFP=(Afp*pf+j*k*rho*c*Bfp*v_cabinet(:,f+1))./Cfp;
pFP_allf(:,f)=pfFP;%all frecuencies included here. the rows are the
    angles from 0 to 2pi and the columns the frequency from 1 to 500Hz

```

```

save('vibrating_cabinet_loop-temp.mat');
close all;

end

%
-----

%
% PLOTTING, POSTPROCESSING AND VERIFICATION
%
-----

%plot fieldpoints, to make sure that they are well defined
% figure; plot3(xyzFP(:,1),xyzFP(:,2),xyzFP(:,3)); xlabel('x'); ylabel
('y'); zlabel('z');
%open('workspace_vibrating_cabinet(24-6-08).mat')
PALL=ans.pFP_allf;

save('workspace_Allcabinet.mat');

%PLOT is a dummy variable created just to plot the polar plots with
the 0
%angle represented in the center of the plot
PLOT=circshift(PALL,-180);

figure;
imagesc(50:600,(180/pi)*theta,20*log10(abs(PALL(:,50:600))/20e-6),[0
40]);
title('SPL_radiated_by_the_cabinet_at_1m_distance_[freq_vvs_azimuth_
angle]');
xlabel('f'); ylabel('azimuth_angle_[deg]');
colormap([linspace(1,0.2,10)' linspace(1,0.2,10)' linspace(1,0.2,10)
']);
xlim([50 350]); colorbar; shading interp;

figure;
imagesc(50:600,(180/pi)*(theta-pi),20*log10...
(abs(PLOT(1:360,50:600))/20e-6),[0 40]);
title('SPL_radiated_by_the_cabinet_at_1m_distance_[freq_vvs_azimuth_
angle]');
xlabel('f'); ylabel('azimuth_angle_[deg]');
colormap([linspace(1,0.2,10)' linspace(1,0.2,10)' linspace(1,0.2,10)
']);
xlim([50 350]); colorbar; shading interp;

figure;

```

```

contour(50:600,(180/pi)*(theta-pi),20*log10(abs(PLOT...
    (:,50:600))/20e-6),10:1:40);
title('SPL radiated by the cabinet at 1m distance - Isobar=1dB-');
xlabel('f'); ylabel('azimuth angle [deg]');
xlim([50 350]); colorbar;
colormap([linspace(1,0.2,10) ' linspace(1,0.2,10) ' linspace(1,0.2,10)
    ']);

figure; contour(1:500,linspace(180,-180,360),angle(PLOT(:,1:500)),8);
title('Phase at 1m from the cabinet [freq vs polar angle] - (Isobar= $\pi$ 
    /4)-');
xlabel('f'); ylabel('azimuth angle [rad]');
xlim([50 350]); colormap([0 0 0 ; 0 0 0]); grid on;

%% COMPARISON WITH THE TOTAL PRESSURE OF THE LOUDSPEAKER

Cabinet_SPL=20*log10(abs(PALL(1,:))/(20e-6));
Total_SPL=20*log10(sqrt(abs(p_35))/(20e-6));

figure; semilogx(1:500, Cabinet_SPL(1:500), 'linewidth',2)
hold on; plot(1:500, Total_SPL(1:500), '—', 'linewidth',2);
title('SPL radiated from the cabinet compared to the total SPL');
legend('Cabinet', 'Total');
xlabel('log(f) [Hz]'); ylabel('SPL [dB]'); xlim([50 600]); grid on;

% Side radiation of the cabinet (at -90deg)
figure;
semilogx(1:500,20*log10(abs(PALL(271,1:500))/20e-6), 'linewidth',2)
hold on;
semilogx(1:500,20*log10(sqrt(abs(p_side_35(1:500)))/20e-6), '—', '
    linewidth',2)
title('SPL radiated from the side of the cabinet compared to the
    total');
xlabel('log(f) [Hz]'); ylabel('SPL [dB]'); xlim([50 600]); grid on;
Legend('Cabinet', 'Total')

%Back radiation of the cabinet
figure;
semilogx(1:500,20*log10(abs(PALLall(180,1:500))/20e-6)+1, 'linewidth'
    ,2, 'color', 'r')
hold on;
semilogx(1:500,20*log10(sqrt(abs(p_back_35(1:500)))/20e-6), '—', '
    linewidth',2)
title('SPL radiated from the back of the cabinet compared to the
    total');
xlabel('log(f) [Hz]'); ylabel('SPL [dB]'); xlim([50 600]);
grid on; Legend('Cabinet', 'Total')

```

```

%% POLAR PLOT
figure; polar(theta, 20*log10(abs(PALL(:, 84))/20e-6));
hold on; polar(theta, 20*log10(abs(PALL(:, 150))/20e-6), '—');
hold on; polar(theta, 20*log10(abs(PALL(:, 182))/20e-6), ':');
Legend('85Hz', '150Hz', '182Hz')
% title('SPL of the main natural frequencies of the cabinet at 1 m')
;
% Legend('85Hz', '150Hz', '182Hz', '220Hz')

%
-----

%% PLOT THE PHASE & MAGNITUDE OF THE VELOCITY
% THIS IS DONE IN ORDER TO SEE THE DEFLECTION SHAPES MORE OR LESS
%
%%%%%%%%%%%%%%%%%%%%%%%%%%%%%%%%%%%%%%%%%%%%%%%%%%%%%%%%%%%%%%%%%%%%%%%%%%%%%%

%phase=atan(imag/real)
%At 150Hz, for the nodes at 18cm height
%figure; contour(150, 17:32, angle(v_cabinet(17:32, 150)), 8); title('
Phase at 1m from the cabinet [freq vs polar angle] — (Isobar=pi/4)
—'); xlabel('f'); ylabel('azimuth angle [rad]');

fernandez=circshift(angle(v_cabinet(49:64, 83)), 19); %fernandez=unwrap(
fernandez);
figure; plot(linspace(-pi, pi, 16), (fernandez)); grid on;
title('Velocity phase on the surface of the cabinet [83 Hz]'); xlabel(
'polar angle (aprox.)'); ylabel('phase(rad)');
fernandez=circshift(abs(v_cabinet(49:64, 83)), 19); %fernandez=unwrap(
fernandez);
figure; plot(linspace(-pi, pi, 16), (fernandez)); grid on;
title('Velocity magnitude on the surface of the cabinet [83 Hz]');
xlabel('polar angle (aprox.)'); ylabel('magnitude(m/s)');

fernandez=circshift(angle(v_cabinet(49:64, 99)), 19); %fernandez=unwrap(
fernandez, 2);
figure; plot(linspace(-pi, pi, 16), (fernandez)+1.5); grid on;
title('Velocity phase on the surface of the cabinet [99 Hz]'); xlabel(
'polar angle (aprox.)'); ylabel('phase(rad)');
fernandez=circshift(abs(v_cabinet(49:64, 99)), 19); %fernandez=unwrap(
fernandez);
figure; plot(linspace(-pi, pi, 16), (fernandez)); grid on;
title('Velocity magnitude on the surface of the cabinet [99 Hz]');
xlabel('polar angle (aprox.)'); ylabel('magnitude(m/s)');

fernandez=circshift(angle(v_cabinet(49:64, 140)), 19); fernandez=unwrap(
fernandez);

```

```

figure ; plot (linspace(-pi, pi, 16), (fernandez)+8); grid on;
title ( ' Velocity_phase_on_the_surface_of_the_cabinet_[140_Hz] ' );
    xlabel ( ' polar_angle_(aprox.) ' ); ylabel ( ' phase(rad) ' );
fernandez=circshift (abs(v_cabinet (49:64,140)),19);%fernandez=unwrap(
    fernandez);
figure ; plot (linspace(-pi, pi, 16), (fernandez)); grid on;
title ( ' Velocity_magnitude_on_the_surface_of_the_cabinet_[140_Hz] ' );
    xlabel ( ' polar_angle_(aprox.) ' ); ylabel ( ' magnitude(m/s) ' );

fernandez=circshift (angle(v_cabinet (49:64,182)),19);%fernandez=
    unwrap(fernandez);
figure ; plot (linspace(-pi, pi, 16), (fernandez+1.5)); grid on;
title ( ' Velocity_phase_on_the_surface_of_the_cabinet_[182_Hz] ' );
    xlabel ( ' polar_angle_(aprox.) ' ); ylabel ( ' phase(rad) ' );
fernandez=circshift (abs(v_cabinet (49:64,184)),19);%fernandez=unwrap(
    fernandez);
figure ; plot (linspace(-pi, pi, 16), (fernandez)); grid on;
title ( ' Velocity_magnitude_on_the_surface_of_the_cabinet_[182_Hz] ' );
    xlabel ( ' polar_angle_(aprox.) ' ); ylabel ( ' magnitude(m/s) ' );

fernandez=circshift (angle(v_cabinet (49:64,210)),19); fernandez=unwrap
    (fernandez);
figure ; plot (linspace(-pi, pi, 16), (fernandez)-4.5); grid on;
title ( ' Velocity_phase_on_the_surface_of_the_cabinet_[210_Hz] ' );
    xlabel ( ' polar_angle_(aprox.) ' ); ylabel ( ' phase(rad) ' );
fernandez=circshift (abs(v_cabinet (49:64,210)),19);%fernandez=unwrap(
    fernandez);
figure ; plot (linspace(-pi, pi, 16), (fernandez)); grid on;
title ( ' Velocity_magnitude_on_the_surface_of_the_cabinet_[210_Hz] ' );
    xlabel ( ' polar_angle_(aprox.) ' ); ylabel ( ' magnitude_(m/s) ' );

```

C.2 Calculation of the sound radiated by the loudspeaker

[loudspeaker-radiation.m]

```

%% Vibrating loudspeaker, based in laser measurements
%still to do: check the vibration levels, the vibration velocities
%should be
%around 0.6585 m/s at 80Hz
%also measure the phase of the speaker,

%% INITIALIZATION
clear;
clc;

open('Velocity_speakr.mat');
v_driver=ans.v_driver;
v_cabinet=ans.v_cabinet;
open('Velocity_cab.mat');
%v_cabinet=ans.v_cabinet;
v_speakr=v_cabinet+v_driver;
%v speaker contains the velocity of the cabinet and of the drivers

%% Get measurements of the pressure
%pressure measured 1m in front of the speaker
p_35=ans.p_35; p_35=p_35';
p_back_35=ans.p_back_35; p_back_35=p_back_35';
p_side_35=ans.p_side_35; p_side_35=p_side_35';

%pFP_allf=zeros(360,600); %this is for all the polar angle, around
%the speaker
pFP_allf=zeros(3,600); %this is for fewer points ( front side back)

for f=1:400

Rfp=1; % radius of the arc of field points (half a circle in the z-
%y plane)
k=2*pi*f/343; % Wavenumber, m-1
nsingON=1; % Deal with near-singular integrals
% CONDICIONES AMBIENTALES
pa = 101325; % Presion Atmosferica (Pa)
t = 20; % Temperatura ( C)
Hr = 50; % Humedad relativa (%)
[rho,c,cf,CpCv,nu,alfa]=amb2prop(pa,t,Hr,1000);

%% Read Geometry (mesh)
% Read nodes and topology.
nodes=readnodes('Node_list_ok.lis');
elements=readelements('Element_list_ok.lis');

M=size(nodes,1); N=size(elements,1);

```

```

% check geometry and add body numbers
[nodesb, topologyb, toposhrinkb, tim, segmopen]=bodyfind(nodes, elements)
    ;axis equal;
topologyb=toposhrinkb;

%% BC's: Velocity (vibrating cabinet)

% Calculate the BEM matrices and solve the pressures on the surface
%[A,B,CConst]=TriQuadEquat(nodesb, topologyb, topologyb, zeros(N,1),k,
    nsingON); % quadrilateral
[A,B,CConst]=TriQuadEquat(nodesb, topologyb, topologyb, ones(N,1),k,
    nsingON); % triangular
B=i*k*rho*c*B;
%pf=A\(-B*v_speakr(:,f+1));
pf=A\(-B*v_driver(:,f+1));

% Field points
%This is for fieldpoints 1m away from the loudspeaker, in the
    positions
%that were measured. In the front in the side and in the back of it.
    Three points:
%front-side-back respectively
xyzFP=[0 0.35 1.2 ; 1.2 0.35 0 ; 0 0.35 -1.2 ];
%plot fieldpoints, to make sure that they are well defined
%figure; plot3(xyzFP(:,1),xyzFP(:,2),xyzFP(:,3)); xlabel('x'); ylabel('
    y'); zlabel('z');

% Calculate field points
[Afp,Bfp,Cfp]=point(nodesb, topologyb, topologyb, ones(N,1),k,xyzFP,
    nsingON); % triangular
%pfFP=(Afp*pf+j*k*rho*c*Bfp*v_speakr(:,f+1))./Cfp;
pfFP=(Afp*pf+j*k*rho*c*Bfp*v_driver(:,f+1))./Cfp;
pFP_allf(:,f)=pfFP;%all frequencies included here. the rows are the
    positions fron, side, back. The columns are the frequencies
close all;
save('workspace_vibrating_drivers_2','pFP_allf','pfFP')
end

open('workspace_vibrating_cabinet(24-6-08).mat')
PALL=ans.pFP_allf([1 270 180],:); %the division is done for
    calibration
clear ans
open('workspace_vibrating_drivers.mat');
PALLsp=ans.pFP_allf;

%%
-----

%%

```



```
%% PLOTTING
%%
```

```
-----

figure; semilogx(1:801, 20*log10(abs(v_driver(6,:))/(1e-9)), 'linewidth', 2);
hold on; semilogx(1:801, 20*log10(abs(v_driver(76,:))/(1e-9)), 'linewidth', 2);
title('vibration velocity of the Woofer and the Midrange');
xlabel('log f [Hz]'); ylabel('dB (ref 1mm/s)');
grid on; xlim([50 500]); ylim([50 150])
```

```
Driver_SPL=20*log10(abs(PALLsp)/(20e-6));
Total_SPL=20*log10(sqrt(abs(p_35))/(20e-6));
Total_BEM=20*log10(abs(PALL+PALLsp)/(20e-6));
```

```
%front radiation
```

```
figure; semilogx(1:500, Total_BEM(1,1:500), 'linewidth', 2, 'color', 'k');
hold on; plot(1:500, Total_SPL(1:500), '—', 'linewidth', 2, 'color', 'k');
title('SPL radiated from the loudspeaker BEM compared to measurement');
legend('BEM', 'Measurement');
xlabel('log(f) [Hz]'); ylabel('SPL [dB]'); xlim([50 350]); grid on;
ylim([50 64]);
```

```
figure; semilogx(1:500, Total_BEM(1,1:500), 'linewidth', 2, 'color', 'k');
hold on; plot(1:500, Driver_SPL(1,1:500), '—', 'linewidth', 2, 'color', 'k');
title('Total SPL from the loudspeaker compared to the loudspeaker unit');
legend('Total', 'Loudsp. unit');
xlabel('log(f) [Hz]'); ylabel('SPL [dB]'); xlim([50 350]); grid on;
ylim([55 62]);
```

```
% Side radiation of the cabinet (at -90deg)
```

```
% figure; semilogx(1:500, Total_BEM(2,1:500), 'linewidth', 2);
% hold on;
% semilogx(1:500, 20*log10(sqrt(abs(p_side_35(1:500)))/20e-6), '--');
% title('SPL radiated from the side of the loudspeaker (90deg)');
% xlabel('log(f) [Hz]'); ylabel('SPL [dB]'); xlim([50 350]);
% grid on; Legend('BEM', 'Measurement')
% ylim([50 60]);
```

```
%Back radiation of the cabinet
```

```
figure; semilogx(1:500, Total_BEM(3,1:500), 'linewidth', 2, 'color', 'k');
hold on;
semilogx(1:500, 20*log10(sqrt(abs(p_back_35(1:500)))/20e-6), '--');
title('SPL radiated from the back of the loudspeaker');
```

```

xlabel('log(f) [Hz]'); ylabel('SPL [dB]'); xlim([50 350]); ylim([50
60]);
grid on; Legend('BEM', 'Measurement')

figure; semilogx(1:500, Total_BEM(3, 1:500), 'linewidth', 2, 'color', 'k')
hold on; semilogx(1:500, Driver_SPL(3, 1:500), '—', 'linewidth', 2, 'color', 'k')
title('Total SPL radiated from the back compared to the Loudspeaker unit');
xlabel('log(f) [Hz]'); ylabel('SPL [dB]'); xlim([50 350]); ylim([50
60]);
grid on; Legend('Total', 'Loudsp. unit');

figure; semilogx(1:500, Total_BEM(3, 1:500), 'linewidth', 2, 'color', 'k')
hold on; semilogx(1:500, Driver_SPL(3, 1:500), '—', 'linewidth', 2, 'color', 'k')
hold on; semilogx(1:500, 20*log10(sqrt(abs(p_back_35(1:500)))/20e-6), '
:');
title('SPL radiated at the back of the loudspeaker (180°)');
xlabel('log(f) [Hz]'); ylabel('SPL [dB]'); xlim([50 350]); ylim([50
60]);
Legend('Total-BEM', 'Loudsp. unit-BEM', 'Total-Measured')

figure; semilogx(1:500, Total_BEM(3, 1:500), 'linewidth', 2, 'color', 'k')
hold on; semilogx(1:500, Driver_SPL(3, 1:500), '—', 'linewidth', 2, 'color', 'k')
hold on; semilogx(1:500, 20*log10(sqrt(abs(p_back_35(1:500)))/20e-6), '
:');
hold on; semilogx(1:500, 20*log10(abs(PALL(3, 1:500))/20e-6), '-.')
title('SPL radiated at the back of the loudspeaker (180°)');
xlabel('log(f) [Hz]'); ylabel('SPL [dB]'); xlim([50 350]); ylim([30
60]);
Legend('Total-BEM', 'Loudsp. unit-BEM', 'Total-Measured', 'Cabinet-BEM')

```

C.3 Time domain characteristics (Impulse response & decay)

[cabinetradiation-TimeDomain.m]

```

%%TIME DOMAIN RESPONSE
%This script performs an IFFT on the response of the cabinet, in
order to
%know what is the time domain response. In principle plotting the
frequency
%against the time (i.e. waterfall plot)

%The phase should be referenced to the electrical input
%For that reason, tn extra transfer function phase should be added
from the
%electrical response to the vibration reference point on top of the
woofer.
%Such a function is called H0 (which is Ref/Rel)

clear ; clc ;

open( 'workspace_vibrating_drivers.mat' )
pfdriver=ans.pFP_allf(1,1:350); clear ans;
%in the case of the back direction;
%pfdriver=ans.pFP_allf(3,1:350); clear ans;
%figure; plot(abs(pfdriver));
open( 'workspace_vibrating_cabinet(24-6-08).mat' )
H0real=ans.H0real';
H0imag=ans.H0imag';
H0mag=sqrt((H0real.^2)+(H0imag.^2));
H0ph=angle(H0real+i*H0imag); H0phase=unwrap(H0ph); clear H0ph;
PALL=ans.pFP_allf; clear ans;

%
%%%%%%%%%%%%%%%%%%%%%%%%%%%%%%%%%%%%%%%%%%%%%%%%%%%%%%%%%%%%%%%%%%%%%%%%%%%%%%

%CASE OF ALL THE CABINET VIBRATING (with the Bottom)
%this doesn't work because the imp response is too long and there is
time
%aliasing. Thus, there is another script called Cabbottom(which is
exactly
%the same as this one, with a longer time span (of two seconds))
%open( 'Velocity_cab_All.mat' )
%PALL=ans.pFP_allf; clear ans;
%
%%%%%%%%%%%%%%%%%%%%%%%%%%%%%%%%%%%%%%%%%%%%%%%%%%%%%%%%%%%%%%%%%%%%%%%%%%%%%%

```

```

%PALL contains the freq domain information of the complex frequency
    over
%all angles in 1degree resolution and 1Hz resolution PALL(0,:) is
    the front
%angle
%DEFINITION OF THE PARAMETERS INVOLVED IN THE ANALYSIS
dir=1;%direction in degrees for which the calculation is done
%complex pressure on the angle dir with the electrical phase
pf=(PALL(dir,1:350)').*(H0phase(1:350)./abs(H0phase(1:350)));
pf(351:700)=conj(pf(350:-1:1));

%VERIFICATION OF THE LOADED DATA
%figure;plot(abs(pf));
%figure;plot(angle(pf));figure;plot(20*log10(abs(pf)/20e-6));
%figure;plot(abs(pfdriver));
%figure;plot(angle(pfdriver));figure;plot(20*log10(abs(pfdriver)/2e
    -5));

%%
-----

%% IMPULSE RESPONSE OF THE CABINET — Using freq. up to 300Hz

df=1;%Hz
N=1024;
fs=N/df;

ptime=(350)*ifft(pf,N,'symmetric'); %350=factor for the ifft
    amplitude
figure;plot(0:1/fs:(1-1/fs), real(ptime),'linewidth',1.5);%plot
    until 1 sec
xlabel('time_(s)');ylabel('Sound_Pressure_(Pa)');
title('Impulse_response_of_the_cabinet_Pressure_at_1m-')
grid on;xlim([0 300e-3]);ylim([-0.05 0.05]);

% %interpolation (for beauty reasons)—not necesary and not used
% %in any case for results—

% tint=1/4096;%fint=1/tint;
% tinterp=(0:tint:(1-tint))';
% ptimeint=interp1((0:1/fs:1-1/fs),ptime,tinterp,'spline');%'linear
    ');
% figure;plot(0:tint:(1-tint), real(ptimeint),'linewidth',1.5);%plot
    until 1 sec
% xlabel('time (s)');ylabel('Sound Pressure (Pa)');
% title('Impulse response of the cabinet —Pressure at 1m-')
% grid on;xlim([0 300e-3]);ylim([-0.05 0.05]);

```

```

% Verification of the impulse response obtained
%check=fft((ptime),N);
%figure;plot(0:df:N/2-1,abs(check(1:N/2)));

%figure;plot(0:1/fs:1,(abs(ptime(1:(fs+1)))/abs(max(ptime))));
%grid on;%normalized decay
figure;plot(0:1/fs:(1-1/fs),real(ptime(1:fs)), 'linewidth',1.5);%
    until 1sec
xlabel('time_(s)');ylabel('Sound_Pressure_(Pa)');
title('Impulse_response_of_the_cabinet_Pressure_at_1m-')
grid on;xlim([0 300e-3]);ylim([-1.5e-3 1.5e-3]);

%%
-----

%% IMPULSE RESPONSE OF THE DRIVER - Using freq. up to 300Hz
%%%%%%%%%%%%%%%%%%%%%%%%%%%%%%%%%%%%%%%%%%%%%%%%%%%%%%%%%%%%%%%%%%%%%%%%%% GOOD %%%%%%%%%%%%%%%%%%%%%%%%%%%%%%%%%%%%%%%%%%%%%%%%%%%%%%%%%%%%%%%%%%%%%%%%%%%

Nd=1024;
fsdriver=Nd/df;
%fsd=Nd/df;%which means fsdriver=Nd
pdrivertime=(175)*ifft(pfdriver,Nd,'nonsymmetric');
%175= factor for the ifft amplitude (since 175 lines are used)

figure;plot(0:1/Nd:(1-1/Nd),real(pdrivertime), 'linewidth',1.5);%
    until 1sec
xlabel('time_(s)');ylabel('Sound_Pressure_(Pa)');
title('Impulse_response_of_the_loudspeaker_unit_Pressure_at_1m-')
grid on;xlim([0 300e-3]);ylim([-1.5e-3 1.5e-3]);

% Verification of the impulse response obtained
% check2=(1/175)*fft((pdrivertime),Nd);
% figure;plot(0:fsdriver/Nd:Nd-1,abs(check2));%
% figure;plot(0:fsdriver/Nd:Nd-1,20*log10(abs(check2)/2e-5));
%
%interpolation (to have the same dimensions as the cabinet)
tdinterp=(0:(1/1024):(1-(1/1024)))';
pdrivertimeint=interp1((0:1/Nd:1-1/Nd),pdrivertime,tdinterp,'linear',
);
% figure;plot(tdinterp,real(pdrivertimeint));%plot until 1 sec
% xlim([0 300e-3]);ylim([-1 1]);

%%%%%%%%%%%%%%%%%%%%%%%%%%%%%%%%%%%%%%%%%%%%%%%%%%%%%%%%%%%%%%%%%%%%%%%%%%
%
% LOAD & COMPARE IMPULSE RESPONSE BY B&O
%%%%%%%%%%%%%%%%%%%%%%%%%%%%%%%%%%%%%%%%%%%%%%%%%%%%%%%%%%%%%%%%%%%%%%%%%%

open('workspace_impulseBO.mat');

```

```

impulseBO=ans. impulseBO_eq;%we use the equalized one, since it is
    the one
                                %implemented when the measurement was
                                done
%impulseBO=ans. impulseBO;
clear ans;
%remove the offset;
offset=40;%samples of offset until the maximum
figure;
plot(-offset/5000:1/5000:((2000 - offset)/5000 - 1/5000), (impulseBO)*1e
    -4);
xlabel('time_(s)'); ylabel('Sound_Pressure_(Pa)');
title('Impulse_response_of_the_loudspeaker_unit_Measured-');
grid on; xlim([0 300e-3]); %ylim([-1.5e-3 1.5e-3]);

%%
-----

%% COMPARISON - PLOTTING

figure; subplot(2,1,1);
plot(0:1/fs:(1-1/fs), real(pdrivertimeint), 'linewidth', 2); %plot
    until 1 sec
grid on; xlim([0 300e-3]); ylim([-1e-1 1e-1]);
xlabel('time_(s)'); ylabel('(Pa)');
title('Impulse_response_of_the_driver_and_the_cabinet_Pressure_at_1
    m-');
subplot(2,1,2)
plot(0:1/fs:(1-1/fs), real(ptime), 'linewidth', 1.5); %plot until 1 sec
grid on; xlim([0 300e-3]); ylim([-1e-1 1e-1]);
xlabel('time_(s)'); ylabel('(Pa)');

figure; %dB-SPL decay
plot(0:1/fs:(1-1/fs), 20*log10(abs(pdrivertimeint(1:fs))/(2e-5)));
    grid on;
hold on;
plot(0:1/fs:(1-1/fs), 20*log10(abs(ptime(1:fs)+pdrivertimeint(1:fs))
    /(2e-5)));
title('Totla_SPL_decay_compared_to_the_loudspeaker_unit_SPL_at_1m-
    ');
grid on; xlim([0 100e-3]); xlabel('time_(s)'); ylabel('SPL(dB)'); %ylim
    ([0 50]);
legend('Driver_only', 'Total_(driver+cabinet)'); grid on; %dB-SPL decay

%
%%%%%%%%%%%%%%%%%%%%%%%%%%%%%%%%%%%%%%%%%%%%%%%%%%%%%%%%%%%%%%%%%%%%%%%%%
```

```

%
%%%%%%%%%%%%%%%%%%%%%%%%%%%%%%%%%%%%%%%%%%%%%%%%%%%%%%%%%%%%%%%%%%%%%%%%
%%
-----

%
%%SPECTROGRAM-WATERFALL PLOT Calculation (from the Time domain)
%
-----

%
%%%%%%%%%%%%%%%%%%%%%%%%%%%%%%%%%%%%%%%%%%%%%%%%%%%%%%%%%%%%%%%%%%%%%%%%
%
%%%%%%%%%%%%%%%%%%%%%%%%%%%%%%%%%%%%%%%%%%%%%%%%%%%%%%%%%%%%%%%%%%%%%%%%

%Try to compare the decay using ffts

n=256;
t=1e-3;
twin=29e-3;%half of the sliding time window used

%Compare the time windows that could be used
win1=Hann(2*twin*fs);
win2=rectwin(2*twin*fs);
win3=tukeywin(2*twin*fs+1,0.15);
win4=tukeywin(2*twin*fs+1,0.4);
wvtool(win1,win2,win3,win4);
wvtool(win4);
%find the best compromise for the window. the one with narrower
    mainlobe
%and smaller side-lobes.
win=win4;
figure;
subplot(1,2,1)
plot((0:1/fs:length(win)/fs-1/fs),20*log10(win),'linewidth',2,'color',
    'k');
title('cosine_tapered_window_(tukey)_-time-');
grid on;xlabel('time_[s]');ylabel('Amplitude');ylim([-35 1]);
subplot(1,2,2)
plot(0:fs/n:fs-1/n,20*log10(fft(win,n)),'linewidth',2,'color','k');
xlim([0 300]);grid on;title('cosine_tapered_window_(tukey)_-
    frequency-');
grid on;xlabel('f_[Hz]');ylabel('Mag_[dB]');
%t=0ms

t=[1 30 50 70 100 130 150]*1e-3;

```

```

for count=1:(length(t))
    if count==1
        estring=win(twin*fs:(2*twin)*fs).*ptime(1:(t(count)+twin)*fs);
        %just a string containing the data transformed, to avoid
        %problems with the indexes
        decaycab(:,count)=fft(estring,n);decaycab(:,count)=decaycab(
            :,count)/(n/2);%(length(estring));
        estringd=win(twin*fs:(2*twin)*fs).*pdrivertimeint((1:(t(
            count)+twin)*fs));
        decaydriv(:,count)=fft(estringd(:,count),n);decaydriv(:,
            count)=decaydriv(:,count)/(n/2);%(length(estringd));
        figure;plot(0:fs/n:(fs/2)-1/fs, 20*log10(abs(decaydriv(1:n
            /2,count)))/2e-5,'linewidth',2,'color','k');
        hold on;plot(0:fs/n:(fs/2)-1/fs, 20*log10(abs(decaycab(1:n
            /2,count)))/2e-5,'linestyle','—','linewidth',2,'color','k
            ');
        xlim([0 300]);ylim([5 63]);
        Legend('Loudsp. unit', 'Cabinet');grid on;xlabel('f [Hz]');
        ylabel('SPL [dB]');title('Spectrum of the decay of the
            cabinet and the driver at t=0ms');
    else
        estring=win.*ptime(round((t(count)-twin)*fs:(t(count)+twin)*
            fs));%just a string containing the data transformed, to
        %avoid problems with the indexes
        decaycab(:,count)=fft(estring,n);decaycab(:,count)=decaycab(
            :,count)/(n/2);%(length(estring));
        estringd=win.*pdrivertimeint(round((t(count)-twin)*fs:(t(
            count)+twin)*fs));
        decaydriv(:,count)=fft(estringd,n);decaydriv(:,count)=
            decaydriv(:,count)/(n/2);%(length(estringd));
        figure;plot(0:fs/n:(fs/2)-1/fs, 20*log10(abs(decaydriv(1:n
            /2,count)))/2e-5,'linewidth',2,'color','k');
        hold on;plot(0:fs/n:(fs/2)-1/fs, 20*log10(abs(decaycab(1:n
            /2,count)))/2e-5,'linestyle','—','linewidth',2,'color','k
            ');
        xlim([0 300]);ylim([5 60]);
        Legend('Loudsp. unit', 'Cabinet');grid on;xlabel('f [Hz]');
        ylabel('SPL [dB]');title(['Spectrum of the decay of the
            cabinet and the loudspeaker unit at t=',num2str(t(count)*1
            e3),'ms']);
    end
end

figure;
for count=1:(length(t)-1)
    subplot(3,2,count);plot(0:fs/n:(fs/2)-1/fs, 20*log10(abs(
        decaydriv(1:n/2,count)))/2e-5,'linewidth',2,'color','k');

```



```

    hold on; plot(0:fs/n:(fs/2)-1/fs, 20*log10(abs(decaycab(1:n/2,
        count))/2e-5), 'linestyle', '—', 'linewidth', 2, 'color', 'k');
    grid on; xlim([0 300]); title(['t=', num2str(t(count)*1e3), 'ms']);
end
Legend('Cabinet', 'Driver'); xlabel('f [Hz]'); ylabel('SPL [dB]');

f=(0:fs/n:(fs/4)-1/fs)';
[T F]=meshgrid(t, f);
figure; mesh(T, F, 20*log10(abs(decaydriv(1:n/4, :))/2e-5), 'MeshStyle', 'column', 'linewidth', 2); alpha(.1)
title('Sequency of the decay of the loudspeaker unit');
colormap(1-white); xlabel('time [s]'); ylabel('f [Hz]'); zlabel('SPL [dB]');
view([35 25]); %zlim([0 70])

figure; mesh(T, F, 20*log10(abs(decaycab(1:n/4, :))/2e-5), 'MeshStyle', 'column', 'linewidth', 2); alpha(.9)
title('Sequency of the decay of the cabinet');
colormap(1-white); xlabel('time [s]'); ylabel('f [Hz]'); zlabel('SPL [dB]');
view([35 25]); %zlim([0 70]);

f=(0:fs/n:(fs/4)-1/fs)';
[T F]=meshgrid(t(2:5), f);
figure; mesh(T, F, 20*log10(abs(decaydriv(1:n/4, 2:5))/2e-5), 'MeshStyle', 'column', 'linewidth', 2); alpha(0.001)
hold on; mesh(T, F, 20*log10(abs(decaycab(1:n/4, 2:5))/2e-5), 'MeshStyle', 'column', 'linewidth', 2, 'linestyle', '—'); alpha(.001)
colormap(1-white); xlabel('time [s]'); ylabel('f [Hz]'); zlabel('SPL [dB]'); Legend('Loudsp. unit', 'cabinet');
title('Comparison of the decay of the loudspeaker unit and the cabinet');
view([27 25]);

figure; mesh(T, F, 20*log10(abs(decaydriv(1:n/4, 2:5))/2e-5), 'facecolor', 'green', 'edgecolor', 'none'); alpha(0.9)
hold on; mesh(T, F, 20*log10(abs(decaycab(1:n/4, 2:5))/2e-5), 'facecolor', 'red', 'edgecolor', 'none'); alpha(0.9)
colormap(1-white); xlabel('time [s]'); ylabel('f [Hz]'); zlabel('SPL [dB]'); Legend('Loudsp. unit', 'cabinet');
title('Comparison of the decay of the loudspeaker unit and the cabinet');
view([42 25]);

```

C.4 Testing of the method (Test Box)

[testbox-radiation.m]

```

%% Vibrating test box, based in measurements
%%
clear;
clc;
open('Velocity_box.mat'); %Opens the script Velocity_cab.mat...
%... which contains the data obtained from the measurements
v_box=ans.v_box;
pres025=ans.pres025;
pres05=ans.pres05;
pFP_allf=zeros(2,600);
fmax=600;

for f=1:500
k=2*pi*f/343; % Wavenumber, m-1
nsingON=1; % Deal with near-singular integrals
% CONDICIONES AMBIENTALES
pa = 101325; % Presion Atmosferica (Pa)
t = 20; % Temperatura ( C)
Hr = 50; % Humedad relativa (%)
[rho , c , cf , CpCv , nu , alfa]=amb2prop(pa , t , Hr , 1000);

%% Read Geometry (mesh)
% Read nodes and topology.
nodes=readnodes('NLISTbox.lis');
elements=readelements('ELISTbox.lis');

M=size(nodes,1); N=size(elements,1);
% check geometry and add body numbers
[nodesb , topologyb , toposhrinkb , tim , segmopen]=bodyfind(nodes , elements)
;axis equal;
topologyb=toposhrinkb;

%% BC's: Velocity (vibrating cabinet)

% Calculate the BEM matrices and solve the pressures on the surface
%[A,B,CConst]=TriQuadEquat(nodesb , topologyb , topologyb , zeros(N,1) , k ,
nsingON); % quadrilateral
[A,B,CConst]=TriQuadEquat(nodesb , topologyb , topologyb , ones(N,1) , k ,
nsingON); % triangular
B=i*k*rho*c*B;
pf=A\(-B*v_box(:,f+1));
% Field points
%coordintaes of the field point
%centre at two heights 50cm and 25cm (+44cm height of the box)=94 &
69 cm

```

```

xyzFP=[0.221 0.94 0.221 ; 0.221 0.69 0.221];
% Calculate field points
%[Afp,Bfp,Cfp]=point(nodesb,topologyb,topologyb,zeros(N,1),k,xyzFP,
    nsingON); % quadrilateral
[Afp,Bfp,Cfp]=point(nodesb,topologyb,topologyb,ones(N,1),k,xyzFP,
    nsingON); % triangular
pfFP=(Afp*pf+j*k*rho*c*Bfp*v_box(:,f+1))./Cfp;
pFP_allf(:,f)=pfFP;%all frequencies included here. the rows are each
    field point and the columns the frequency from 1 to 500Hz

%% Plot solution
% figure;
% %subplot(2,1,1)
% plot(theta*180/pi,20*log10(abs(pfFP)/(20e-6))); grid
% xlabel('Angle [deg]'); ylabel('| pressure on field points [dB]| ');
% title(['Contribution of the loudspeaker cabinet, f=',num2str(f),'
    Hz at r=',num2str(Rfp),'m and height=',num2str(height),'m']);%
    subplot(2,1,2)

%plot fieldpoints, to make sure that they are well defined
% figure; plot3(xyzFP(:,1),xyzFP(:,2),xyzFP(:,3)); xlabel('x'); ylabel
    ('y'); zlabel('z');

save('vibrating_box_loop_temp.mat');
close all;
end

save('workspace_vibrating_box.mat')

PALl=pFP_allf;
pFP_allf=circshift(pFP_allf,[0 1]);

figure; plot(1:801,20*log10(sqrt(abs(pres025)))/(20e-6)), 'linewidth',
    ,2);
hold on; plot(20*log10(abs(pFP_allf(2,:)))/(20e-6)), '-.', 'linewidth',
    ,2);
title('Test_Box-Comparison-between_BEM_and_measurement_(at_0.25m_
    height)');
ylabel('SPL [dB]'); xlabel('freq [Hz]');
grid on; legend('Measurement','BEM')
figure; plot(1:801,20*log10(sqrt(abs(pres05)))/(20e-6)), 'linewidth',2)
;
hold on; plot(20*log10(abs(pFP_allf(1,:)))/(20e-6)), '-.', 'linewidth',
    ,2);
title('Test_Box-Comparison-between_BEM_and_measurement_(at_0.5m_
    height)');
ylabel('SPL [dB]'); xlabel('freq [Hz]');
grid on; legend('Measurement','BEM')

```

```

%
%%%%%%%%%%%%%%%%%%%%%%%%%%%%%%%%%%%%%%%%%%%%%%%%%%%%%%%%%%%%%%%%%%%%%%%%%

% MODES IN THE TEST BOX – very approximate, just to have an idea –
% 44by44by44 cm box made out of fiber board, on the top surface there
% is a
% 1mm thick aluminium plate driven by an inertial exciter
h=1e-3;
l=0.42%length of the sides
n1=1;%mode
n2=3;
%aluminium
rho=2.7e3;
E=7.1e10;v=0.33;
m=rho*h;
B=(E*h^3)/(12*(1-v^2));
wn=((n1*pi/l)^2+(n2*pi/l)^2)*sqrt(B/m);
f=wn/(2*pi);

```

Appendix D

SHELL63 Elastic Shell

SHELL63 has both bending and membrane capabilities. Both in-plane and normal loads are permitted. The element has six degrees of freedom at each node: translations in the nodal x, y, and z directions and rotations about the nodal x, y, and z axes. Stress stiffening and large deflection capabilities are included. A consistent tangent stiffness matrix option is available for use in large deflection (finite rotation) analysis. See Section 14.63 of the ANSYS Theory Reference for more details about this element. Similar elements are SHELL43 and SHELL181 (plastic capability), and SHELL93 (mid-side node capability). The ETCHG command converts SHELL57 and SHELL157 elements to SHELL63.

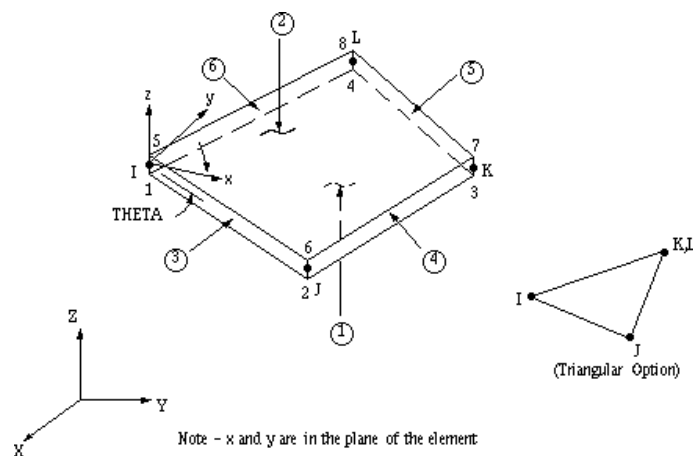


Figure D.1: *SHELL63 Elastic Shell*